UNIVERSITY OF CAPE TOWN
IYUNIVESITHI YASEKAPA • UNIVERSITEIT VAN KAAPSTAD

UNIVERSITY OF CAPE TOWN

FACULTY OF ENGINEERING AND THE BUILT ENVIRONMENT

Department of Civil Engineering

Effect of anti-corrosive coatings on the bond between corrosion-damaged rebar and concrete repair materials

Muhammad Ameen Moolla

Student Number: MLLMUH011

Supervisors: Professor Hans Beushausen & Nicholas Jarratt

Date: 11th February 2022

A dissertation submitted to the Department of Civil Engineering, University of Cape Town, in partial fulfilment of the requirements for the degree of Master of Science in Civil Engineering.

Acknowledgements

I would like to thank the University of Cape Town and more specifically the Civil Engineering department for allowing me the opportunity to conduct this investigation. I am grateful to CoMSIRU for providing me with the platform to conduct this study. Thank you very much to the National Research Foundation who has provided me with financial assistance throughout my postgraduate studies, allowing me to complete my MSc degree.

Much appreciation is owed to the lab staff in the construction materials laboratory as they have contributed largely to assisting with the experimental work and without their dedicated efforts, this investigation could not have been conducted.

Thank you, to Professor Hans Beushausen and Mr Nicholas Jarratt in assisting largely with this investigation to develop my thesis.

A big thank you goes out to all my friends in supporting me with constant motivation throughout my studies. Thank you to my parents, Haseena & Suleiman Moolla, and loving wife Khadija, who has largely supported me. Lastly, all praise is due to the almighty Allah for granting me this opportunity.

UNIVERSITY OF CAPE TOWN
IYUNIVESITHI YASEKAPA • UNIVERSITEIT VAN KAAPSTAD

Plagiarism declaration

1. I know that plagiarism is wrong. Plagiarism is to use another's work and pretend that it is one's own.

2. I have used the Harvard convention for citation and referencing. Each contribution to, and quotation in, this thesis from the work(s) of other people has been attributed and has been cited and referenced.

3. This thesis is my own work.

4. I have not allowed and will not allow anyone to copy my work with the intention of passing it off as his or her own work.

5. This thesis/dissertation has been submitted to the Turnitin module (or equivalent similarity and originality checking software) and I confirm that my supervisor has seen my report and any concerns revealed by such have been resolved with my supervisor.

Signature: Signed by candidate

Date: 11th February 2022

Abstract

Reinforcement corrosion is the largest contributor to the deterioration of existing RC structures worldwide. The aggressive electrochemical process causes destruction to the steel by a loss in cross section and rib height, which in turn affects the bond between steel and concrete and consequently the structural performance of reinforced concrete structures. During a repair strategy, when the patch repair method is considered, one of the steps usually involves the application of a protective coating to the corroded and subsequently cleaned steel. It is well-accepted that protective coatings offer corrosion resistance to the steel in reinforced concrete repaired elements. However, information on how well the coated rebar bonds to the new surrounding repair concrete is limited. Hence, developing an understanding on the bond performance of repaired coated rebar is important for engineers in the construction repair industry. One commercially available epoxy-modified, cementitious coating material was considered in this study, Sika ® Armatec ® -110- EpoCem, and applied with one or two coats of 0.6 mm each. Rebar corrosion damage levels of 0%, 10% and 20% (of steel mass loss) were simulated by mechanical grinding of sound rebar samples, attempting to represent the condition of cleaned corroded rebar. Two steel bars, Y12 and Y16, of different diameters were considered. Three repair materials with CEM I 52.5N were considered in this study, which included one concrete with a w/b ratio of 0.45 and two mortars with w/b ratios of 0.47 and 0.65, referred to as C45, M45 and M65, respectively. Pull-out testing was conducted on a total of 108 specimens to assess the effect of coating thickness on the bond with respect to the different parameters of this study. The results indicate that the w/b ratio of the mortars had a significant influence on the bond and the addition of stone showed no difference on the failure loads obtained. There was no significant effect of the rebar diameter on the pull-out force for uncorroded rebar, although with cleaned corroded rebar the effect was significant. Specimens with 10% mass loss had larger reductions in pull-out force compared to those with 20% mass loss. While coatings reduced the bond of uncorroded and cleaned corroded rebar, the thickness of the coating had practically no influence on the pull-out force. Using C45-12 with two coats on 20% corroded steel, the pull-out force was 80% compared to before corrosion. Failure of uncorroded specimens was dominated by splitting, and slip was mostly seen for cleaned corroded specimens. With coatings applied to uncorroded bars, slip coating failure was evident with uncorroded steel while splitting with coating failure was evident especially with Y16. From the corroded coated specimens, there appeared to be good contact between the cleaned corroded steel and repair material.

Table of contents

List of figures

List of tables

1. Introduction

1.1 Background

Reinforcement corrosion is the dominant cause for premature failure of concrete structures worldwide, due to its detrimental effects on a member's durability and structural load-bearing capacity (Lin *et al.*, 2019). A substantial amount of aging infrastructure experiences degradation as a result of reinforcement corrosion, resulting in significant costs to restore their capacity and prevent further deterioration and failure (Guettala and Abibsi, 2006). Environmental exposure of the concrete to deleterious substances, allows processes such as carbonation and chloride ingress to occur, which under the right conditions can initiate and sustain reinforcement corrosion. This electrochemical process consequently causes oxidation of the steel to form rust where the reinforcement bears a loss in cross-section (Mackechnie and Alexander, 2001). Furthermore, corrosion of the reinforcement destroys the ribs and lugs on deformed bars, which are responsible for providing the bond that allows for the composite action and load transfer between the steel and concrete. Carbonation-induced corrosion occurs relatively uniformly over the steel surface, whereas chloride-induced corrosion results in localized pits, where the damage is more severe. Independent of the cause for corrosion initiation, the damaging effects from either process can cause major destruction to the embedded reinforcement, if corrosion progresses and insufficient remedial action is taken.

Many structures experience early deterioration because of reinforcement corrosion where their durability, and hence, service life is compromised. As a result, large amounts of capital are invested annually in concrete repairs. Patch repairs are a common repair method for damaged concrete structures suffering from reinforcement corrosion. The procedure involves the removal of the defective concrete, followed by cleaning the surface of the steel to remove all corrosion products (Ballim, Alexander and Beushausen, 2009). A protective coating is then usually applied, and the concrete section restored. The function of an anti-corrosive coating agent on the reinforcement is to mitigate further corrosion and reinstate the bond strength that was initially provided by the ribs on the uncorroded steel. There are a variety of commercially available coatings, however, the limitations of poor workmanship on-site, such as not cleaning the steel thoroughly from corrosion products or not coating the cleaned steel properly, can lead to further and continuous corrosion. Furthermore, if the coating is not correctly applied, the bond between the steel and repair material may be impacted, which would affect stress transfer and hence the load bearing capacity of structural repaired members. It is well understood that repair coatings provide sufficient corrosion control however there is little understanding of how

repair coatings bond to the cleaned corroded steel. The purpose of this study is to evaluate how coatings affect the bond when applied to cleaned corroded steel at different degrees of corrosion damage and used in combination with various concrete repair materials and rebar sizes.

1.2 Problem statement and justification

Repair and rehabilitation of corrosion-damaged reinforced concrete structures has been a concern for many decades. However, there are still areas in the concrete repair industry that require further investigation. For example, there is not much literature available with regards to how repair coatings affect the bond between the steel and repair material. Due to a lack of research on the issue, no guidelines in repair standards currently exist to allow engineers assessing this effect in their evaluation of the structural capacity of repaired members and structures.

Mackechnie and Alexander (2001) report that, during a typical patch repair procedure, after cleaning of the corroded steel, either an anti-corrosion epoxy coating or zinc-rich primer should be applied to the steel. These coatings act as barriers against carbonation, chlorides, and moisture to prevent further corrosion. Epoxy-modified cementitious coatings are commonly used in the concrete repair industry, especially in South Africa. According to Jorge, Dias-da-Costa and Júlio (2012), these types of coatings reduce the bond strength of uncorroded steel and, therefore, should not be considered in new construction. Natino *et al* (2021) report that coatings may restore up to 90% of the bond strength when the bars are repaired after 10% steel mass loss. There is, however, little insight into how the coating thickness affects the bond of corroded steel, which makes it difficult for engineers to specify a suitable coating thickness in a repair strategy, or how these coatings perform when applied to steel at different stages of corrosion damage. Hence, there is a need to understand how the thickness of epoxy-modified cementitious coatings affect the bond of corroded repaired rebar and the degree to which they can restore the bond at different levels of steel mass loss. Furthermore, the effect of repair material properties on the bond strength to the prepared and coated steel reinforcement needs to be investigated.

1.3 Aims and outcome

The current research study aims to investigate the effect of the coatings on the bond of corroded repaired rebar. The objectives of this study are:

- To determine if the levels of corrosion damage have an influence on the bond strength between steel and repair material.
- To assess whether the thickness of coatings affects the bond of corroded specimens by pull-out testing and to quantify how much of the original bond is reinstated after repair.
- To assess the performance of coatings in combination with mortar or concrete of varying compressive strength.
- To assess the effect of coatings when applied to reinforcing bars of different size.

The predicted outcome of this study is to assess by how much of the bond is reduced by coatings to corrosion-damaged rebar. In addition, this investigation will contribute to providing guidance on appropriate coating thicknesses to be used. This work will also demonstrate how coatings perform in relation to the rebar diameter and repair material used. Lastly, the results from this research will provide a basis for further researchers to contribute to a better understanding on the performance of anti-corrosive coatings used for corrosion repair.

1.4 Scope and limitations

This research is concerned with the application of anti-corrosive coatings as a remedial measure for corrosion damage and quantifying how much of the original bond can be restored. In this study, the repair of existing corroded RC structures is considered, where the protective coating is applied during one of the steps during the patch repair process. This study is limited to one commercially available epoxy-modified cementitious coating (Sika Armatec® -110 EpoCem). Other coating types are out of the scope of this research. Two different size rebar of 12 mm and 16 mm are chosen for this experiment.

Time restrictions prevented the actual corroding of reinforcing bars for the experimental investigations. Therefore, corrosion damage was simulated using an angle grinder. A steel mass loss of 10% and 20% was chosen, with the aim of representing the condition of the steel after cleaning in a typical repair scenario. Further testing on natural corrosion damaged steel can support the findings from this investigation. The repair materials included one concrete with w/b ratio of 0.45, and two mortars with w/b ratios of 0.47 and 0.65, referred to as C45, M45 and M65, respectively. Compressive strength testing and pull-out testing was considered to characterize the repair material mixes and assess the pull-out performance, respectively. A

curing period of 7 days was used in this study. The pull-out failure loads were analyzed to identify clear influences of the parameters on the bond as factors such as corrosion and the coating changes geometrical properties of the mechanical bond at the steel-concrete interface.

1.5 Overview of the thesis structure

The content of this paper is sectioned into six chapters: Chapter 1 - Introduction, Chapter 2 - Literature review, Chapter 3 - Methodology, Chapter 4 - Results and discussion and Chapter 5 - Conclusions and Chapter 6 - Recommendations. Chapter 1 provides a basis for the study starting with a background, problem statement, aims and outcomes of the study, as well as the scope and limitations of the investigation. Chapter 2 provides detailed literature into bond strength, reinforcement corrosion and its influence on bond strength, repair of corrosion-damaged RC as well as suitable rebar coatings used for repair. Chapter 3 presents the test methods and experimental approach on how the specimens were prepared and tested. Chapter 4 presents and discusses the results from experimental testing and, lastly, Chapters 5 and 6 provide the conclusions drawn from the thesis and recommendations for future work.

2. Literature Review

2.1 Overview

The bond strength in reinforced concrete is based on the properties of both the steel rebar and surrounding concrete. The composite action between the two materials allows for successful load transfer between different elements in a RC member (Bouazaoui and Li, 2008). The ultimate load-bearing capacity as well as the stiffness of the structural member is affected by the bond. The bond between steel and concrete is hence an important aspect to the structural capacity of a reinforced concrete member, such as resisting shear forces in a truss mechanism against seismic loads (Aryanto and Shinohara, 2012; Plesa *et al.*, 2016). For in-situ structures where corrosion progresses to high degrees of steel mass loss, the bond strength is significantly reduced, due to destruction of the ribs and a loss in cross-sectional diameter of the steel. Corrosion largely decreases the effective bonding area between the steel and concrete.

A common repair strategy for corrosion-damaged rebar includes conducting the patch repair method. This involves removal of the defective concrete, followed by cleaning of the corroded steel and subsequent application of a protective coating which should provide corrosion control and adequate bond strength to the repaired member. At present, the existing concrete repair standards and available literature lacks information pertaining to the application and effects of coatings on the bond and the structural performance of corrosion-damaged steel. As a result, further investigation into the effects of repair coatings on corroded steel is necessary to provide a basis for developing the available concrete repair standards. In doing so, engineers may have a better understanding of the important factors to consider when applying coatings during repair applications.

The following sections of this chapter provide a detailed discussion into the bond between steel and concrete and related influencing factors, the effects of reinforcement corrosion and the need for repair, as well as repair principles with discussions on the available coatings and their potential influence on bond strength between steel rebar and concrete repair materials.

2.2 Bond strength between rebar and concrete

The bond strength at the interface between rebar and concrete occurs by composite action of the two materials. The steel carries most of the tensile load while the concrete supports the member in compression, and in doing so, both materials will experience the same deformation without loss of connection at the steel-concrete interface (Sonebi, Davidson and Cleland, 2011). The bond is responsible for successful stress transfer between the steel and concrete,

and hence is an important aspect to consider for the structural capacity of reinforced concrete members. The bond strength between steel and concrete can be measured by Equation 1,

$$\tau = \frac{P}{\pi DL} \tag{1}$$

where τ is the shear bond strength, P is the applied failure load, D is rebar diameter and L is the embedded length of the steel. There are three main mechanisms that govern the bond strength between rebar and concrete. This includes: chemical adhesion between the concrete and steel surface area, frictional resistance along the bar, and bearing resistance that induces mechanical interlock of the concrete between the ribs of the steel (Diab *et al.*, 2014). Adhesion between the steel reinforcement and concrete occurs because of the chemical bond at the contact interface between the two materials. The bonding by adhesion can be defined as the strength that remains before any slip of the concrete occurs at the interface under tensile load, where proceeding bond-slip mechanisms such as friction and mechanical interlock occur upon the initiation of slip at the steel-concrete interface (Turk, Yildirim and Caliskan, 2003). Frictional forces remain present at the steel when adhesion to the concrete is lost. This bond mechanism is of high concern and the dominating bond force for plain bars. The frictional forces present in deformed bars play a significant role in providing adequate resistance to tensile load, however of a magnitude that is considerably less compared than that provided by the mechanical interlock component (Xiao, Li and Zha, 2004), shown in Figure 1.

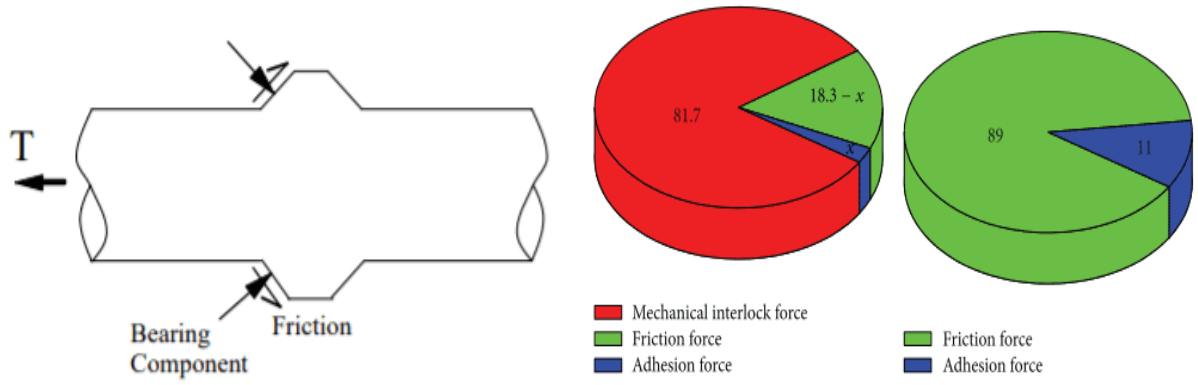

Figure 1: Bond force mechanisms (Xiao, Li and Zha, 2004)

Mechanical interlock is caused by the ribs and lugs on the steel which exert bearing forces on the surrounding concrete when a member is loaded (Diab *et al.*, 2014). Essentially, for deformed rebars, the bond is dependent mainly on bearing stresses due to mechanical interlock, with a small contribution from adhesion and frictional stresses. For plain bars, however, there is no bearing component, due to the absence of deformities along the surface of the bar,

whereby the bond strength in members is comprised of simply adhesion and friction between the surrounding concrete and smooth bar surface. Furthermore, the bearing capacity of the concrete is essential to resist splitting of the surrounding concrete. When the steel in under tensile load, the stress at the interface rapidly increases till the maximum bond strength has been reached. Upon failure, the bond stress gradually decreases as the load is further applied, displayed in Figure 2. A typical bond stress-slip curve represents the relationship between the stress generated at the steel and the corresponding slippage from the surrounding concrete (ACI Committee 408, 2003). Bond strength is quantified by conducting pull-out testing and is further discussed in Chapter 3. The bond between steel and concrete occurs by composite action and is therefore related to properties of both materials. The main factors that influence the bond are:

1. Applied load
2. Geometrical properties of the steel
3. Compressive strength of the concrete

There are other factors that affect the bond such as loading rate, compaction of the mix, type of rebar and concrete used. However, these factors do not play a role as important as the main factors listed above.

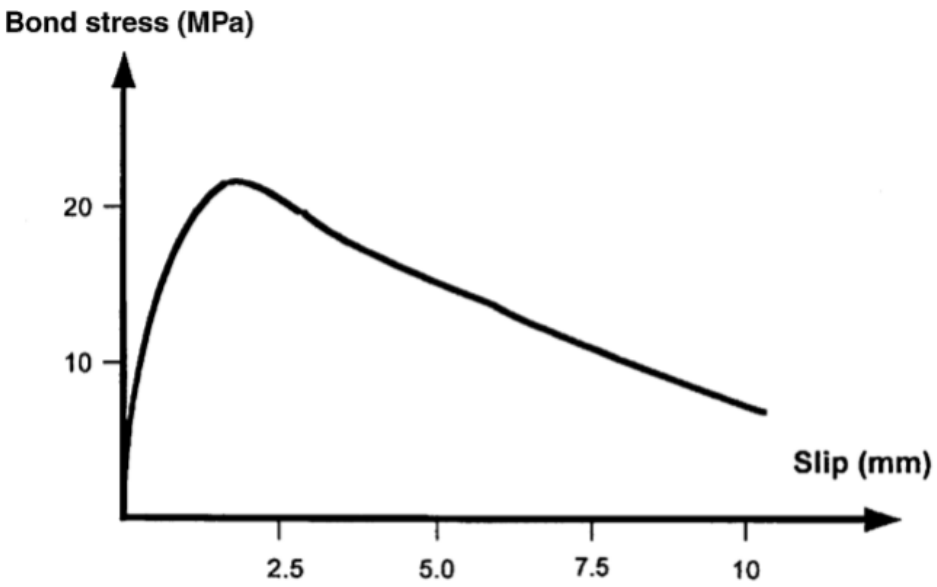

Figure 2: Bond stress-slip relationship (ACI Committee 408, 2003)

2.2.1 Effect of rebar diameter on bond strength

In reinforced concrete design, rebar sizes may vary considerably among different design projects, with the intent of providing a certain structural capacity to the member to attain the performance. The load transfer in structural members are largely dependent on the strength of the bond between the rebar and surrounding concrete substrate (Pothisiri *et al.*, 2018). Whilst in design, further calculations are performed on the basis that there is adequate bond strength at the steel-concrete interface. Therefore, ensuring sufficient bond strength is imperative. Changing the size of reinforcement in members can have a serious effect on the bond strength, depending on the scenario. It is well known in literature that increasing the rebar diameter relates to a distinct size effect, which is illustrated in Figure 3. This means to say that an increase in rebar diameter will result in a higher load (kN) to cause bond failure but also a lower bond strength (MPa) when the effective steel surface area is considered (Turk, Yildirim and Caliskan, 2003). When a reinforced concrete element is loaded, the force exerted at the steel-concrete interface increases the relative bond strength of the reinforced concrete composite system under load, prior to the initiation of bond slip. This increase in bond strength takes place at a higher rate for smaller sized reinforcing bars (De Larrad et al., 1993). Therefore, from Equation 1 it is seen that the bond strength is dependent on the geometrical properties of the steel and loading condition. It is noted that for larger bar diameters, there occurs a thicker interfacial transition zone (ITZ) between the steel and concrete that holds more water under the ribs (Teresa *et al.*, 2008). Furthermore, in reinforced concrete beams, the smaller diameter rebars have a higher ductility, meaning that while the bond strength might increase, the stiffness is lowered.

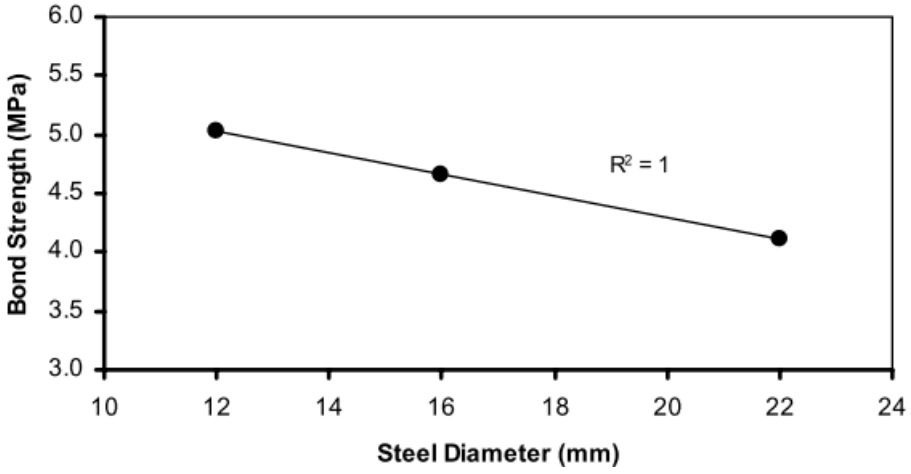

Figure 3: Bond strength vs. rebar diameter (Turk et al., 2003)

Increasing the bar diameter from 12 to 15 mm will cause a reduction of 25% in the bond strength (Metelli and Plizzari, 2014). During a study on rebar diameter and concrete quality on bond strength, a significant influence on improvement in bond strength performance (80% compared to normal strength concrete) is indicated by the effects of high strength concrete and a small bar size (10 mm diameter), where this performance effect is substantially reduced (to 30%) by an increase in the bar diameter to 25 mm with the use of normal strength concrete. This demonstrates the effects of rebar size and concrete quality on the bond strength. Whilst investigating the effects of bar diameters on bond strength performance of reinforced concrete beams, increasing the bar diameter results in a reduction in bond strength and deflection behaviour at midspan, though the stiffness of beams is increased (Sukru, 2004).

Other factors such as concrete cover depth and confinement also influences the effect of rebar diameter on the bond strength. During pull-out tests on different concrete and bar properties, larger cover depths in specimens, up to 52 mm, and presence of confinement through transverse reinforcement reduces the size effect i.e., for smaller bar diameters, the result of increased bond strength is complimented with adequate cover depth and presence of transverse reinforcement (Ichinose, 2004).

2.2.2 Effect of relative rib area on bond strength

The relative rib area of reinforcing bars, also known as the bond index, has the greatest influence on the bond strength and the member stiffness (Metelli and Plizzari, 2014). The rib area can be characterized by the ratio between the rib area in line with the perpendicular plane and the bar surface area between successive ribs, shown in Figure 4, where a – rib height, b – rib width, α – rib face inclination, β – rib inclination, s – rib spacing.

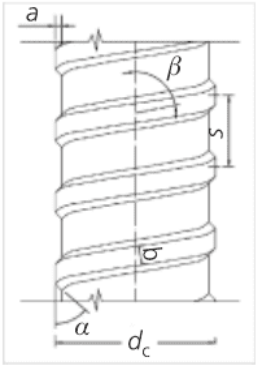

Figure 4: Distinction between rib dimensions (Metelli and Plizzari, 2014)

The relative rib area f_R, is defined by Equation 2 below where *de* is the external bar diameter, *di* the internal core diameter, *d* the nominal diameter and *s* the rib spacing.

$$f_R = \frac{de^2 - di^2}{4ds} \quad (2)$$

Metelli and Plizzari (2014) report that increasing the relative rib area from 0.04 to 0.10 will increase the bond strength by as much as 40%, as a result of highly ribbed bars producing a smaller wedging action to the concrete. Additionally, Darwin and Graham (1993) report a small increase in the bond strength of 10% achieved by varying the bond index from 0.05 – 0.20. The authors further note interdependency between the rib spacing and rib height. A 30% increase in the bond strength was achieved when the bond index was raised from 0.05 to 0.10 due to the lower bursting forces generated by bars with a high rib frequency. The lower wedging action generated by highly ribbed bars has the potential to reduce the risk of splitting failure of concrete while an increase in bond strength can be achieved (Metelli and Plizzari, 2014). Different rib geometry arrangements are shown in Figure 5.

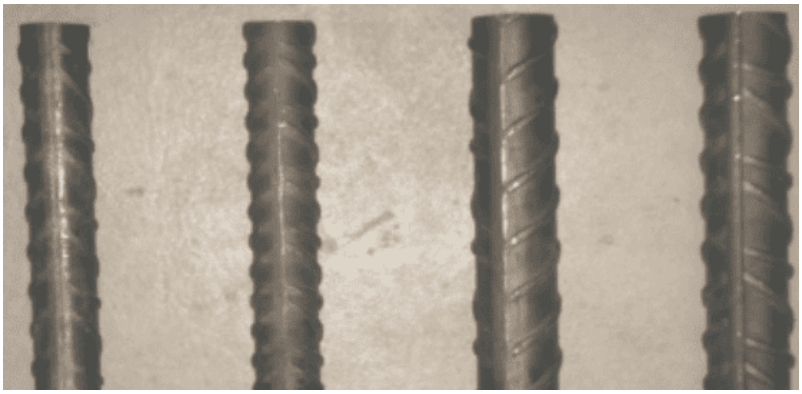

Figure 5: Various rib geometries of deformed bars (Metelli and Plizzari, 2014)

2.2.3 Effect of concrete compressive strength on bond strength

The bond strength of reinforced concrete is highly dependent on the compressive strength of concrete. Wang (1963) investigated the water-cement ratio against the compressive strength and bond strength, whose results are illustrated in Figure 6. It is evident that for high strength concretes, with low water-cement ratios, the relative bond strength is also of a high magnitude. For application with plain bars, however, varying the compressive strength of concrete will result in no considerable influence on the bond strength due to the absence of ribs.

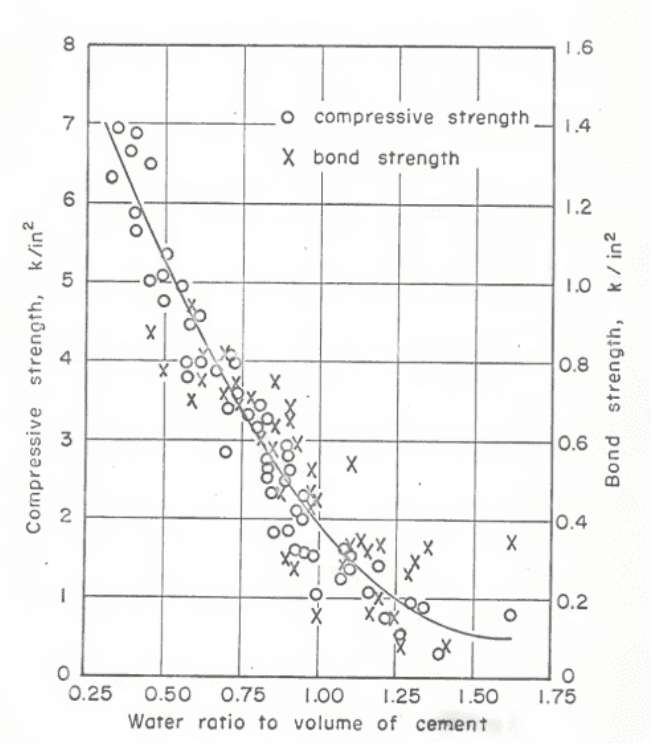

Figure 6: Concrete compressive strength and bond strength relationship with water-cement ratio (Wang, 1963)

There are other relating factors to compressive strength that increase the bond strength between steel and concrete, such as the aggregate composition and cement content (Wang, 1963). It can therefore be seen that the compressive strength of concrete in contact with steel has a significant effect on the bond strength, which is a result of mechanical interlock. Considerable research has been conducted in order to characterize and quantify the influence of different concretes on maintaining the bond between steel and concrete. New innovative construction concretes have been developed, which offers a higher bond strength to reinforcing steel when compared to conventional concrete, such as self-compacting concrete (Qasim and Ahmed, 2018). Other innovations in material technology have led to the use of steel fibres for high strength characteristics. In this application, a higher strength concrete is achieved but the ductility is lowered. As a result, steel fibres are used to maintain adequate bond strength while also increasing tensile strength, to the benefit of crack resistance. The workability of concrete in new construction during placement should be manageable enough to spread thoroughly between the entire rib area on the steel surface. In doing so, a proper contact area is secured between the two materials to sustain a good bond. The consistency of concrete has the potential to influence the bond quality largely, where a higher consistency of concrete contributes to settlement and bleeding, which could also further lead to plastic settlement cracking. The bond in this manner is compromised due to the accumulation of bleed water under steel, particularly

important to consider when casting top reinforcing bars in RC beams and slabs (Darwin, 1987). This issue can, however, be mitigated through adequate compaction effort using vibration. Compaction of the mix is particularly important to ensure proper contact to the steel.

2.3 Reinforcement corrosion

Existing concrete structures worldwide are experiencing current deterioration as a result of many causes including inadequate mix design and cover provision, as well as poor construction practices such as insufficient placement, compaction and curing methods. Reinforcement corrosion is to date the largest cause for premature deterioration in concrete structures, requiring early repair and maintenance that is extremely costly (Mackechnie and Alexander, 2001). Reinforcement corrosion affects the durability of reinforced concrete structures while inflicting major damage and requiring major costs to repair worldwide every year. The effect of rebar corrosion is detrimental as the rust component formed during corrosion is expansive, causing internal stresses. The corrosion products formed induces tensile stress within the concrete cover till reaching its tensile capacity, thereafter, causing cracking of concrete. Furthermore, subsequent delamination and spalling of the concrete cover occurs as the corrosion process continues. As a result, the rebar is exposed to the atmosphere with sufficient oxygen and moisture that will accelerate corrosion further (Zhang *et al.*, 2020). As such, the damaging effects to RC members subject to ongoing reinforcement corrosion progresses, where the durability and performance of corrosion affected RC structures are significantly compromised, as seen in Figure 7.

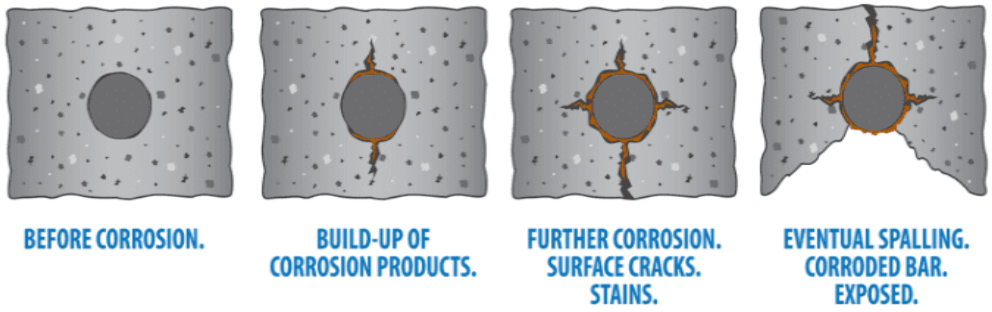

Figure 7: Corrosion propagation damage (Dhawan, et al., 2014)

2.3.1 Corrosion process

Reinforcement corrosion is an electrochemical process that incorporates the flow of charge through electrons and ions from the location of the anode to cathode on the steel surface. Figure 8 illustrates a typical corrosion process for reinforced concrete. In order for the corrosion process to occur there needs to be present an anode, cathode, metallic path and electrolyte

(Mackechnie and Alexander, 2001). The anode is the area on the rebar surface at which corrosion takes place and the location from which electrons flow, where the metal is oxidized. The cathode is the site where no corrosion takes place and the location to which electrons will flow, where oxygen is reduced to form hydroxyl ions. The steel reinforcement itself acts as the metallic path and serves as the connection between the anode and cathode to complete the circuit. An electrolyte containing O_2 and H_2O needs to be present, which flows through the concrete pore solution, carrying current and so allowing the ion transfer (James *et al.*, 2019).

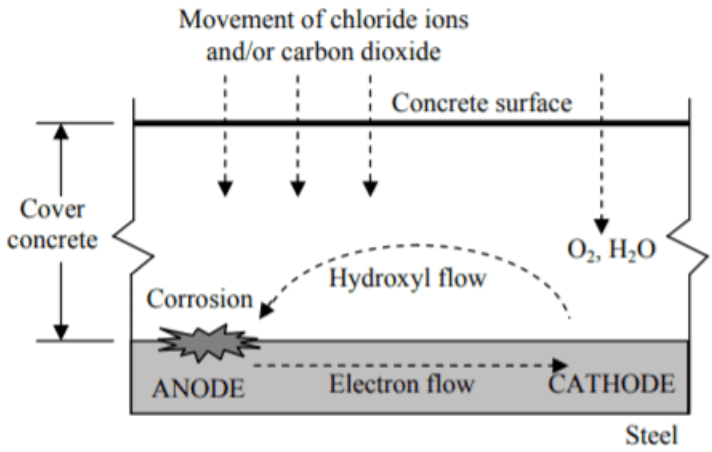

Figure 8: Overall corrosion process (Mackechnie et al., 2001)

Reinforcement corrosion can be categorized into the anodic and cathodic processes. The flux of ions produced at the steel surface together with the electrons can be used to measure the corrosion rate. The processes are shown in the following equations:

$$\textbf{Anodic reaction: } 2Fe \rightarrow 2Fe2 + 4e - \quad (3)$$

$$\textbf{Cathodic reaction: } O2 + 2H2O + 4e- \rightarrow 4OH - \quad (4)$$

$$\textbf{Corrosion reaction: } 2Fe + 2H2O + O2 \rightarrow 2Fe(OH)2 \quad (5)$$

Equations 3, 4 and 5 represent the initial process of corrosion between the anode and cathode. In order for rust to be formed, further stages of corrosion must occur whereby $Fe(OH)_2$ (ferrous hydroxide) forms 4Fe(OH)3 (ferric hydroxide) and finally Fe2O3.H2O (hydrated ferric oxide) commonly termed ‘rust’. Equations 6 ,7 and 8 describes the process by which rust is formed.

$$Fe^{2+} + OH^{-} \rightarrow Fe(OH)2 \quad (6)$$

$$4Fe(OH)_2 + O_2 + 2H_2O \rightarrow 4Fe(OH)_3 \quad (7)$$

$$2Fe(OH)_3 \rightarrow Fe_2O_3.H_2O + 2H_2O \quad (8)$$

Reinforcement corrosion can be classified into two stages, namely the initiation and propagation phase, while the second stage can be further categorised into a propagation stage and further accelerated corrosion propagation stage (Ballim, Alexander and Beushausen, 2009). In the initiation phase, aggressive chemical agents from the environment penetrate and move through the concrete cover to de-passivate the steel and induce corrosion. In the propagation phase however, corrosion damage is induced which extends to cover cracking and spalling that causes cause major damage to in-service RC structures. Important to the bond strength of corrosion-affected steel is the formation of ferric oxide which is largely responsible for the destruction of the steel ribs, reducing the bond strength.

2.3.2 The effect of reinforcement corrosion on bond strength

The influence that reinforcement corrosion has on a RC member's structural behavior arises mainly from degradation of the bond at the steel-concrete interface. It is commonly known that reinforcement corrosion destroys the ribs and lugs which largely comprises the bond in uncorroded deformed rebar (Lin *et al.*, 2019). The cross-sectional diameter of the steel is reduced and thereby the strength of the member is affected by corrosion activity. Deterioration of the bond due to corrosion therefore has a significant effect on reducing the service life of RC members where the serviceability and ultimate load-carrying capacity are altered as a result. Furthermore, in instances where corrosion progresses to high levels, the failure mode of the concrete can be changed from ductile to brittle failure, which can be a major problem for in-service RC structures if no remedial action is taken. Figure 9 displays an overview of the damaging effects due to reinforcement corrosion on the bond that exists in RC members.

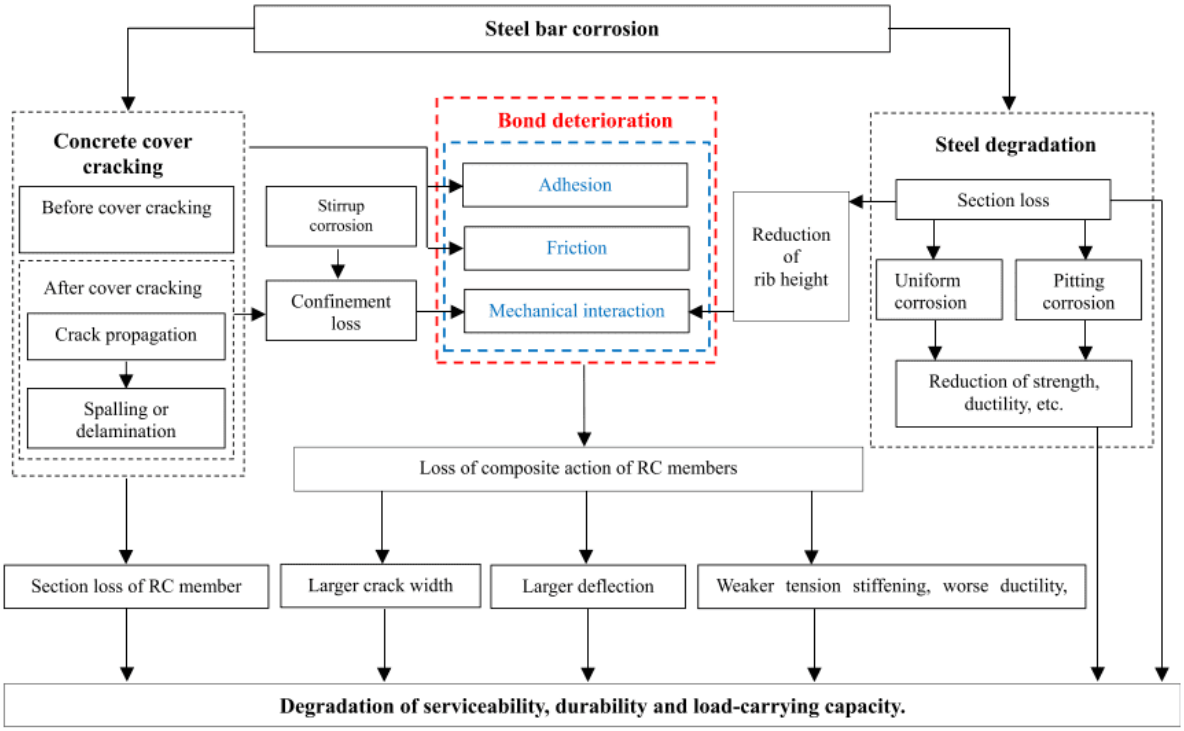

Figure 9: Reinforcement corrosion effects on structural performance (Lin et al., 2019)

Although corrosion occurs on the steel, the effects are imposed on the surrounding concrete cover region, which too experiences deterioration as a result. For the steel, the geometrical properties are affected by a cross-section reduction where the strength and ductility mostly are negatively affected (Lin *et al.*, 2019). For low corrosion levels of 5% and high corrosion levels of 10% steel mass loss, the ductility can be lowered by as much as 20% and 40% respectively (de Brito *et al.*, 2020).

The effects of reinforcement corrosion on deterioration of the bond have been widely investigated by many authors. The relationship between bond strength and corrosion level in terms of mass loss is shown in Figure 10. A general trend is noticed, where the bond strength is increased during the initial stages of corrosion, till a critical corrosion threshold is reached. Thereafter, the bond strength decreases as the corrosion level increases (Lin *et al.*, 2019). During the initial stages of corrosion, up to about 5% steel mass loss, the expansive corrosion products seep into open pores, creating a denser and stronger ITZ between the corroded steel and concrete. This seepage also creates a confining pressure, thereby further enhancing the frictional component of the bond (Lin *et al.*, 2019). Almusallam *et al.*, (1996) noted that, at this corrosion level, the ultimate bond strength had increased by 13% of its original bond strength, before corrosion had occurred.

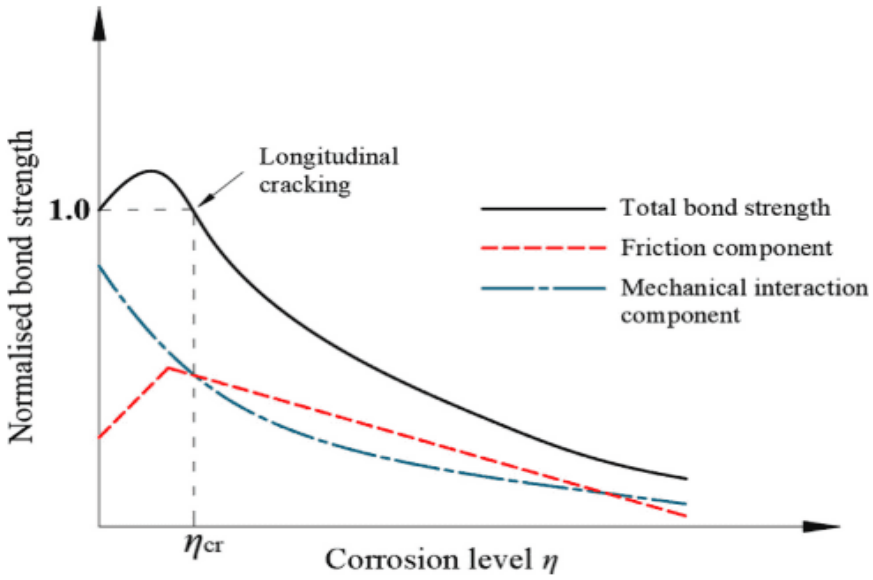

Figure 10: Idealized bond strength relationship with corrosion level (Lin et al., 2019)

The mechanical interlock is, however, affected when corrosion initiates and can be attributed to the radial pressure from corrosion counteracting the stresses from mechanical interlocking. Regardless of this reduction, the enhancement of frictional resistance from the initial firm rust has a larger effect, as seen in Figure 10. Hence, reinforcement corrosion has a positive influence on the bond strength during early stages of damage (Lin *et al.*, 2019). Almusallam *et al.*, (1996) reported that despite a rib loss of 25% occurring during early stages of corrosion, the enhanced friction enabled an increase in bond strength. It is important to note that there is no specific guideline as to which specific corrosion level will induce a certain level of damage by cracking or spalling of the concrete cover. This could be due to several influencing factors, in both the steel and concrete, whereby researchers have adopted different mix parameters, materials, equipment, testing methods and accuracy of results. Though researchers have noted the bond strength initially increases with corrosion, up to levels as high as 5%, the bond may also start to deteriorate at levels as low as 2%, which Kearsley and Joyce (2014) reported to be the critical point where the bond starts to deteriorate.

As corrosion progresses to a higher stage, the bond deteriorates and hence the serviceability of members becomes a concern. Degradation of the bond occurs by accumulation of more rust that starts to behave as a lubricant, decreasing adhesion and ultimately the bond strength at the steel-concrete interface (de Brito *et al.*, 2020). The rust produced from corrosion generates expansive stresses within the concrete cover where at severe stages of corrosion can cause cracking once the tensile resistance of the concrete is exceeded. Here the radial pressure caused

from the rust is allowed to relax, however, major deterioration of the ribs exist (Lin *et al.*, 2019). The presence of ribs on a corroding reinforcing bar subject to pull-out load, initiates the development of tensile hoop stress that progress through the concrete cover and facilitates cracking in this region. As a result, the width of cracks are increased significantly where the corrosion level is considerable enough to cause cracking i.e. above approximately 5% mass loss (Kearsley and Joyce, 2014). The point at which minor corrosion cracks begin to occur on the concrete surface, can be related to significant damage of the ribs. Here the reduction in rib profile can reach as much as 43% (Almusallam *et al.*, 1996). While the ribs degrade to this extent, there is a steep reduction in the bond strength. When the level of corrosion reaches a point above approximately 8%, where extensive cracking or spalling of the concrete cover is present, the effects of rib loss are detrimental to the mechanical interlock provided by the ribs (Almusallam *et al.*, 1996). Here, the rust mass that has been produced drastically reduces the frictional resistance of the bond. Additionally, the loss of rib profile at this stage of corrosion is approximately half that of the original geometrical make-up. The ribs are therefore seen to play an imperative role and when affected by corrosion, the bond strength between steel and concrete is severely impacted. It is important, therefore, to establish a corrosion level threshold (% mass loss) where bond degradation is critical to the performance of the structure (de Brito *et al.*, 2020). There is a near-linear relationship between the mass loss, due to corrosion, and the bond strength of reinforcing bars, which is illustrated in Figure 11. With regards to rebar size influence, it can be noted that as the corrosion degree increases, the pull-out failure load will reduce at a faster rate for larger bars (El Alami *et al.*, 2022).

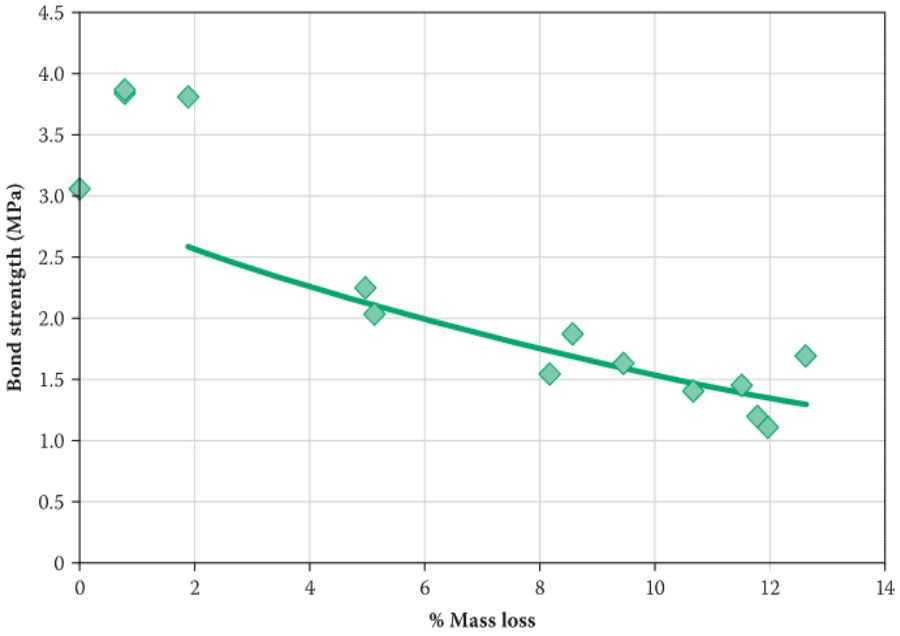

Figure 11: Bond strength deterioration according to steel mass loss (Kearlsly and Joyce, 2014)

The presence of cracks poses a large concern to the structures service life. There is a strong correlation between the surface crack width of concrete and the corrosion degree (Lin *et al.*, 2017). It is therefore necessary to monitor existing structures for visible damage by corrosion as failure of members by insufficient bond strength can lead to major safety concerns if no remedial action is taken to repair the damage and restore capacity. The extent to which a structure's capacity is restored depends on the level of damage that is present due to corrosion. Further, with excessive cracking of the cover region coupled with a loss in cross-section, there is the possible scenario of brittle failure occurring when a RC member is subject to structural loading. In cases where corrosion has only progressed to low levels below 10% steel mass loss, patch repairs with application of anti-corrosive coatings are seen to be an effective method to restore a significant portion of a members original load-carrying capacity (Natino *et al.*, 2021). Corrosion damaged structures are usually repaired when the extent of corrosion is controllable, typically around 20% mass loss, as destruction to the ribs beyond this stage of corrosion may be unacceptable for sustaining adequate bond strength.

The influence of corrosion on the condition of the bar surface has a major impact where the cross-sectional diameter is no longer uniformly circular, after damage has occurred. The geometrical properties of the bar are therefore altered by corrosion, affecting the mechanical properties and hence, structural response of the steel. Also, the residual yield stress in the steel decreases as the corrosion degree increases, while there is no significant change in the elastic modulus of the bars (Taha and Morsy, 2016).

2.4 Repair and rehabilitation of corrosion damaged RC structures

2.4.1 Repair principles for corrosion control

Over the past decades, the topic of repair and rehabilitation of existing reinforced concrete structures has become a major concern. This is mostly due to structures experiencing pre-mature deterioration from several harmful mechanisms but mostly owed to reinforcement corrosion. As a result, the need for structural engineers with knowledge on how to repair these damaged RC structures is becoming more apparent, to an extent where it is predicted that in the future, engineers will spend less time on designing new structures, while rehabilitating more existing structures as infrastructure development continues. With the widespread demand for repair, the industry requires a set of standards or guidelines which helps the engineer to make

correct informed decisions on how to successfully repair a damaged RC structure. A common repair standard adopted in most countries worldwide, known as EN1504, is a comprehensive European standard that advises on concrete repair processes in terms of the assessment, planning, design and quality control (Raupach and Büttner, 2014). The standard also includes guidelines to various test methods adopted in the concrete repair industry. The aim of EN1504 is to alleviate the problem most engineers and contractors make in applying a conventional repair with no proper consideration to the underlying cause of deterioration, suitable repair materials, methods of application and service life required from the repair, which is mostly the case due to a lack of experience.

The standard does not provide adequate information regarding the use of anti-corrosive coating materials in the case of concrete repair. Most of the commercially available products promoted in the building and construction industry provide instructions on applying coating substances. The manufacturers provide specifications in terms of the coating thickness, though not proven through experimental investigation whether the application method is in fact effective to restore the bond that is lost due to corrosion.

2.4.2 Patch repairs

Patch repairs are a common repair method for corrosion damaged RC structures and have been used extensively in the concrete repair industry. Its application involves repair of concrete that has deteriorated as a result of reinforcement corrosion and aims to reinstate the old section and re-passivate the steel, following the repair principle of concrete restoration (Raupach and Büttner, 2014). The patch repair process involves:

(1) Removal of the defective, contaminated concrete
(2) Surface preparation of the steel by cleaning all rust
(3) Application of a protective coating
(4) Casting of a suitable repair mortar
(5) Application of protection to the exterior concrete surface

Cleaning of the steel is essential where the rust should be completely removed from the steel before application of a protective coating. The coating is applied to the bare corroded steel to mitigate further corrosion and reinstate the bond strength that has been lost due to corrosion. Typical coatings used in the repair of corroded reinforcement is discussed in Section 2.5. If corrosion has damaged the steel to a considerable level, replacement of the steel is necessary.

Additionally, galvanic cathodic protection in the form of sacrificial anodes is required in some cases to avoid corrosion adjacent to the repair patch.

2.4.2.1 Cleaning of the corroded steel

To completely remove all corrosion products thoroughly, when removing the defective concrete surrounding a corroding rebar, it is essential that the method used ensures that the cleaned bar is free from rust, as this would largely affect the bond between the corroded coated steel. There are many different methods to clean corroded steel before repair; though, there may be difficulty with applying certain methods on site. The methods of brushing or cleaning with acid allows portions of rust to remain, which are not easily visible and can lead to future corrosion. Most of the concrete repair operations employ the use of metallic wire brushes to clean the corroded steel, due to its ease of application. While this method may appear to be effective, this is not always the case. Al-Dulaijan *et al.* (2002) reports that adopting sandblasting methods aided better results, with respect to corrosion resistance of repaired concrete elements. Fernandez, Lundgren and Zandi (2018) investigated the effects of various rebar cleaning methods, including wire brush, sandblasting and acid cleaning, see Figure 12. The results indicate a lower removal capacity from brushing and acid cleaning due to the remains of minor corrosion products that are not visually observable. The authors note sandblasting to be the most effective method to clean corroded steel, as all corrosion products are ensured to be removed, exposing corrosion pits successfully. Although some researchers assume sandblasting to have a significant effect on altering the surface texture of the bar, this is not the case as confirmed by (Fernandez, Lundgren and Zandi, 2018).

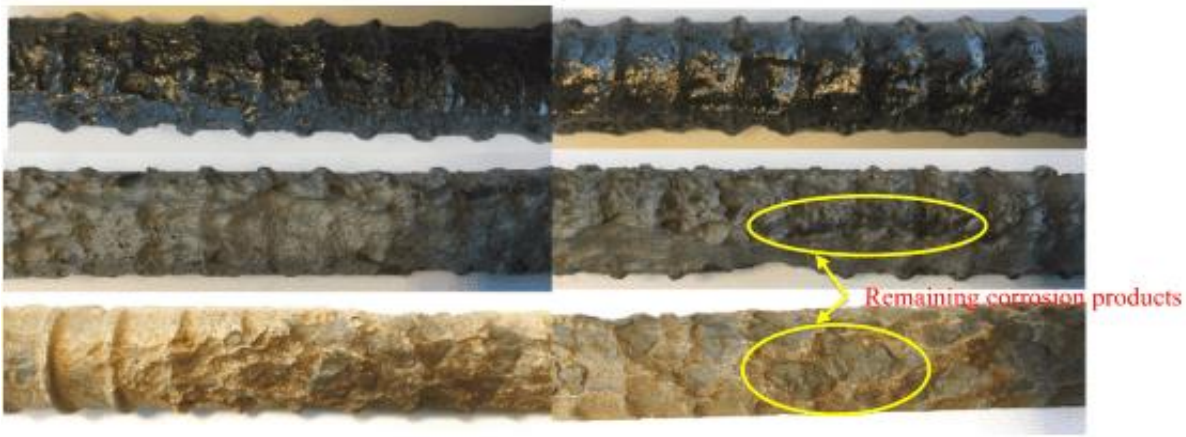

Figure 12: Corroded rebar cleaned using metallic brush (top), sandblasting (middle) and acid immersion (bottom) (Fernandez et al., 2018)

2.4.2.2 Coating the cleaned corroded rebar

The popular coating substances available for application in reinforced concrete are manufactured with a cementitious, epoxy, or urethane base, further discussed in Section 2.5. The bond strength and corrosion resistance offered by different coatings varies significantly because of their chemical and physical properties. Investigations on coatings that are both effective in this regard is present in existing findings to some extent.

Anti-corrosive coatings with good adhesive properties may be necessary to not only protect the steel from further corrosion, but to restore the bond that was initially provided by the ribs. Different coating materials, due to their chemical composition, viscosity, and application, display varying geometrical surface conditions around the bar, where some enhance or reduce the effective rib area that allows for interlock of the surrounding concrete. In other words, cement-based coatings which are thick will drastically reduce the rib area while epoxy coatings have no considerable effect in this regard (Natino *et al.*, 2021). Pure epoxy based coatings offers no friction however as a result of its smooth finish, and therefore has a large impact on the bond (Seddelmeyer *et al.*, 2000). While the coating type may affect the surface roughness of the bar, the overall influence on the geometrical properties is primarily dependent on the condition of the rebar after corrosion and cleaning.

2.5 Rebar coatings

Coating systems are commonly applied to rebar during new construction and repair of corrosion damaged rebar. The function of a coating is to protect the steel from aggressive conditions that may cause rebar corrosion (Sørensen *et al.*, 2009). There are various coatings commercially available for the application of repairing RC structures damaged by reinforcement corrosion, such as passivating and non-passivating epoxy coatings, polymer-modified cement slurry and zinc-rich coatings. Often, these coatings are modified with binders for enhanced mechanical properties.

Two coating types commonly used in concrete repair projects are cementitious epoxy-modified coatings and zinc modified polyurethane primers, referred to as ‘anti-corrosive’ coatings and recommended for application in repairing corrosion damaged steel (Mackechnie and Alexander, 2001). These products are commercially available and are well known for their protection against corrosion, however, little knowledge exists on how well they bond to the cleaned steel.

2.5.1 Coating protective mechanisms

The mechanisms of protection from coatings can be categorized into barrier, galvanic or inhibitive effects to resist corrosion (Sørensen *et al.*, 2009), shown in Figure 13. Anti-corrosive coating systems can comprise of single or multiple coating layers, which can be of a metallic, organic, or inorganic nature.

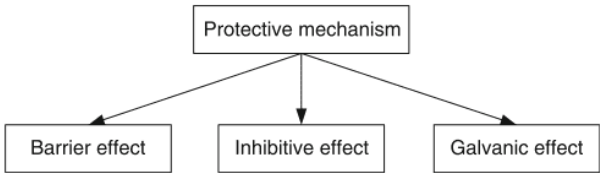

Figure 13: Coating protective mechanisms (Sørensen, et al., 2009)

Most manufactured coating products have a base component for a specific protective effect and modified for additional benefits where the base component lacks. For example, in concrete repair application, common repair coatings include a barrier effect from a cementitious base component that is modified with polymers for corrosion resistance. Similarly, zinc sacrificial and inhibitive coatings are modified with urethanes for enhanced physical resistance and adhesion to the steel (Sørensen *et al.*, 2009).

2.5.2 Coating types

2.5.2.1 Sacrificial coatings

Sacrificial coatings, unlike barrier coatings, function through the mechanism of galvanic corrosion, where the reinforcement is protected from corrosion by a metal with a higher electronegativity. Sacrificial coatings have been widely used in the construction industry and applied as a primer, due to its reliance on full contact with the steel, resulting in a coating that is anodically active, while the steel acts as the cathode (Natino *et al.*, 2021). Sacrificial coatings and primers function by the flow of current, which requires high zinc-pigmentation to ensure adequate conductivity. In this way, the steel can be galvanically protected where the actual corrosion resistance occurs by flow of galvanic current from the sacrificial zinc primer (Sørensen *et al.*, 2009). As a result of the high zinc pigmentation needed in sacrificial coatings and primers, the remainder percentage of binder by weight in the anti-corrosive substance is quite low. Hence, desirable mechanical behavior of these coatings and primers are not always achieved, due to low cohesion and adhesion to the concrete (Sørensen *et al.*, 2009). Most zinc-rich primers are thus modified with epoxies or urethanes to enhance their mechanical performance, and ultimately contribute to an increased bond strength, when compared to pure

zinc-based primers. Concerning galvanic coatings, the low presence of components required to ensure good mechanical resistance renders these systems not suitable to concrete repair application for restoring the lost bond (Sørensen *et al.*, 2009).

2.5.2.2 Inhibitive coatings

Inhibitive coatings function by passivating the substrate and is comprised of a protective layer with insoluble metallic pigments. These coatings are often primers, operating by reaction between the dissolved particles and the steel. Inorganic salts form the inhibitive pigments within these coatings and are partly water soluble. Hence, when the primer is in contact with water, some inhibitive pigments dissolve and are transported to the steel surface where they react to passivate the steel (Sørensen *et al.*, 2009).

2.5.2.3 Barrier coatings

Barrier coatings create a film of a certain thickness, normally applied in layers, that protects the steel from corrosive conditions, hence increasing its physical resistance. Due to practices during repair construction, where time is saved through application of less coats of greater thickness, the geometrical properties of the bar is affected drastically, where the rib area is substantially reduced (Natino *et al.*, 2021). Barrier coating systems, which contain polymers that bear hydrolysable bonds, such as urethanes, display more pronounced adhesion to metal substrates (Sørensen *et al.*, 2009). Popular barrier coatings used in new construction due to their excellent corrosion resistance, are epoxy-based coatings. These coatings if carefully handled during placement are effective in protecting the rebar from harsh conditions, though the bond strength is significantly reduced because of the high reduction in surface roughness, when compared to uncoated bars.

One of the most extensively used coating types, especially in South Africa, is cementitious barrier coatings. Cementitious coatings maintain a high alkalinity to re-passivate the steel, however, most coating systems are modified with epoxies and polymers for enhanced corrosion resistance (Sørensen *et al.*, 2009). The characteristics of a suitable binder that can offer successful performance in terms of corrosion resistance and bond improvement to a damaged reinforcement bar should feature properties such as good mechanical strength, low permeability, cohesion of the coating substance and adhesion of the coating substance to the steel, such as epoxies (Ramaswamy, S. N., Varalakshmi, 2016). Epoxy coatings are popular in the construction industry due to their excellent corrosion resistance. The epoxy molecule contains stable carbon-carbon bonds that provides chemical stability when well cured

(Sørensen *et al.*, 2009). However, epoxy-based coatings have shown to reduce the bond strength in reinforced concrete considerably when pure epoxy-based coatings are used. Properties of the steel such as an increasing bar diameter has a more severe effect on reducing the bonding performance of epoxy-coated bars (Choi *et al.*, 1991). The reduction in bond strength increases with thicker coatings due to the smooth finish of the epoxy producing no irregularities for the surrounding concrete to bond. Pure epoxy-based coatings are, therefore, not recommended for application in repairing corrosion damaged RC structures. Epoxy resins have however been popular as a modifier to cementitious based coating materials for enhanced corrosion resistance and mechanical properties. Such coatings are referred to as anti-corrosive cementitious coatings. Vaysburd and Emmons (2000) note that the effective performance of anti-corrosive cementitious coatings will not decrease the bond strength significantly, while still maintaining high alkalinity to resist corrosion. Hence, this coating system serves as a probable solution to restore the lost bond in repairs that results from the damaging effects by reinforcement corrosion (Kamde and Pillai, 2020). Polymer-modified cementitious coatings have been of recent interest due to their high functionality, which includes (i) creation of a physical barrier to protect the steel from transport of aggressive species that may initiate corrosion and (ii) hinders ionic flow between the anodic and cathodic regions. In this way, the corrosion resistance of cement-based coatings is enhanced. When comparing untreated and cementitious coated rebars, the angle of the resultant force, from friction and bearing components, is reduced by the presence of cementitious coatings along the bar surface (Natino *et al.*, 2021).

2.6 Performance of coatings

2.6.1 Uncorroded coated steel

The performance of cementitious based coatings, modified for corrosion resistance, has been investigated but knowledge on how well the coated steel bonds to the surrounding concrete is limited. The thickness effect of cementitious coating causes accumulation of the material in the corners between ribs, reducing the relative rib area and hence the ultimate bond strength, shown in Figure 14.

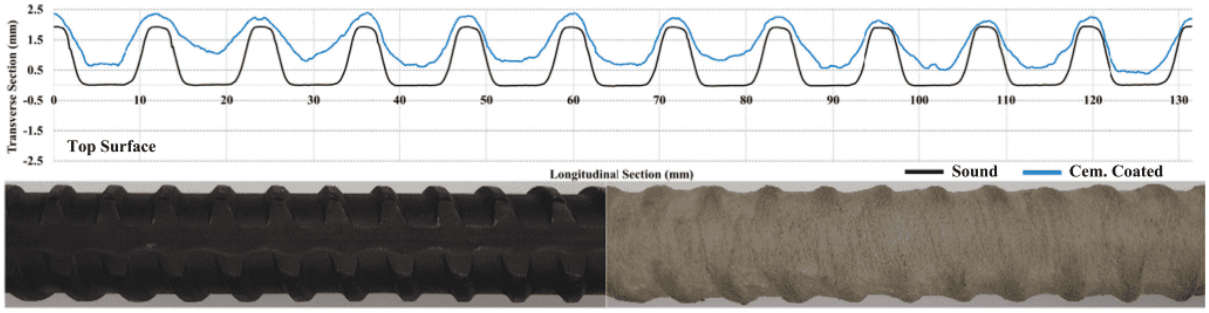

Figure 14: Effect of cementitious coating on rib area of uncorroded steel reinforcement (Natino et al., 2021)

Cementitious coatings affect two properties of uncorroded steel bars, surface roughness and relative rib area, which are parameters that considerably affect the bond strength (Natino *et al.*, 2021). The cementitious coating, when applied, results in an uneven surface due to its low workability. Cementitious coatings possess a high viscosity and, therefore, leads to a low workability during application, making it difficult to achieve the coating thickness desired. Due to the nature of cementitious coatings, the surface roughness compared to untreated steel is enhanced.

2.6.2 Corroded coated rebar

When corrosion occurs, the cross-sectional diameter of the steel along with its ribs deteriorates and reduces in height. This affects the mechanical interlock of the bond as corrosion changes the surface profile of the bar. A typical repair scenario requires the cleaned corroded steel to be coated, which further reduces the relative rib area along the steel shown in Figure 15.

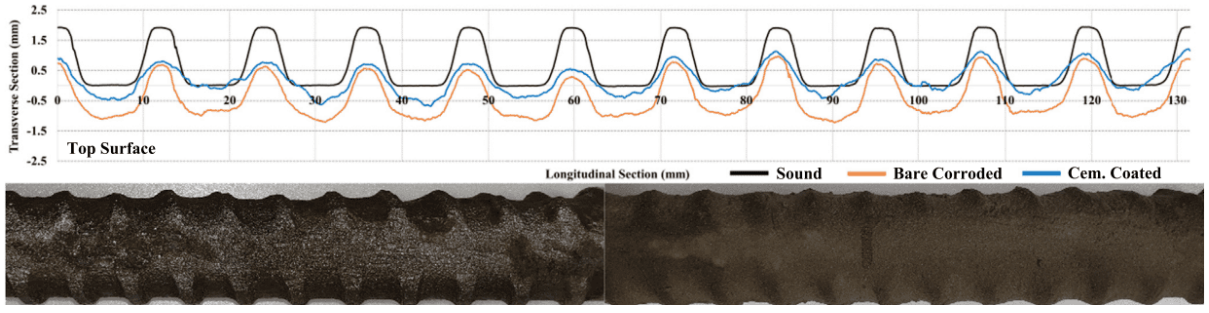

Figure 15: Effect of cementitious coating on rib area of corroded steel reinforcement (Natino et al., 2021)

Figure 16 depicts the average bond strengths achieved by pull-out testing of a variety of commercial repair systems presented by Jorge, Dias-da-Costa and Júlio (2012).

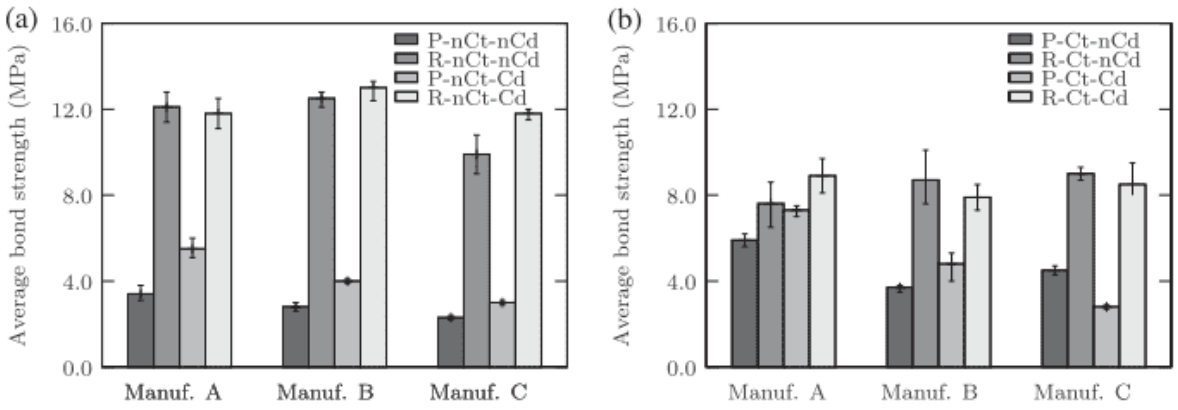

Figure 16: Bond strength pf uncoated (left) and coated (right) series for plain (P) and ribbed (R) rebar with cementitious coatings - coated (Ct), uncoated (nCt), corroded (Cd) or uncorroded (nCd), (Jorge, Dias-da-Costa and Julio, 2012)

The repair systems included cement-based epoxy-modified resin, cementitious mineral and synthetic resin coatings on plain and deformed steel bars, corroded to 5% and 3% mass loss, respectively. Coating thicknesses of 1.8 mm and 1.5 mm were applied to the plain and deformed bars, respectively, recommended by manufacturer specifications. In this investigation, repair concretes including cementitious grout with silica fume, fibre-reinforced plain cement and a hydraulic binder with silica fume were considered. Three combinations of a single coating and repair mortar was adopted, namely Manufacturers A, B and C. For the uncoated steel, the initial bond failure mechanism in plain bars was controlled by adhesion loss whereas for deformed bars it was governed by mechanical interaction of the ribs and concrete. For plain bars, the bond strength was observed to increase by application of the coating due to an enhanced surface roughness (Jorge, Dias-da-Costa and Júlio, 2012). Hence, anti-corrosive cementitious coatings should be applied to plain bars, as this would strengthen the frictional component of the bond. For deformed bars, however, the use of these cementitious coatings reduced the bond strength by up to 40% of the original capacity (Jorge, Dias-da-Costa and Júlio, 2012). This observation was, however, for a low corrosion degree of 3% steel mass loss. Natino *et al.*, (2021) investigated the effect of anti-corrosive coatings on the bond behavior of repaired rebar at higher corrosion levels. Figure 17 displays the bond-slip curves for anti-corrosive cementitious coatings used on bars corroded up to 13% steel mass loss.

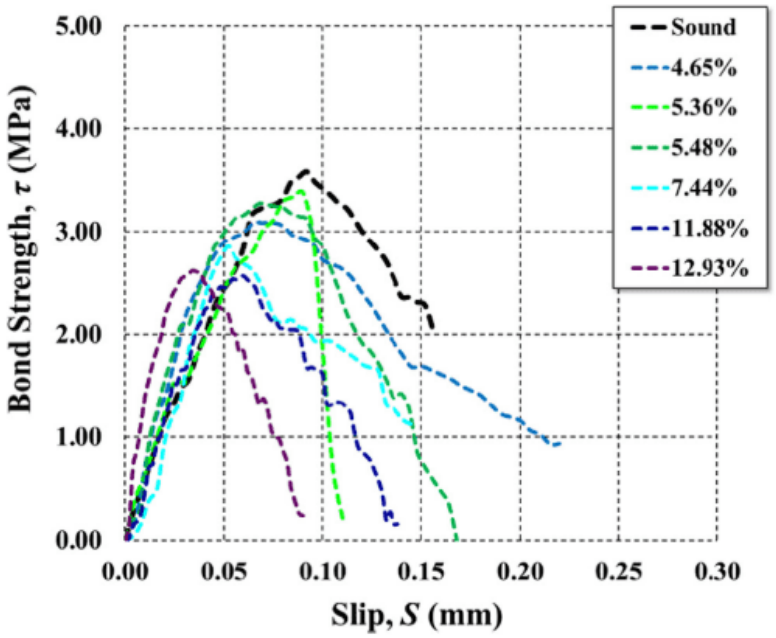

Figure 17: Bond-slip relationship for cementitious coatings on corroded steel (Natino et al., 2021)

Two-end pull-out testing was conducted to investigate the bond-slip behavior of a commercial polymer-modified cement slurry coating and an epoxy coating on corroded specimens. One coating application of 1 mm (recommended by the manufacturer) was performed. Ordinary Portland cement was used for the repair concrete with a 14-day compressive strength of 40 MPa. The results showed that as the degree of corrosion increased, the ultimate bond strength of the coated rebar reduced, and there was also less slippage of the bar, suggesting more abrupt failure of the concrete. Shearing of the surrounding concrete with bar slip caused a rapid decrease in the bond stress till approximately 80% of the original bond capacity. Furthermore, the residual strength between the crushed concrete surrounding the rebar, as a result of shearing of the bar, causes a gradual decrease in the bond stress-slip curve. Natino *et al.* (2021) concluded that polymer-modified cementitious coatings can restore the bond strength up to 70% of its original capacity at about 12% steel mass loss.

2.7 Summary of literature review

This chapter introduced aspects related to the bond between steel and concrete, factors affecting the bond, and the resulting damage due to corrosion. Repair methods were also discussed and the influence of coatings on the bond between cleaned corroded steel and repair materials.

The bond allows for transfer of load between the steel and concrete and is important to the structural capacity of reinforced concrete members. The bond mechanism is characterized by

three forces, namely chemical adhesion between the steel and concrete, friction and mechanical interlock. The mechanical interlock component is responsible for most of the bond between deformed bars and concrete, due to the presence of ribs. The ribs comprise the relative rib area, which offers bearing forces to the surrounding concrete, and plays a significant role in resisting slippage of the bar when loads are applied.

The main factors that affect the bond between steel and concrete includes the diameter relative rib area of the bar and the compressive strength of the surrounding concrete. As the bar diameter increases, the bond strength decreases due to an increased surface area of the steel. This relates to a higher pull-out force, but a lower bond strength according to Equation 1. Furthermore, for larger bars, the ITZ between the steel and concrete is thicker, due to more water contained between ribs (Teresa *et al.*, 2008). The bond strength will increase with a greater relative rib area on the steel surface (Metelli and Plizzari, 2014). Lastly, the compressive strength of the concrete has a direct influence and is proportional to the bond strength.

When corrosion occurs, a positive effect on the bond strength is usually observed up to a corrosion degree of 5% steel mass, where the bond strength can increase by as much as 13% compared to uncorroded steel (Almusallam *et al.*, 1996). As corrosion continues to higher stages, though, the effects become detrimental to the bond, which is an important aspect to consider when repair of corrosion damaged steel takes place. Patch repairs are often conducted where the defective concrete is removed, followed by cleaning of the steel and subsequent application of a suitable coating. The function of this coating is to provide corrosion control to the steel, but should also act to provide adequate bond between the corroded repaired steel and repair material, as the bond strength can be significantly reduced by corrosion damage.

In the concrete repair industry, engineers follow guidelines from recognized standards such as EN1504. This comprehensive standard, as well as the available literature lacks guidelines on how to assess the bond of corroded repaired steel and repair materials when coatings are used, which is an important aspect to consider for the structural capacity of repaired concrete members.

There exist various rebar coatings that are commercially available for use in new construction and for repair of corroded steel. The available literature, however, suggests a lack of information concerning the use of these coatings and how they may affect the bond between cleaned corroded rebar and concrete repair materials. One of the coating types commonly used

is a barrier coating with a cementitious base, but often modified with polymers for enhanced corrosion resistance. Jorge, Dias-da-Costa and Júlio (2012) showed that cementitious coatings increase the bond for plain bars, however, they can reduce the bond of uncorroded deformed bars by as much as 40%, although no detailed explanation for this observation was provided. Natino *et al.* (2021) demonstrated that applying a cementitious coating reduced the bond strength of uncorroded steel due to the accumulation of the coating in the corners between the ribs of the steel, which affects the mechanical interlock component of the bond. The bond strength was reduced by 70% due to corrosion at 12% steel mass loss.

From the available literature, it is noted that the bond is negatively affected by corrosion and cementitious coatings have been found to reduce the bond between concrete and cleaned corroded steel. There is, however, no information on how the thickness of the coatings affect the bond between steel (both uncorroded and cleaned) and concrete. In addition, the application of cementitious coatings to corroded rebar at higher corrosion degrees has not yet been investigated. Engineers also require information pertaining to the use of these cementitious coatings, when used in combination with common bar sizes and repair material properties. An investigation into the above-mentioned factors is thus needed to better understand the bond between cleaned corroded steel and cementitious repair materials. In doing so, a basis can be provided onto which the structural capacity of corroded coated steel can be evaluated.

3. Experimental methodology

3.1 Overview

The experimental approach for this investigation considered an epoxy-modified, cementitious coating (Sika ® Armatec ® -110- EpoCem) that was applied to uncorroded and corroded (simulated) steel bars of varying cross-sectional diameter (Y12 and Y16). Corrosion damage was simulated to 10% and 20% steel mass loss using an angle grinder. Thereafter, the steel was coated with either one or two coats, with each coat being 0.6 mm thick. The different repair materials considered in this study included one concrete with a w/b ratio of 0.45 and two mortars with w/b ratios of 0.47 and 0.65, referred to as C45, M45 and M65, respectively. The specimens were cured for a duration of 7 days before pull-out testing. The experimental tests carried out in this study are shown in Table 1. Four specimens were tested for each result to avoid errors from atypical samples.

Table 1: Experimental tests

Test type	Purpose	Standard
Compressive strength	Characterizing the repair mixes	SANS 5863 (2006)
Pull-out testing	Analysis of the bond behavior of pull-out specimens	SANS 920 (2011)

3.2 Experimental program

The control specimens for this study included the untreated, uncorroded reinforcement bars. This control allowed the effect of the coating thickness to be analysed independently, with each repair material and bar diameter. Furthermore, the parameters are not interrelated and act in in isolation due to uncorroded specimens representing new construction cases, whereas corrosion and coated specimens represent repair scenarios.

From the results obtained for each tested group, the parameters (bar diameter, corrosion degree, repair material) could be compared for the different specimen arrangements (Table 2) with respect to the main tested variables i.e., coating thickness. Figure 18 depicts the experimental procedure adopted for this study.

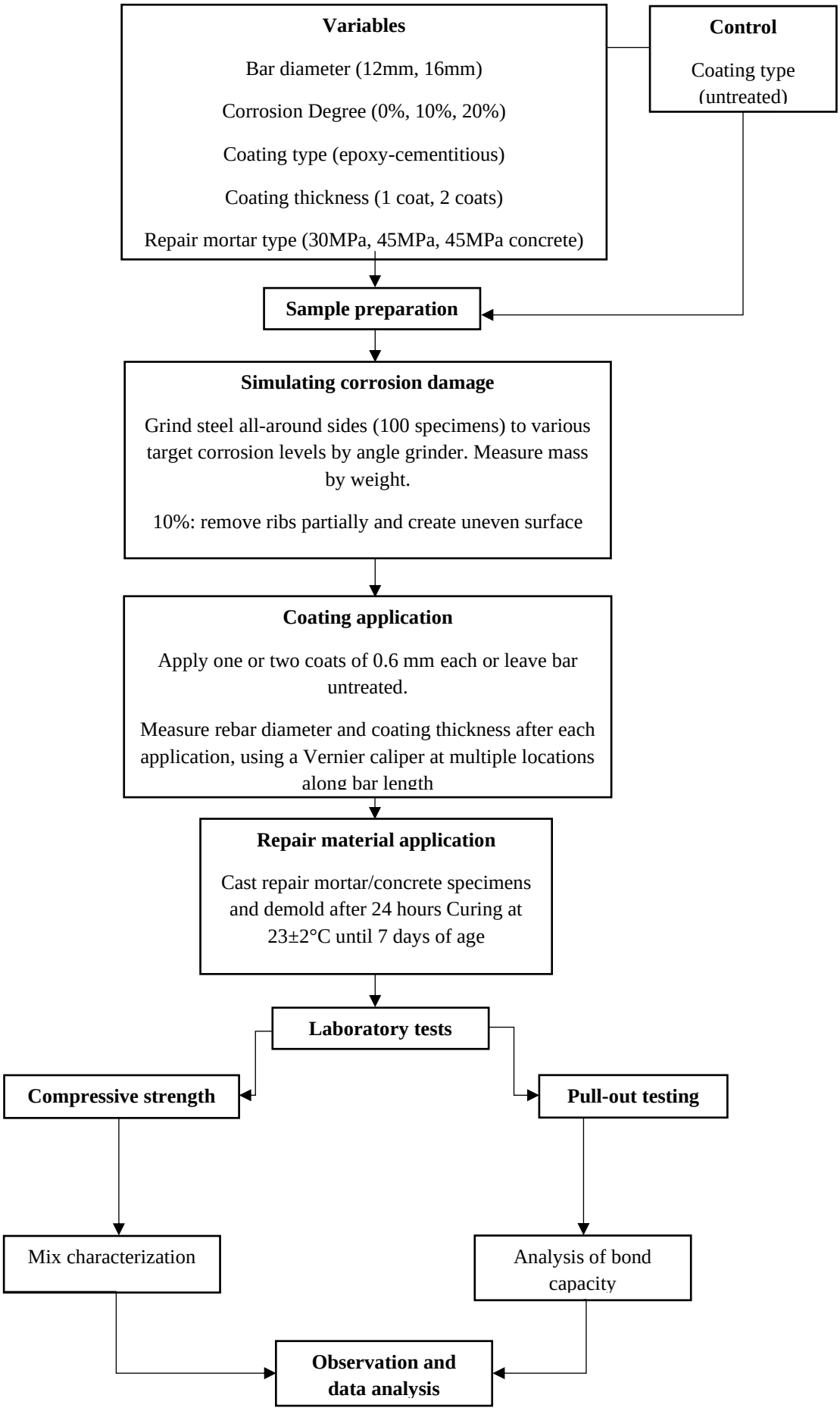

Figure 18: Experimental tests

3.3 Experimental parameters

The experimental parameters for this study is presented in Table 2.

Table 2: Combined parameter arrangement

Bar diameter	Corrosion degree	Coating	Repair material
12 mm	0%	Untreated	M65
			M45
			C45
		One coat	M65
			M45
			C45
		Two coats	M65
			M45
			C45
	10%	Untreated	M65
		One coat	M65
		Two coats	M65
	20%	Untreated	M65
			M45
			C45
		One coat	M65
			M45
			C45
		Two coats	M65
			M45
			C45
16 mm	0%	Untreated	M65
		One coat	M65
		Two coats	M65
	20%	Untreated	M65
		One coat	M65
		Two coats	M65

The effects of rebar diameter on bond strength have already been addressed by previous researchers, as well as the effects of w/b ratio, and low corrosion levels of 10% steel mass loss. Hence, it was decided to assess the performance of the coating at all corrosion levels and both bar diameters for the normal strength mortar M65. The performance of the higher strength mortar and concrete was assessed for the 12 mm diameter bar only, in the uncorroded state and 20% steel mass loss, as this study is largely focused on the coating's performance at high corrosion degrees.

3.3.1 Corrosion degree

Corrosion has a significant effect on the bond strength due to the destruction of the ribs and a reduction in cross-sectional diameter of the deformed rebar (Lin et al., 2019). Target corrosion levels of 10% and 20% of steel mass loss were chosen to simulate corrosion damage and present a scenario in which in-situ deteriorated structures would require repair.

Corrosion degrees higher than 20% of steel mass loss would result in a significant reduction in the steels cross-sectional area, meaning the steel would likely be replaced in practice. In addition, the performance of cementitious coatings used on corrosion-damaged steel of a more severe nature i.e., higher corrosion degrees than 10% (Natino et al., 2021), has not yet been investigated. It was therefore decided to mainly investigate the effects of the coating on 20% corroded steel, by checking the performance of all three repair materials i.e., M65, M45 and C45. For the 10% corroded steel, only M65 was considered based on the aims of this research and limitations to the number of tested parameters.

3.3.2 Coating thickness

The selected product was Sika ® Armatec ® -110- EpoCem (Epoxy-modified, cementitious), which is a typical coating used in repair application (Mackechnie and Alexander, 2001). The composition of the coating includes Portland cement, epoxy resin, fine aggregates, and additives. This coating type is commonly used in South Africa but little information on the bond strength characteristics between concrete and steel in new construction and repair scenarios exists.

According to the product manual, this coating has excellent adhesion to concrete and steel and is an excellent bonding bridge for cement or epoxy-based repair mortars. The coating is also marketed as a material with high shear strength and high resistance to water and chloride penetration. The product manual recommends applying two coats of 1 mm thickness each. It

was expected that the thickness of the coating may impact the bond negatively, hence it was decided to apply a coating thickness of 0.6 mm per coat.

3.3.3 Repair materials

Three repair materials were considered to represent suitable repair mortars/concrete with OPC cement. A type CEM I 52.5N Ordinary Portland Cement (OPC) was chosen as the binder for both mortars and the concrete. This cement is locally produced, and a common cement type used in South African RC structures. A w/b ratio of 0.47 and 0.65 was chosen for the mortars. The two w/b ratios for the mortars were selected to identify how the chosen coating performs in combination with a normal and high strength repair mortar, respectively. One concrete mix, with a w/b ratio of 0.45, was considered to investigate the effects of coarse aggregate on the bond performance.

3.3.4 Rebar diameter

The relative rib area has a large influence on the bond in uncorroded deformed bars (Metelli and Plizzari, 2014). Two different bars were chosen for this study, which includes 12 mm and 16 mm diameter deformed high-yield steel bars, known as Y12 and Y16. These bar configurations were in accordance with SANS 920:2011 and were chosen as they represent the most common bar types used for reinforced concrete in South African RC structures.

3.4 Mix design and constituents

The mix design proportions for the three repair materials chosen is displayed in Table 3 and material quantities used are provided in Appendix A.

Table 3: Mix design proportions

Mix ID	M65	M45	C45
w/b ratio	0.65	0.47	0.45
CEM I 52.5N	465	640	411
Water	300	300	185
Fine aggregate (dune sand)	738	650	426
Fine aggregate (crusher sand)	738	650	426
Coarse aggregate (19 mm Greywacke)	-	-	1040
Flow/Slump (mm)	570 - 630	530 - 550	85 - 90

The concrete mix design adopted for the corroded specimens was performed in accordance with the Cement and Concrete Institute (C&CI), using the volumetric mix design method (Ballim, Alexander and Beushausen, 2009). Before casting of the specimens, trial mixes were performed to determine the water content for the three mixes used in this study. The detailed results for the two trial mixes performed is provided in Appendix F.

A 50/50 blend of Philippi dune sand and greywacke crusher sand was chosen for the fine aggregates in the repair mixes. This blend was considered as the dune sand contributes to better workability due to its rounded shape and smooth texture (Ballim, Alexander and Beushausen, 2009), while the crusher sand compensates for the lack of smaller particles from the dune sand. A sieve analysis for the 50/50 blend of dune and crusher sand was carried out in accordance with SANS 201:2008.

For the sieve analysis, the dust content in the selected sample was removed by wet sieving, as recommended by the standard. The grading curve for the fine aggregates is shown in Figure 19. The grading curves for the individual aggregates is provided in Appendix B. Only fine aggregates were used for the mortars, M65 and M45. The concrete C45 included Greywacke stone of 19 mm, which is commonly referred to as Malmesbury Shale in the Western Cape Province. Furthermore, mixes supplemented with stone aggregate for concrete can account for reduced costs associated with the repair material, especially when large sections are restored (Morgan, 1996).

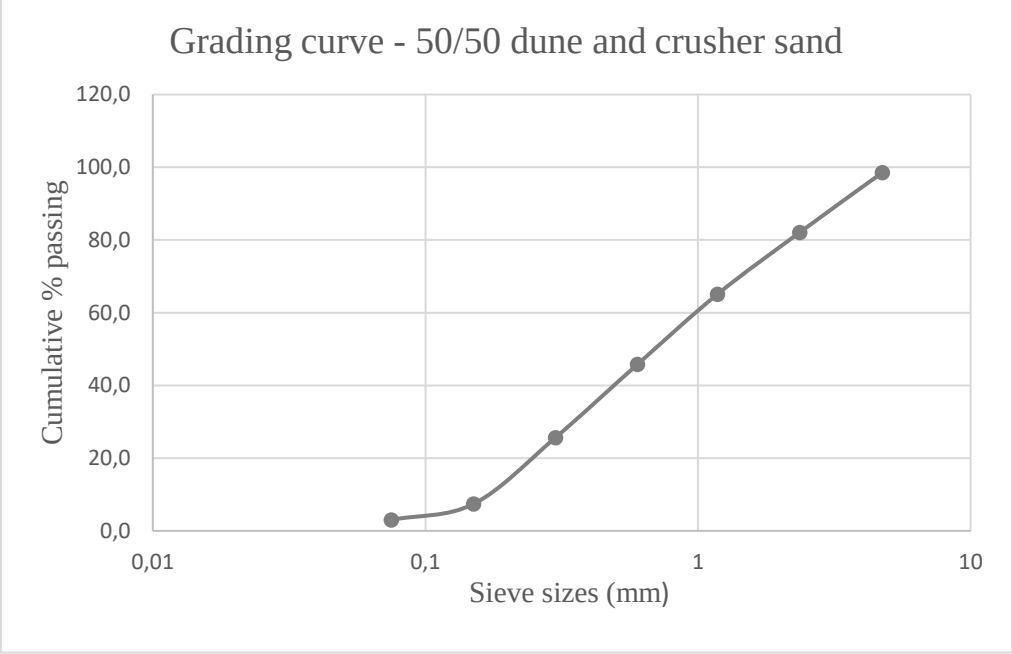

Figure 19: Grading curve for fine aggregate

3.5 Steel preparation

Corrosion was simulated using an angle grinder. The condition of the steel surface was analysed and measured by weight loss using a digital scale to an accuracy of 0.1 g. This method of corrosion damage simulation was chosen due to time constraints and was considered to not significantly deviate from natural corrosion damage. Hence, the state of the steel surface should represent that of a corroded cleaned bar, after the rust has been removed. To achieve a desired corrosion degree of an equivalent 10% mass loss, some of the ribs were removed and an uneven surface created, shown in Figure 20. For 20% mass loss, all the ribs were removed, and an uneven surface created, shown in Figure 21. To accurately remove the correct amount of steel, the bars were grinded and weighed continuously until they were ± 1.5 % steel mass loss from the respective corrosion target levels. Furthermore, when all the ribs were removed the surface profile of the steel was smooth and similar to a plain bar, hence it was decided to create minor indentations along the bar surface to represent chloride -induced corrosion damage. The mass of the grinded steel bars used in this study is provided in Appendix C.

Figure 20: 10% cleaned corroded steel

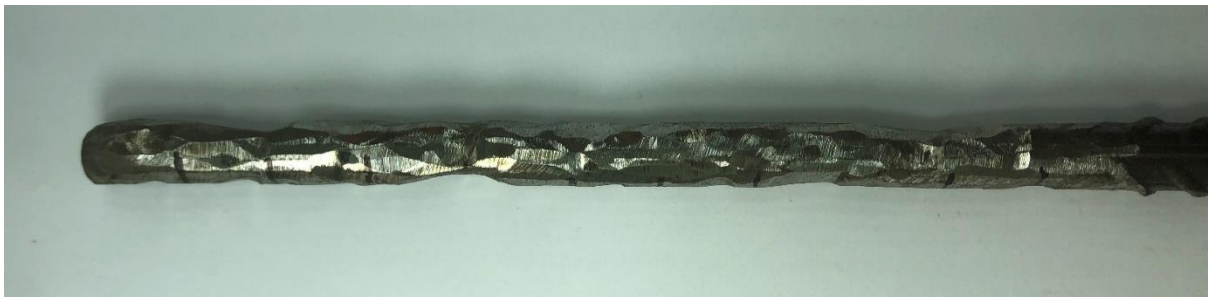

Figure 21: 20% cleaned corroded steel

3.6 Coating application

The coating was applied using a paint brush to the steel that was secured in a vice grip, shown in Figure 22. The time interval between applying the first and second coat was 2 hours, while the repair material was placed after 2 hours of drying of the coating. The average coating

thickness of the bars was measured using a Vernier Calliper, as seen in Figure 22. Readings were taken at 15 mm intervals along the length of the steel by comparing the diameter of the uncoated bar to the coated bar at the same location. The detailed rebar diameter measurements and coating thickness measurements for each bar can be found in Appendices D and E.

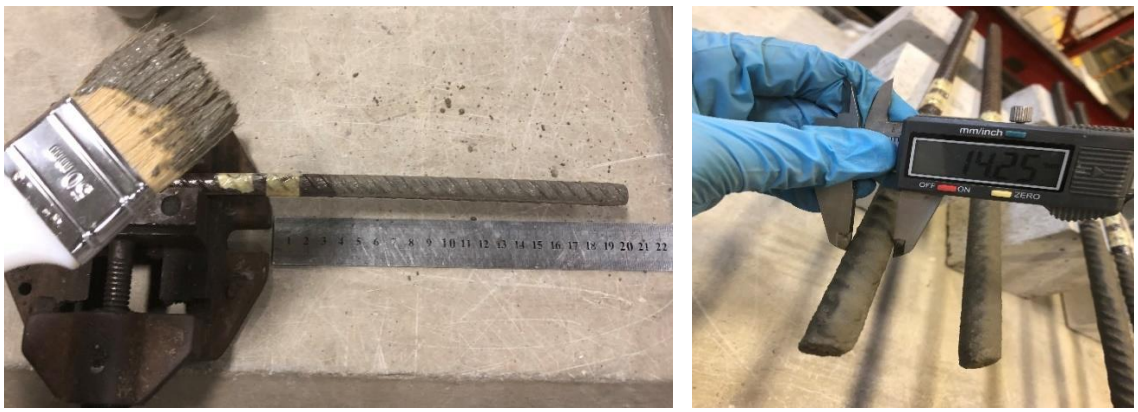

Figure 22: Coating application and thickness measurement

3.7 Mixing, casting, and curing

Mixing of the mortar and concrete was conducted by firstly mixing the dry materials sufficiently, thereafter, adding small quantities of mortar to the mix in increments till the desired workability of the mix was achieved. The mixing of fresh mortars and concrete was performed in accordance with SANS 6255: 2006 and SANS 5861-1: 2006, respectively. Before the fresh mixes were placed into moulds, see Figure 23 (a), their workability was assessed by means of the slump test for concrete and the flow test for mortars, which was conducted in accordance with SANS 5862-1:2006 and SANS 5862-2:2006, respectively. Figure 23 (b) displays the spread from M65 mortar of high workability from the flow test.

Figure 23: (a) Plastic mould, and (b) mortar flow

The specimens used for this investigation were cast in 150 x 150 x 150 mm cubic specimens for pull-out testing and 100 x 100 x 100 mm cubic specimens for compressive strength testing. Once the repair material was placed into the moulds, the rebar was positioned perpendicularly to the top surface of the pull-out specimen and left to cure in laboratory conditions for 24 hours before de-moulding. Adequate compaction was achieved by means of a vibrating table for a duration of 10 seconds for the concrete (C45), five seconds for the higher strength mortar (M45) and no compaction for the low strength mortar (M65), due to its high workability. Once the repair concrete was placed, compacted, and demoulded after 24 hours, the specimens were cured in a moisture curing tank until seven days of age to obtain the pull-out specimens for testing, shown in Figure 24. The specimens were cured until 7 days of age to shorten the testing period. The ACI Committee 301 suggests that 70% of the compressive strength is achieved after 7 days age.

Figure 24: Test specimens after demoulding and curing

3.8 Experimental tests

3.8.1 Compressive strength testing

The compressive strength of the different repair materials was conducted for the purpose of mix characterization. Three specimens were tested after 7- and 28-days age, to monitor strength gain. The compressive strength test was performed in accordance with SANS 5863:2006. The cubes were removed from the curing tank, followed by lightly wiping their surfaces of water before to determine the mass of each specimen in a saturated state. The specimens were placed back into the curing tank to maintain a saturated state for the compressive strength test. The specimens were placed on one of its sides and aligned directly on the centre of the base plate of the Amsler testing machine to ensure a uniform load distribution.

3.8.2 Pull-out testing

The pull-out test is a well-known method that has been used successfully to assess the bond strength between steel and concrete. RC specimens are cast with an embedded steel rod in the centre of the mould. This involved testing the tensile pull-out force between a cast-in reinforcing bar and concrete. The maximum load is measured as the load corresponding to failure of bond between the steel and concrete. Figure 25 (a) displays the Dension Universal Testing Machine used for pull-out testing. The pull-out test was carried out with a carbon steel chamber (16 mm plates) constructed and used for placement and fitting of the pull-out specimens, displayed in Figure 25 (b). A tensile load was applied to the steel manually in increments to carefully achieve a constant load rate of 0.1 MPa/s.

Figure 25: (a) Pull-out test machine (left), and (b) Specimen arrangement (right)

4. Results and discussion

This chapter provides the results obtained for the experimental tests described in Chapter 3. A detailed discussion on the compressive strength and pull-out force results are presented. Statistical analysis was performed to determine whether there was any significant difference between the mean pull-out force of the different tested parameters i.e., degree of corrosion (0%, 10%, 20% steel mass loss), coating thickness (untreated, 1 coat, 2 coats), bar diameter (12 mm, 16 mm) and repair material (M65, M45, C45). This provided a basis to make observations and decisions concerning the effect of coatings on the bond strength of corroded repaired specimens.

4.1 Compressive strength

The compressive strength was determined for the three mixes used in this study. This included a total of nine batches that were casted, consisting of two mortars (M65 and M47) and a concrete (C45). For each batch, three cubes each were tested after 7 and 28 days to determine the compressive strength development of the repair materials. The detailed compressive strength results for each batch are provided in Appendix F. Figure 26 shows the average compressive strength for M65, M45 and C45 at 7 and 28 days. The values for M65-12 represent the average compressive strength of five 45 L batches, whereas M45-12 and C45-12 displays the average compressive strength of two 45 L batches each.

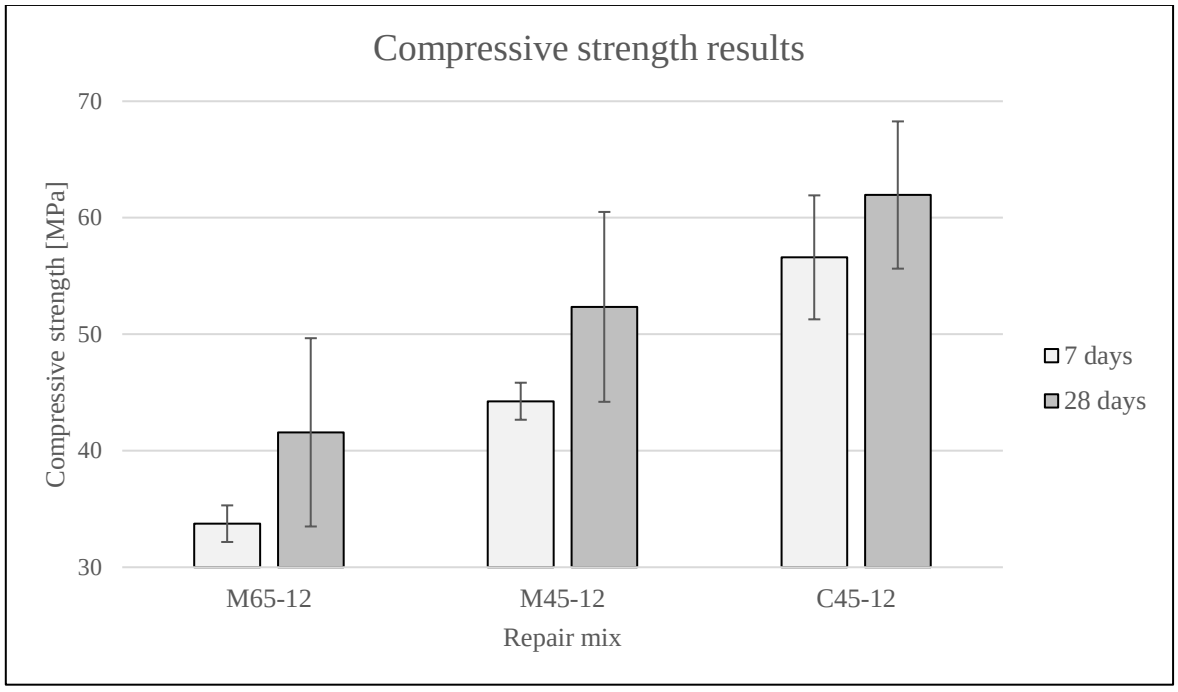

Figure 26: Average compressive strength results for each mix

The average compressive strength of M65 ranged between 32 – 36 MPa at 7 days age. Comparing this to M45, where the compressive strength ranged from 42 – 46 MPa, there was a clear increase in compressive strength as the w/b ratio was lowered for the mortars. As the w/b ratio decreased, the permeability was lowered which provided a stronger matrix structure. Mix C45 displayed strengths in the range of 51 – 62 MPa, which was considerably higher than M45 due to the presence of coarse aggregate in the mix. The aggregate is the strongest component in a concrete mix and offers enhanced dimensional stability to the material. The degree to which coarse aggregate affects strength, depends on the strength of the concrete which means that for stronger concretes, the influence of aggregate is more pronounced (Ballim, Alexander and Beushausen, 2009). Mix C45 with a w/b ratio of 0.47, similar to that of M45, displayed compressive strengths above 50 MPa at 7 days age, with values exceeding 60 MPa at 28 days.

Curing of the specimens for a longer period had a direct influence on the compressive strength of all tested mixes, indicating a stronger concrete/mortar with increasing age. This is because curing promotes the hydration reaction (Ballim, Alexander and Beushausen, 2009). The strength at 7 days age as a percentage of the 28 days compressive strength was 81%, 85% and 91% for M65, M45 and C45 respectively. It can be seen therefore that the strength gain for concrete is quicker than for the mortars.

4.2 Pull-out test results

4.2.1 Introduction and summary of results obtained

To analyse the bond strength of uncorroded pull-out specimens, Equation 1 is applicable. However, in a repair scenario where corrosion resulted in a variable diameter along the steel surface, Equation 1 could not be used. With the coating being applied to the cleaned corroded steel, there is an additional component that comprises the bond between reinforcement and repair material. Previous researchers calculated the bond strength by measuring the end-to-end stress of the rebar (Natino *et al.*, 2021). Such measurements have not been considered for this investigation; hence it was decided to interpret and analyse the pull-out failure loads instead to provide a more accurate and direct comparison of the differences caused by corrosion and the coating in relation to the various repair materials and bar diameters used. The detailed pull-out test results are provided in Appendix G and the statistical approach adopted for analysis of the results is described in the next section.

4.2.2 Analysis of pull-out results

The pull-out test results were analysed to determine whether coatings have a significant effect on the pull-out force. Statistical analysis was carried out on each data set for the pull-out test results by adopting various statistical methods to identify meaningful trends in the data sets. The methods utilized for the analysis includes hypothesis testing alongside the analysis of variance (ANOVA) test.

Hypothesis testing entails forming a null hypothesis, which states that there is no significant difference in the mean values between two sets of observations. If the null hypothesis is rejected, the alternate hypothesis is accepted and states that there is a statistical difference in the mean values between two results. One-way ANOVA tests were performed to determine the statistical significance between the means of two variables. It must be noted that this test was chosen, as opposed to the two-way ANOVA test, due to the nature of the experiments carried out and the fact that the considered variables do not act collectively, but rather in isolation (new construction or repair scenario). The different corrosion levels represent different times in a structures service life i.e., new structures for uncorroded specimens and corrosion damaged structures requiring assessment and/or rehabilitation for 20% corroded specimens. Furthermore, the parameters pertain to changes in different components (steel-coating-concrete) that make up the bond. A one-way ANOVA was therefore chosen as suitable to observe changes to the bond strength between the treatment levels of each parameter i.e., the difference in mean pull-out forces between repair materials, corrosion degrees, rebar diameters and coating thicknesses.

This statistical test measures the p-value and indicates whether there is a significant difference between the mean of tested groups or not. For instance, an individual one-way ANOVA was performed on each mix to compare the influence of corrosion levels of untreated bars on the pull-out force. Further tests were carried out separately, to identify the effects of the coating thickness on the pull-out force with respect to different corrosion levels, bar sizes and repair materials. The acceptance or rejection of a null hypothesis depends on the significance level. This significance level is evidence of the percentage risk, which means to say there is a 5% chance that the statements associated with accepting or rejecting the hypothesis could be on the contrary. A p-value of less than 0.05 would indicate statistical significance, meaning the null hypothesis is rejected.

The null hypothesis for this study states that there is no significant difference in the mean pull-out force between untreated and coated specimens. The alternate hypothesis states that there is a statistically significant difference in the mean pull-out force between untreated and coated specimens.

Table 4 displays the dominant failure mode for the various parameters tested in this study. The most common failure mode, and number of failed specimens as such, is displayed in brackets. It must also be noted that the number in brackets is only an indication of how many specimens failed in that way, but the total number of failed with sheared coatings for the different tested sets are provided in Appendix H, along with the detailed failure mode of each specimen. The shaded areas refer to shearing of the coating observed on two or more failed specimens per test result. For coated specimens categorized with 'slip' failure, this was exclusively between the coating and rebar. For coated specimens with splitting failure, most of the coating remained attached to the steel. Discussions on the failure modes are presented in parallel with the pull-out test results in Sections 4.2.3 – 4.5.

Table 4: Failure mode summary

Repair mix	**C45**		**M45**		**M65**				
Bar diameter	**12 mm**							**16 mm**	
Corrosion degree	**0%**	**20%**	**0%**	**20%**	**0%**	**10%**	**20%**	**0%**	**20%**
Untreated	Splitting (2)	Slip (3)	Splitting /slip (2)	Slip (3)	Splitting (3)	Splitting (3)	Slip (3)	Splitting (4)	Splitting (2)
One coat (0.6 mm)	Slip (3)	Slip (4)	Slip (3)	Slip (4)	Splitting /slip (2)	Splitting /slip (2)	Slip (4)	Splitting (3)	Slip (4)
Two coats (0.6 mm each)	Slip (3)	Slip (3)	Slip (4)	Slip (4)	Slip (3)	Slip (3)	Slip (3)	Splitting (4)	Slip (3)

The specimen failure modes were categorized as either splitting of the repair material or slip of the rebar. Figure 27 (a) and (b) shows splitting and 15 mm slip from uncorroded rebar, respectively. Figure 27 (c) shows remnants of the uncorroded coated specimens after splitting failure.

Figure 27: Splitting (a), 15 mm slip (b), splitting with coating failure (c)

4.2.3 Repair material properties on pull-out force

Figure 28 displays the pull-out results for the uncorroded untreated specimens with different repair mixes. There was an increase of 18% in the pull-out force when the w/b ratio was reduced from 0.65 to 0.45 for the mortars (M65 and M45). This difference is significant, indicated by the p-value (0.004). M45 contained a higher cement content than M65 but had the same water content, which led to a higher pull-out strength for M45. As the strength of the mix increased, the bond strength also increased as a result of a lower porosity in the interfacial transition zone (ITZ) between the steel reinforcement and cement paste (Teresa *et al.*, 2008).

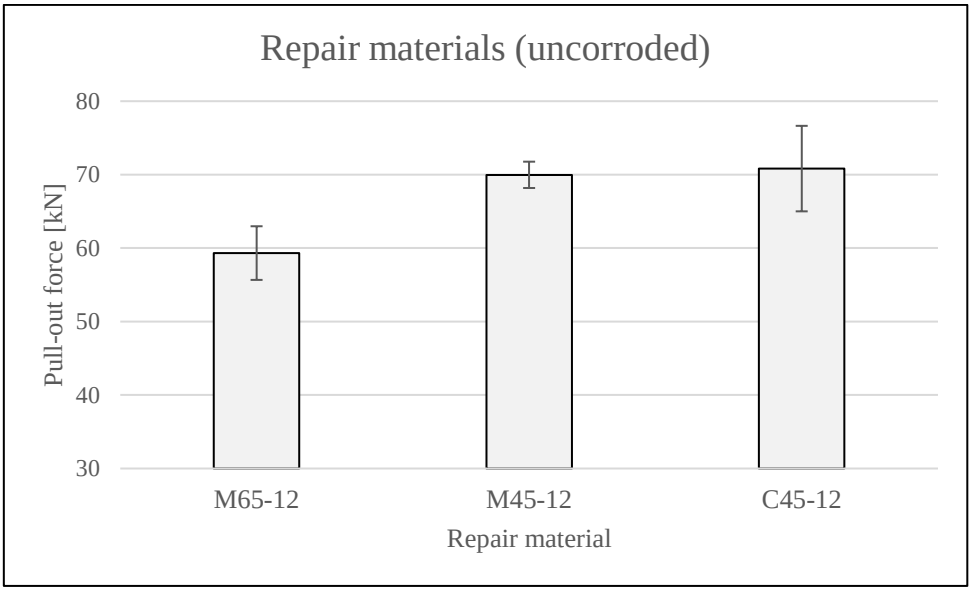

Figure 28: Pull-out test results for uncorroded specimens (Control)

In addition, a more dense ITZ gave rise to a higher bond strength between the concrete matrix and rebar (Bashir, Ansar and Muhammad, 2019). Furthermore, due to minimal compaction of the 'high flow' mortar, more air voids were observed on specimens with mix M65 after curing which could have also affected the compressive strength and therefore the pull-out strength

(Gao, Zhang and Zhang, 2015). The observation from this result shows the effect of compressive strength on the bond strength, and is supported by the findings from previous researchers (e.g., Wang, 1963). C45 specimens (w/b of 0.45) displayed the same average pull-out force than specimens of the mortar mix M45 (w/b of 0.47). The variability in results for specimens with mix C45 can be attributed to differences in stone content or arrangement in the different concrete specimens.

For the uncorroded specimens, splitting of the repair material was seen as the dominant failure mode for C45 and M65, due to bearing forces generated by the ribs on the surrounding repair material. In addition, M65 was also a weaker mix with more air voids present, which could have contributed to specimens with M65 splitting more frequently, than to the other two mixes. Comparing M45 and M65, the higher w/b ratio caused more splitting failure. Splitting occurred for two of the specimens with M45, which was due to the ribs. Slip of the rebar was recorded for the remainder specimens with M45 and could have occured as a results of the ITZ between the steel and mortar failing when the load increased. When slip occurs, the mechanical interlock is lost and the bond relies on friction between the crushed mortar and steel. Between M45 and C45, there appeared to be no influence from the addition of stone on the failure mode according to Appendix H.

4.2.4 Rebar diameter properties on bond strength

From Figure 29, the effect of rebar diameter is clearly seen where a larger bar diameter resulted in a higher pull-out force.

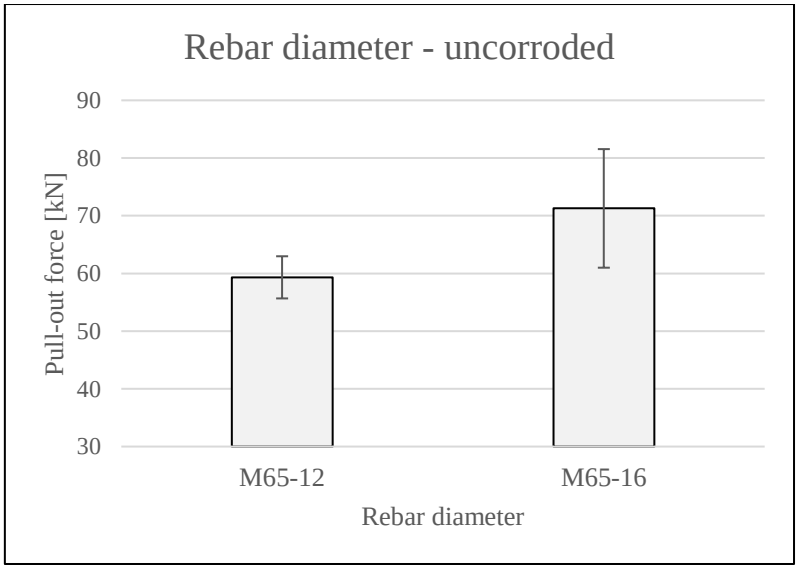

Figure 29: Pull-out test results for various bar diameters of M65

The M65-16 specimens showed a 20% higher pull-out force compared to M65-12 specimens. Khalaf *et al.* (2020) noted 26% increase in the pull-out force when the bar diameter was increased from 12 mm to 16 mm, similar to the results observed from this study. The difference in values between M65-12 and M65-16 is insignificant due to the variability in results, though, and is supported by the p-value (0.106) and overlapping error bars.

The presence of larger ribs on the 16 mm bars, compared to the 12 mm bars, increased the relative rib area (see Equation 2) between the steel and repair material for uncorroded specimens. As a result, the bearing forces increased, allowing greater mechanical interlock between the ribs and surrounding concrete when under load (Angst *et al.*, 2017; Metelli and Plizzari, 2014). Specimens with both bar sizes have w/b ratios of 0.65. Therefore, the low compressive strength in conjunction with larger ribs may have contributed to sudden splitting of the specimens during testing. This could explain the high variability seen for M65-16 results.

When considering the 16 mm bars, the failure mode was dominated by splitting of the repair material. The bearing forces generated within the surrounding concrete was higher for greater size bars, due to larger ribs that led to higher bearing forces in the repair material compared to 12 mm bars. Splitting was recorded at pull-out forces in the range of 52.7 - 70.8 kN. The variation could be due to a combination of factors, which may include rib size variation, load rate variation from manual application, and surface defects on the specimens. Specimens with 16 mm bars showed a 12 kN higher average pull-out force than the 12 mm bars. Furthermore, splitting failure occurred more often for the M65-16 specimens than for the M65-12 specimens, with slip of the rebar evident in some instances (see Appendix H).

It must be noted that the higher pull-out force from M65-16 over M65-12 discussed earlier in this section, does however relate to a lower bond strength when calculated in MPa, as the surface area of steel is inversely proportional to the bond strength, according to Equation 1. From the results, it is observed that as the bar diameter increased, the bond strength decreased, which is in agreement with the findings of previous researchers (Turk, Yildirim and Caliskan, 2003; Diab *et al.*, 2014).

4.2.5 Influence of coatings on uncorroded specimens

Figure 30 displays the average pull-out force for uncorroded 12 mm bars with mixes M65, M45 and C45 that were untreated, coated once or coated twice.

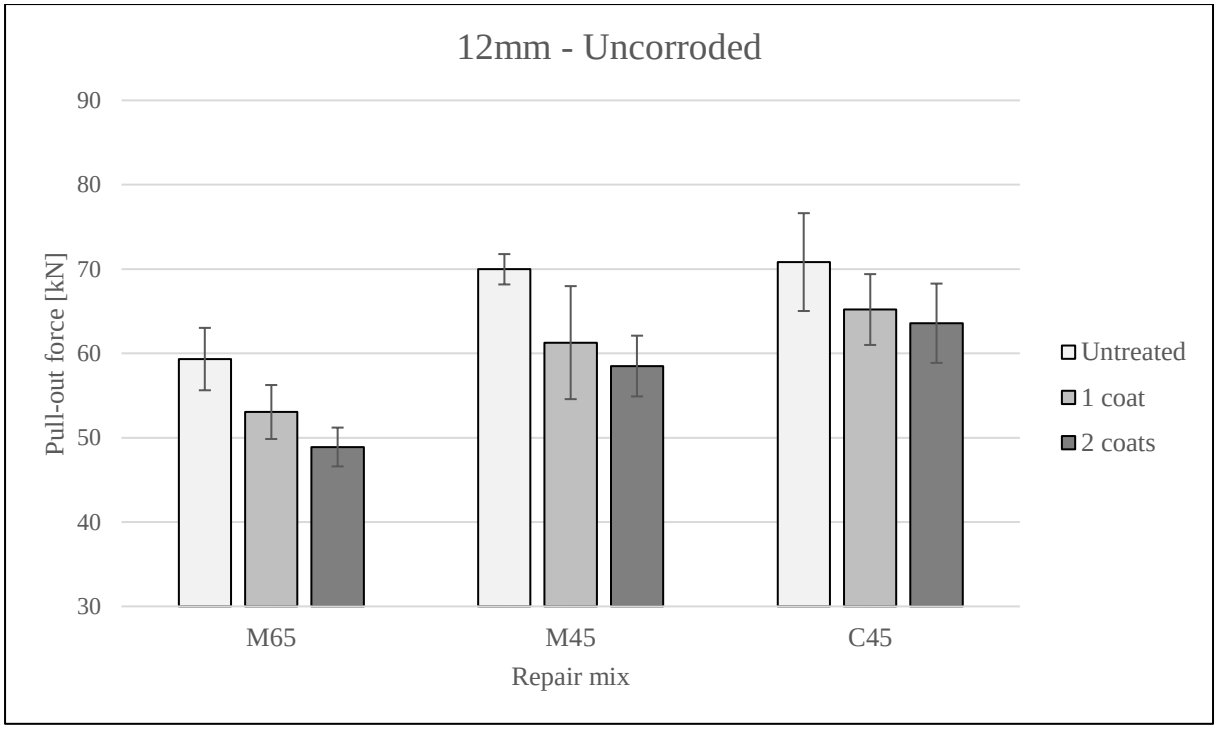

Figure 30: Pull-out test results for uncorroded specimens with 12 mm bars

Coating uncorroded bars was seen to have a negative effect of reducing the pull-out force between steel and concrete. Considering specimens from M65, there was a reduction of 11% in the pull-out force when one coat was applied to untreated bars. The variability in results, however, suggest no statistically significant difference when applying one coat. When two coats are applied, there is a further reduction of 7%, which is significantly different from the M65 control specimens. This is supported by the low p-value (0.006); therefore, the null hypothesis is rejected. The effect of the cementitious coating accumulating between ribs can be clearly seen in Figure 31. When coatings were applied to uncorroded deformed bars, the relative rib area was reduced due to the thickness of the cementitious coating, which tended to accumulate between ribs on the steel surface during application. The bearing area between ribs that comprises the mechanical interlock component of the bond was hence reduced. In this regard, applying one coat lowered the bond forces to the repair material due to a reduction in the relative rib area from the coated steel. When two coats were applied, the bearing area between ribs was further reduced, resulting in further smoothening of the interface between coated steel and concrete. Therefore, the pull-out force of uncorroded reinforcing bars was negatively affected by the coating. The findings in similar studies confirms this observation of cementitious coatings reducing the relative rib area (Natino *et al.*, 2021).

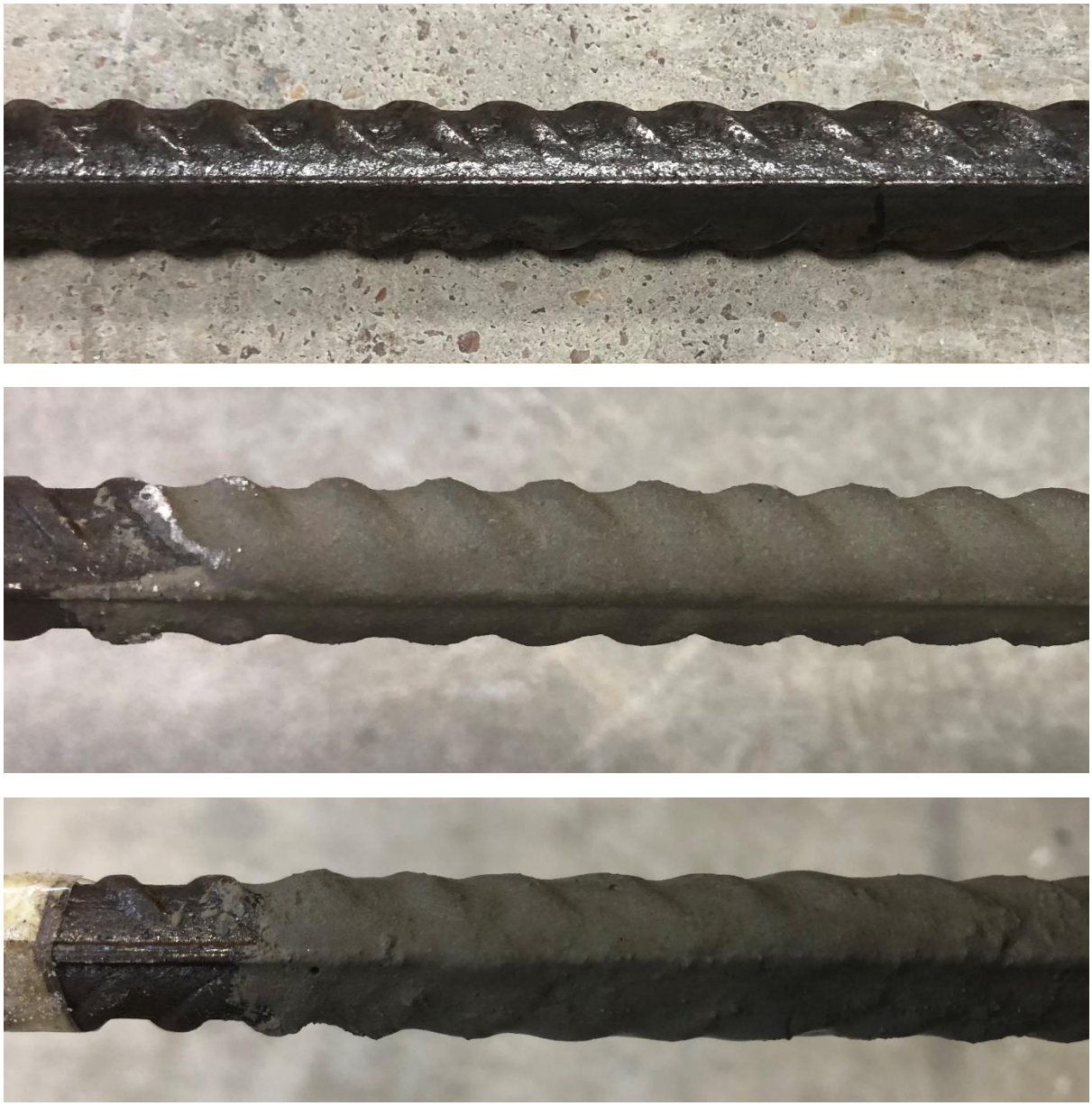

Figure 31: Uncorroded untreated 12 mm steel (top), one coat (centre), two coats (bottom)

For M45, the specimens with one coat experienced a 13% lower pull-out force than the untreated specimens, with a large variation in results for specimens with one coat. Due to this variation, there was no significant difference between specimens that were untreated or those that had received a single coat. This is supported by the p-value (0.07) which is above the threshold. When two coats are applied, there was a reduction of 16% in the mean pull-out force compared to M45 control specimens, however with less variation in the results. The low p-value (0.002) indicates a significant difference in the pull-out force when applying two coats to untreated bars with M45, hence rejecting the null hypothesis. Specimens with C45 that were coated once experienced an 8% lower pull-out force than the untreated specimens. When two

coats were applied, the pull-out force was the same. The variation in results suggest no significant effect of applying one or two coats to untreated bars, which is confirmed by the high p-values (0.2 for one coat and 0.1 for two coats). Hence the null hypothesis is accepted. The performance of M45 and C45 at all treatment levels (i.e., untreated, one or two coats) was similar. Comparing M65 and M45, there was no significant difference when one coat was applied, due to the high variation in results for M45. For two coats, however, there was a meaningful difference in pull-out force between these two mixes, confirmed by the low p-value (0.008). Between all three mixes, the thickness of the coating was seen to have no significant effect on the bond where the difference in pull-out force between coats was less than 10 kN on average for all mixes and bar sizes according to Figures 30 and 34.

For M65-12, slip and splitting failure was equally evident in the test sets for one coat. For two coats, slip of the coated rebar with shear failure was dominant. In general for each repair mix, when coatings were applied to uncorroded steel, the most common failure mode was by slippage of the bar with shearing of the coating. Compared to untreated steel (10 mm), the magnitude of slip was greater when the coating was applied (55 mm), as seen in Figures 32 (a) and (b) respectively. The relatively large slip for the coated specimens compared to the control corresponds to the reductions in pull-out force observed with the coated specimens.

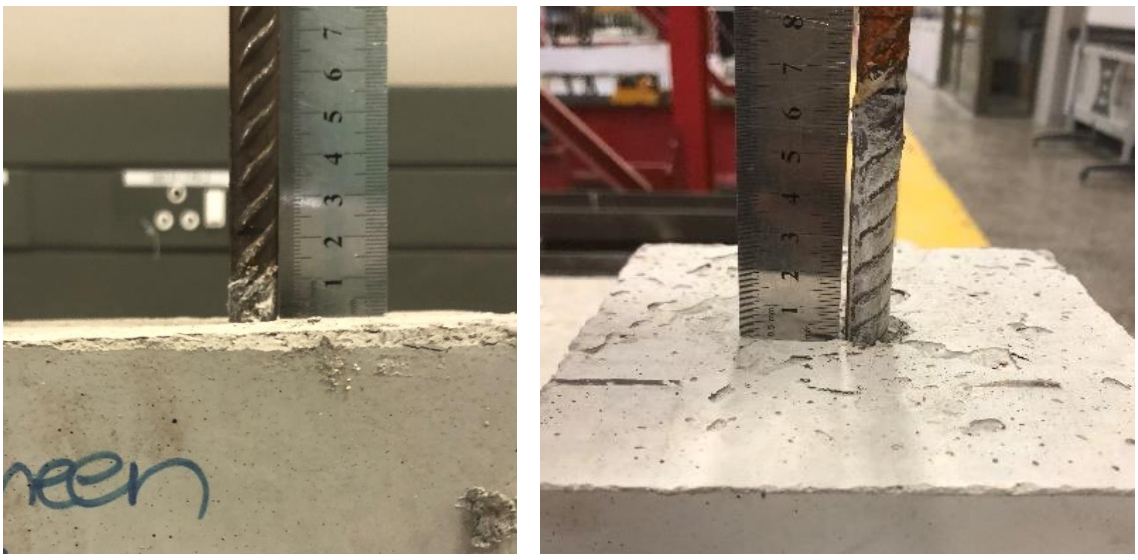

Figure 32: (a) Uncoated bar slip of 10 mm (left), and (b) coated bar slip of 50 mm (right)

The dark patterns on the concrete surface shown in Figure 33 were a result of the underlying ribs, which pulled through the coating material during loading. This can be explained by the compressive strength of the coating, which McClarty (2021) reported to be 25 MPa, while the different repair materials in this study (34 – 57 MPa). Hence, failure occurred within the coating

as the compressive strength of the repair materials was higher than the coating. Therefore, it can be assumed that the coating acted as a weak link between the steel and repair material.

Figure 33: Coating remains and concrete-steel interface after failure

Figure 34 displays the pull-out test results for the 12 mm and 16 mm bars with no corrosion and all coating treatments. The results for M65-12 have already been discussed at the start of Section 4.2.5.

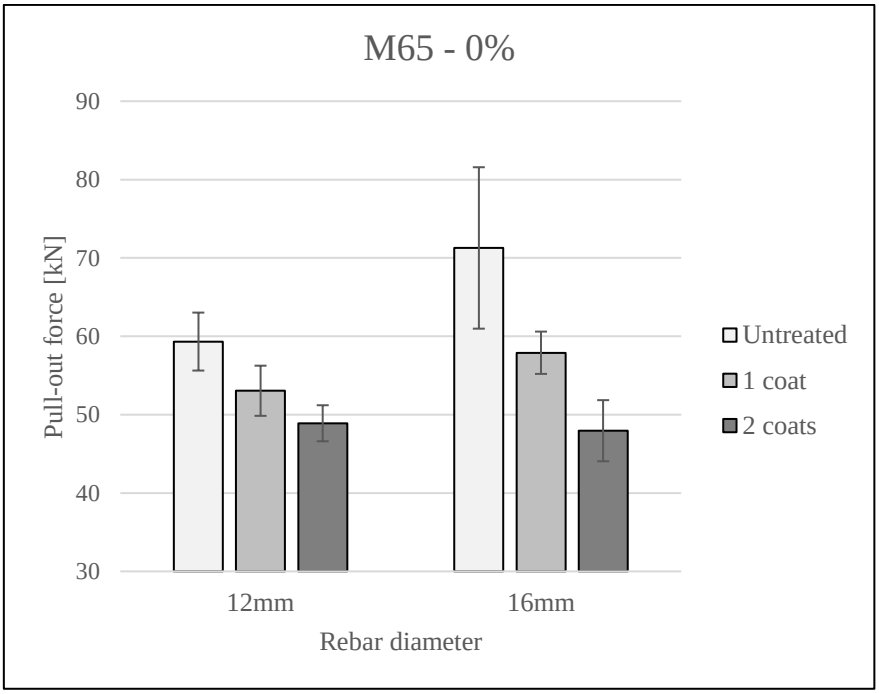

Figure 34: Pull-out test results for uncorroded M65-16

When one coat was applied to corroded 16 mm bars (M65-16), the results showed a decrease of 19% in the mean pull-out force compared to the untreated specimens. The p-value (0.07)

and overlapping error bars, however, suggests this result was not significant, hence accepting the null hypothesis. This can be explained by the presence of larger ribs, and that the first coating does not reduce the relative rib area severely. The same coating thickness that was applied to 12 mm bars (0.6 mm approximately) was used on the 16 mm bars with the larger ribs. Therefore, the coating does not accumulate between rib corners to the degree that it does with 12 mm bars. When the second coat was applied, there was a further reduction of 14% in pull-out force. This difference compared to the untreated specimens (33%) is significant and supported by the low p-value (0.01), rejecting the null hypothesis. This was due to more coating substance accumulating between ribs, which considerably reduced the relative rib area on the steel.

In this manner, coating on 12 mm uncorroded steel does not offer good resistance to pull-out as the bond forces are almost eliminated by the second coat. As highlighted at the end of Section 4.2.4, the variation in results for the untreated uncorroded 16mm bars could be owed to a variety of factors. The coating thickness was seen to have a significant effect on the bond of 16 mm uncorroded steel. Compared to the M65-12 results, the pull-out force for M65-16 was 9% higher when one coat was applied and practically the same when the second coat was applied. The variability in results for both coating applications indicate that there was no significant difference in pull-out force between specimens with 12 mm and 16 mm bars, respectively. This statement is supported by the high p-values (0.09 for one coat and 0.7 for two coats). Failure of the coated M65-16 specimens occurred by shearing of the coating mostly when one or two coats were applied. Figure 35 displays shearing of the coating and splitting failure of the repair material. The applied bearing forces exceeded the strength of the coating, and explains why the coating failed, shown by its remnants between the ribs.

Figure 35: Coating failure with 10% corroded steel

4.2.6 Influence of previously corroded rebar on pull-out force

Figure 36 indicates that corrosion had a negative effect on the pull-out force, which was evident for all mixes.

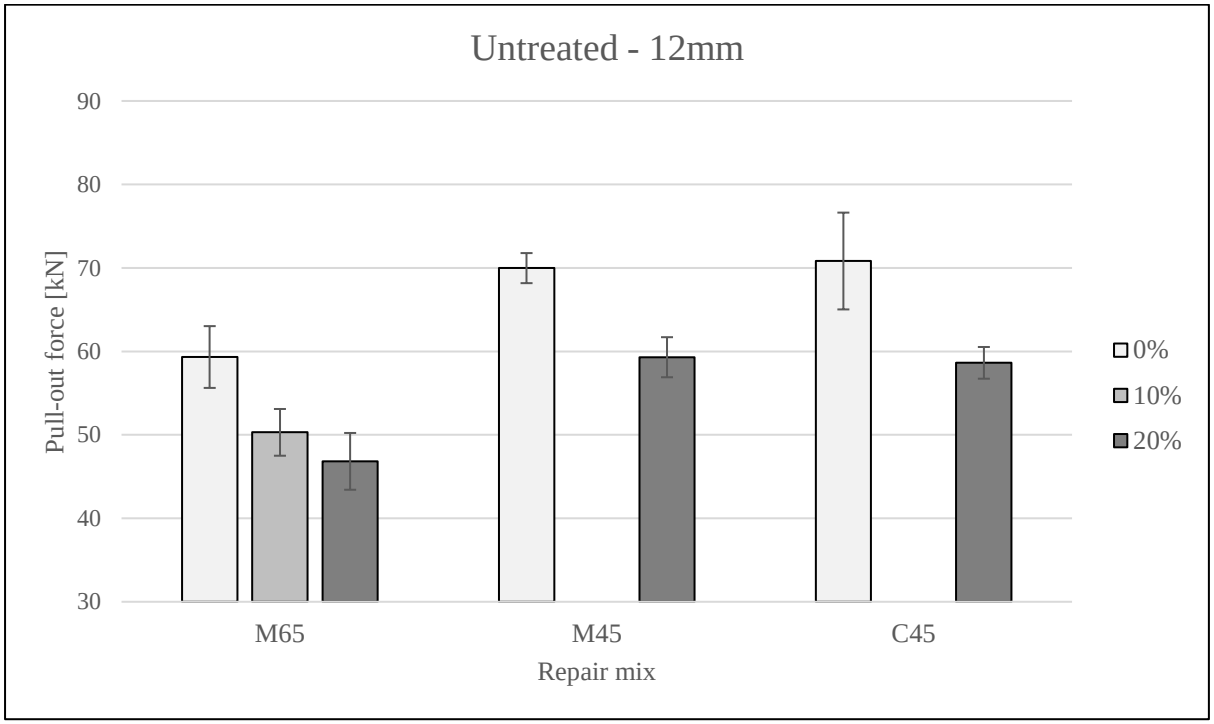

Figure 36: Corrosion influence on pull-out force

Considering mix M65, there was a 15% reduction in pull-out force when 10% corrosion occurred compared to uncorroded specimens. For 10% steel mass loss, the corrosion simulating process constituted a partial reduction in rib height along the bar surface with some areas having all the ribs removed. The reduction in rib height for the 10% corroded specimens yielded a statistical difference in the pull-out force compared to the uncorroded specimens and is indicated by the low p-value (0.015). Due to all the ribs gone on the 20% corroded specimens, there was a 21% reduction in pull-out force compared to the uncorroded specimens. The low p-value (0.014) indicates this reduction is statistically different. For this study, minor indentations were created along the bar surface during the steel cleaning process, in an attempt to simulate a bar surface profile with 20% steel mass loss and similar to what is seen from chloride-induced corrosion damage.

A possible reason for the variation in results for the 20% corroded specimens could be due to different surface conditions of the untreated bars, according to location and size difference of pitting corrosion areas. Therefore, all the bars had similar mass losses but different surface profiles, which would cause variation in the results obtained.

The results from Figure 36 only showed only a 10 – 20 kN reduction in pull-out force when compared to the uncorroded specimens. Therefore, the bond of the cleaned corroded steel is not significantly different compared to the uncorroded steel. It is believed that, while the mechanical interlock was reduced by the loss of ribs, the adhesion and frictional components of the bond increased. This can be confirmed by further investigation through analysing the microstructure between uncorroded and cleaned corroded rebar by image analysis. The reductions in pull-out force due to corrosion was minor compared to those seen from other investigations. A study from Kearsley and Joyce (2014) observed a reduction of about 60% in the ultimate bond when the steel was corroded to 10% mass loss; however, the corrosive products were not removed before pull-out testing. At corrosion levels below 5% steel mass loss, the firm rust produced filles the pores of the surrounding concrete which leads to an increase in the bond strength. However, when corrosion progresses to higher stages, the accumulation of more rust begins to negatively affect the bond between the steel and concrete. It was observed that the bond strength reduction of specimens with 20% corrosion present on the steel can be reached as high as 80% compared to uncorroded specimens (Tondolo, 2015). The results from this study therefore highlights the importance of cleaning the corroded steel. Specimens from both M45 and C45 experienced a 16% reduction in pull-out force when 20% corrosion occurred. This is significantly different compared to the untreated specimens and is supported by the low p-values (0.001 for M45 and 0.005 for C45). The performance of M45 and C45 at 20% corrosion remained significantly higher than M65.

With regards to failure of the corroded specimens compared to uncorroded specimens, it was observed that the failure mode changed from splitting failure to slip of the bar, which was a result of the reduction or complete loss of ribs on the corroded specimens. Figure 37 (a) shows about 15 mm slip, and Figure 37 (b) shows 30 – 35 mm slip for the 20% corroded specimen.

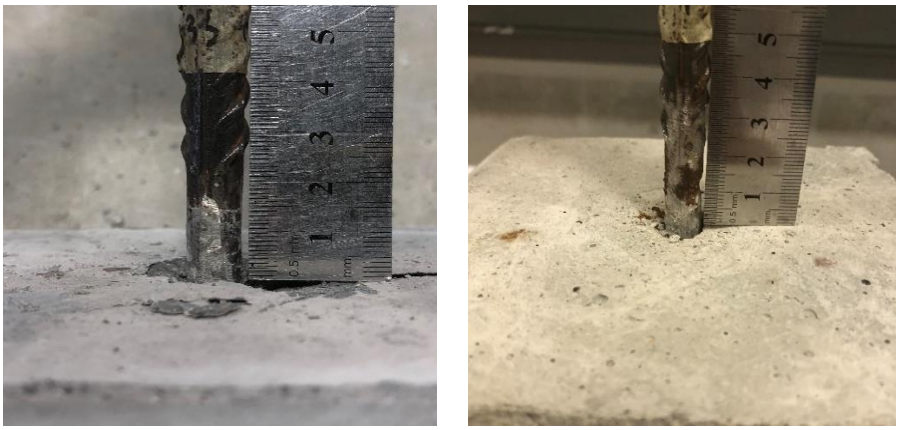

Figure 37: (a) Untreated 20% corroded steel with 15 mm slip, and (b) 30 – 35 mm slip

For the corroded specimens, mechanical interlock no longer existed, and the bond relied on adhesion and friction between the cleaned corroded steel and repair material. The relatively high slip seen for the corroded specimens corresponds to the reductions in pull-out force observed, when compared to the uncorroded specimens.

Figure 38 displays the condition of 20% cleaned corroded rebar with no coating, after being protected by repair material through 7 days wet curing. After the steel cleaning process, the bars were sealed in bubble wrap until application of the coating to prevent exposure to moisture and therefore corrosion of the steel. It can be observed that applying no coating after steel cleaning will result in immediate surface corrosion, even after the repair concrete is applied over the steel. Therefore, during repairs, coating of the steel should be done immediately.

Figure 38: Corrosion effects of untreated steel after 7 days wet curing

4.2.6.1 Effect of corrosion on different size diameter bars

Figure 39 displays the pull-out test results of uncorroded and 20% corroded M65 specimens with different bar diameters. The effects of corrosion on specimens with 12 mm bars have already been discussed. The M65-16 specimens showed an 11% lower pull-out force compared to the uncorroded specimens. Both test results, however, show a high variability. This, along with the high p-value (0.3), indicates there is no significant difference between the uncorroded and 20% corroded specimens with 16 mm bars. Therefore, corrosion negatively affected the pull-out force of M65-12 but did not severely impact the performance of M65-16. For the 20% corroded specimens, the untreated M65-16 displayed a 35% higher pull-out force than for M65-12, indicating the difference between the 12 mm and 16 mm bars is statistically significant, confirmed by the p-values (0.01). The difference between the two bar diameters at 20% corrosion is considerable and was more pronounced than for uncorroded specimens. This can be explained by the fact that for the 20% corroded specimens, all the ribs are gone for both bar diameters, hence the size of the nominal bar diameter, plays a major role in determining the pull-out force. Furthermore, the larger surface area on the 16 mm steel compared to the 12 mm steel means higher adhesion and frictional bond components exist which led to the higher pull-out force.

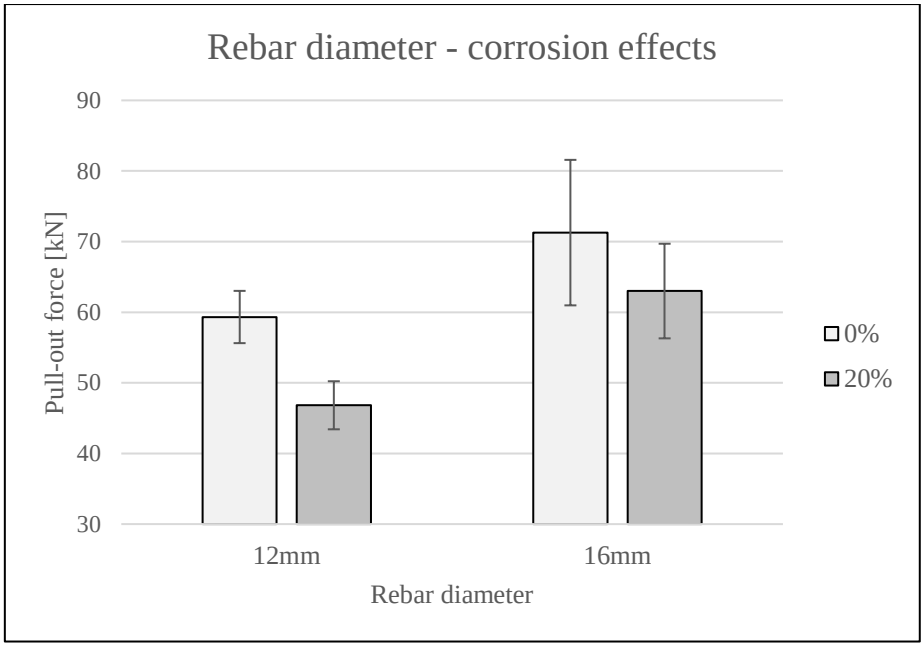

Figure 39: Corrosion influence for different size bars

4.2.7 Influence of coatings on previously corroded specimens

4.2.7.1 Effect of coatings on 10% corrosion-damaged steel

From Figure 40, it is evident that applying one coat had a negative effect on the pull-out force of 10% corroded specimens compared to the untreated specimens, and applying a second coat showed no change in the pull-out force.

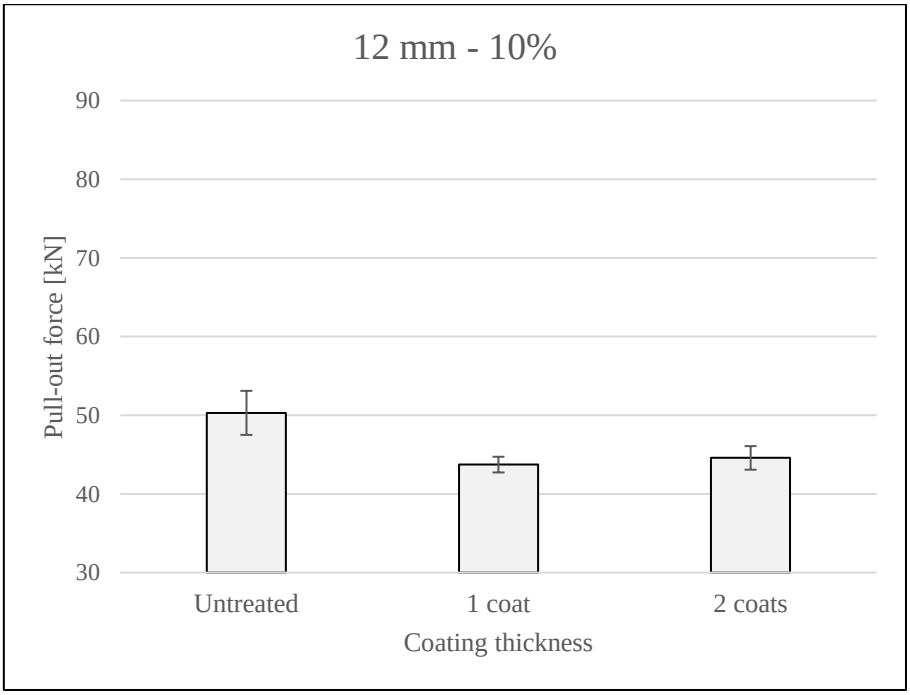

Figure 40: Pull-out test results for 10% corroded M65-12

The pull-out force was reduced by about 12% when applying one or two coats. This reduction, when compared to the untreated specimens, is statistically different and supported by the low p-value of 0.009 for one coat and 0.02 for two coats. Hence, the null hypothesis is accepted. Compared to the untreated specimens, the pull-out force of the coated specimens was only about 6 kN lower, therefore the coating did not significantly reduce the bond. Furthermore, the coating thickness was seen to have no effect on the bond of 10% corroded steel. The reduced rib height on 10% corroded steel displayed a similar profile to that of a plain bar when two coats were applied, shown in Figure 41. Specimens with 10% corrosion were only considered for M65 with 12 mm steel, as the properties of the different repair materials and rebar sizes affect the pull-out performance in the same way at different corrosion degrees.

As some of the rib height was still present on 10% corroded steel, the coating failed due to stresses exerted from the ribs within the coating material. Slip of the rebar and splitting failure occurred equally among the four specimens for the test set with one coat and was accompanied by shearing of the coating. Figure 42 shows splitting with coating shear with two coats. It appeared that the coating completely masked the ribs and hence the specimens failed mostly by slip with the coating shearing.

Figure 41: 10% corroded steel with two coats

Figure 42: Splitting failure with coating shear for 10% corroded specimens

4.2.7.2 Effect of coatings on 20% corrosion-damaged steel

Figure 43 displays the pull-out force results for the 20% corroded specimens, for all coating treatments and mixes tested. Although there is a general trend where coating applications reduce the pull-out force for each of the mixes, this reduction was very small and not as predominant as seen with the uncorroded specimens.

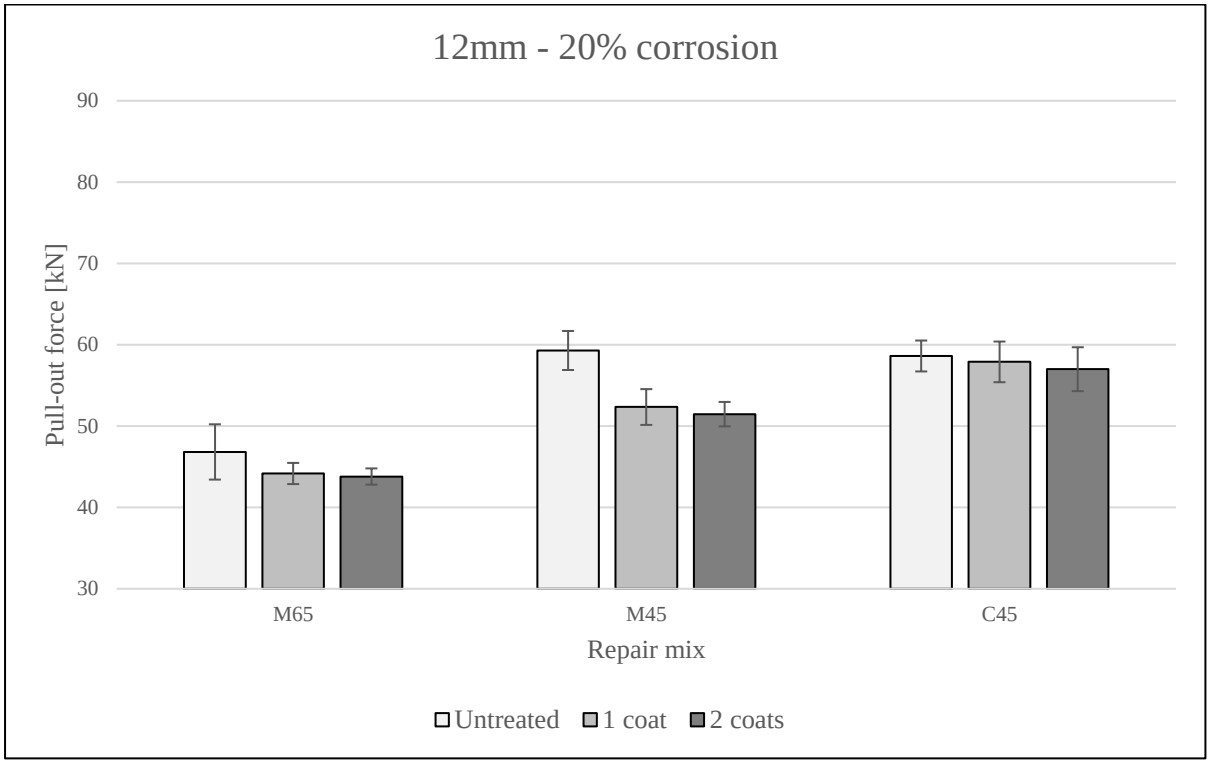

Figure 43: Pull-out results for 20% corroded 12 mm specimens

For mix M65, the pull-out force reduced by 6% when one coat was applied, compared to untreated specimens. When two coats were applied, the pull-out force remained unaffected, similar to the 10% corroded specimens. The high p-values (0.2) indicates no significant reduction in the pull-out force when one coat was applied to untreated specimens of M65-12. The same effect was noticed when applying two coats, with p-value (0.2), hence accepting the null-hypothesis. It is further observed that the surface condition of 10% corroded coated specimens was similar to that of 20% specimens, see Figures 41 and 44. Additionally, the same pull-out force of 44kN was obtained for both groups, indicating that applying two coats to 10% and 20% corroded specimens showed the same pull-out strength. At 20% steel mass, the difference in pull-out force between coats was less than 1 kN on average according to Figure 43 and 46. The only difference in pull-out force between the 10% and 20% corroded steel was in fact only seen for untreated specimens, highlighting that the loss of ribs by corrosion, or the coating's effect of reducing the relative rib area, had reduced the bond.

Figures 44 shows effects of applying the first, then the second coat to the cleaned corroded steel at 20% steel mass loss. The mechanical interlock component of the bond no longer existed due to the loss of ribs at 20% corrosion. Hence, the pull-out force was not as severely affected by the coating for 20% corroded specimens when compared to uncorroded specimens.

Figure 44: 20% corroded untreated (top), one coat (centre), two coats (bottom)

It must be noted that an average coating thickness of 0.6 mm (per coat) was used in this study, except for the A12-20 batch (see Appendix E) of pull-out specimens where the measured average coating thickness on each bar was 1.2 mm per coat. Although the coating thickness was much larger for these specimens, there was statistically no difference between the pull-out force between specimens with coating thickness of 0.6 mm and those with 1.2 mm. This could imply there is minimal effect of the coating thickness in reducing the pull-out force for M65. In theory, this could imply a hyperbolic relationship between the coating thickness and pull-out force, though this could not quantifiably be proven due to the limitation of only adopting two coating thicknesses in this study.

For mix M45, the pull-out force was reduced by 12% when one coat was applied. The low p-value (0.01) indicates there is a significant difference in the pull-out force between untreated and treated specimens with one coat, rejecting the null hypothesis. When two coats are applied, however, there was no difference compared to the first coating. For mix C45, the pull-out force only decreased marginally for the first, and second coat applied respectively, compared to

untreated specimens. This rejects the null hypothesis and shows no effect of the coating on 20% corroded steel. For the 20% corroded specimens, it can be noted that there was no effect of the coating thickness on the bond of cleaned corroded rebar for all tested mixes. When coatings were used, poor performance of M45 was noticed and could be due to the higher strength of the overlay material (M45) compared to the substrate material (coating) in terms of their cement contents. A study by (Beushausen, Höhlig and Talotti, 2017), showed the importance of strength compatibility between the substrate and overlay repair material, in respect to bonded concrete overlays used on repaired concrete surfaces. The conclusions in this regard could support a theory towards the importance of compatibility between coating substrate to overlay repair material. However, there is no evidence in previous literature to support this, and thus further investigation is needed.

The failure mode observed for most of the 20% corroded specimens with coating was slip. When two coats were applied to the 20% corroded specimens, failure within the coating was observed in some instances. In most cases however, there appeared to be good contact between the repair material, the coating, and cleaned corroded steel, shown in Figure 45. Some of the coating detached from the steel during loading however most of the coating remained intact. The coating appeared to break in the top half of the specimen, which could be due to higher stresses in the upper region of the repair material, as seen for uncorroded specimens. This explains why the coating detached with the repair material towards the top surface of the specimen during failure but bonded quite well along the rest of the corroded steel, which was mostly the case for 20% corroded steel.

Figure 45: 20% corroded coated steel after failure

4.2.8 Effect of rebar diameter on previously corroded and coated specimens

Figure 46 shows the pull-out force for the 12mm and 16 mm bars at 20% steel mass loss. There was a decrease of 16% in the pull-out force when one coat was applied to 16 mm bars, compared to untreated specimens.

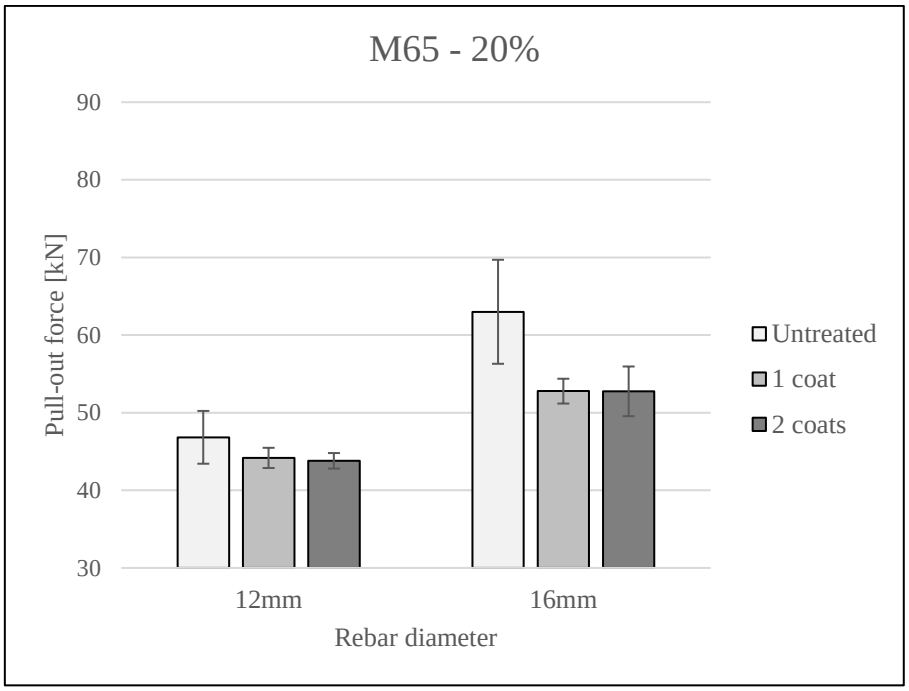

Figure 46: Pull-out test results for 20% corroded M65 specimens of different bar sizes

The low p-value (0.04) suggests this difference is significant, rejecting the null hypothesis. When the second coat is applied, the average test result is the same as for one coat, but with a higher variability in the results. Furthermore, the p-value (0.054) indicates there is no significant difference between the second coat and untreated specimens, hence accepting the null hypothesis. The variation in results for the untreated specimens could be due to the variable surface condition of the cleaned corroded steel.

Furthermore, there is no difference between applying one or two coats to 20% corroded 16 mm bars, indicating that the coating thickness had no effect on the pull-out force.

4.3 Performance of coatings on corroded rebar

Figure 47 displays the effect of corrosion on pull-out strength and the performance of coatings on 10% and 20% corroded specimens in relation to uncorroded untreated specimens. The results indicate a reduction in pull-out force from specimens with cleaned corroded steel, compared to the control. The low p-values, displayed in Appendix G, are all below 0.05 apart from M65-16, indicating there was a statistical difference between the corroded and uncorroded

specimens. Despite this, the reductions in pull-out force compared to the controls were only between 10 to 20 kN, meaning there was no significant impact of corrosion on the pull-out force. In general, between the mixes there was no difference between leaving the bars untreated or applying the coating with C45-12 or M65-12. Furthermore, there was no effect of the coating thickness on the pull-out force and hence the bond. Surprisingly, the pull-out force from corroded coated specimens with M65 at 10% and at 20% steel mass loss was the same.

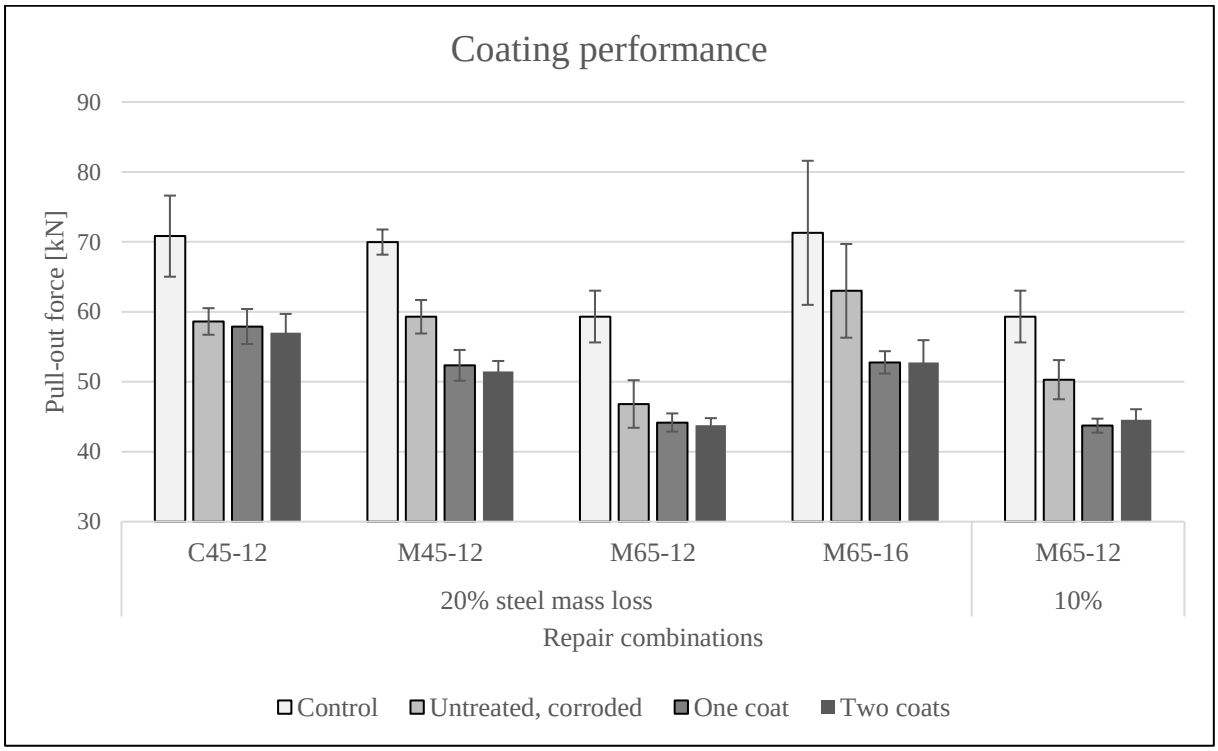

Figure 47: Coating performance on corroded coated specimens

At 10% steel mass loss, the pull-out force of the corroded coated specimens with M65 was 75% compared to the control, and similar to what was observed by Natino *et al.* (2021). For the 20% corroded specimens with two coats, the pull-out force of all mixes ranged from 73 to 80%, compared to their respective controls.

4.4 Summary of discussions

4.4.1 Main trends from study

Influence of repair materials

The pull-out force was affected in the same manner as the compressive strength due to changes in the mortar's w/b ratio, when comparing M65 and M45. As the compressive strength is directly related to the bond strength and hence pull-out force, the pull-out force increased with a lower w/b ratio. With the addition of stone to mix, no difference between the mortar (M45)

and concrete (C45) was observed from the pull-out test results, despite the compressive strength of the concrete being higher.

Influence of rebar diameter

As the rebar diameter was increased, the pull-out force increased, although this difference was not significant for uncorroded specimens.

Influence of coatings on uncorroded specimens

The pull-out force for all three mixes was reduced when one coat was applied to uncorroded rebar, although this reduction was not significant. When two coats were applied to M65-12 and M45-12, the pull-out force was significantly lower than untreated specimens, indicating a negative effect from two coats of 0.6 mm thickness each. The relative rib area was significantly reduced due to accumulation of the cementitious coating between the rib corners on the rebar surface, affecting the mechanical interlock component that forms most of the bond on uncorroded rebar. Mix C45-12 coated specimens performed the best among the sets and displayed no significant reduction in pull-out force when two coats were used, compared to the untreated specimens. The 16 mm steel showed a relatively high pull-out force, due to the large ribs, and was affected the most when the coating was applied.

Influence of rebar corrosion

As corrosion increases from 0 to 10% steel mass loss, the pull-out was reduced and up to 20% steel mass loss, the bond was further reduced, but of a smaller magnitude. The results indicated that the reductions in pull-out force caused by corrosion were higher for an increase in bar diameter. When the ribs were gone at 20% steel mass loss, the influence of rebar diameter on the pull-out force could be noticed by the difference in nominal bar diameter between the 12 mm and 16 mm corroded steel.

Influence of coatings on previously corroded specimens

At 10% steel mass loss, a statistical difference between the untreated and coated specimens were noticed, however the reduction in pull-out force was only 6 kN and therefore not significant. There was no difference between applying one or two coats, showing that the coating thickness had no impact on pull-out force. At 20% steel mass loss, there was no difference between leaving the bars untreated and applying the first coat, which was the case for all mixes besides M65-16. In addition, there was no difference in pull-out force when applying the second coat. The coating thickness appeared to have less effect in reducing the

pull-out force of 20% corroded specimens, compared to uncorroded specimens, which was evident for all three mixes.

Failure mode analysis

For the uncorroded untreated specimens, the dominant failure mode observed was splitting of the repair material because of the ribs. Splitting failure was seen more in M65 than with other mixes which could be due to a weak mortar with high air voids content. Furthermore, splitting was also noticed more frequently for specimens with 16 mm as opposed to 12 mm steel, even when coatings were used. When coatings were used on 12 mm uncorroded steel, the coating appeared to mask the ribs and its bearing forces on the repair material. Due to the lower compressive strength of the coating in relation to the repair mixes, the ribs pulled through and caused shearing of the coating from uncorroded steel. With two coats applied, this observation was more evident, indicating that a thicker coating of this type had a greater potential to fail by shearing with the repair mixes used. When corrosion occurred, most of the specimens failed by slip of the rebar due to the absence of ribs. When coatings were used on 10% corroded specimens, shearing of the coating was observed due to some of the ribs with a reduced height still present after corrosion and cleaning. For the 20% corroded coated specimens, slip was seen most of the time and occurred between the steel and coating. Shearing of the coating was only observed in a few instances, showing that the coating is more applicable to repair applications with cleaned corroded steel, when the ribs are gone.

4.4.2 Factors affecting the bond

Figure 48 shows the ranking of the different parameters' influence on the pull-out force, along with Table 5 indicating the labels for the respective combination of parameters tested.

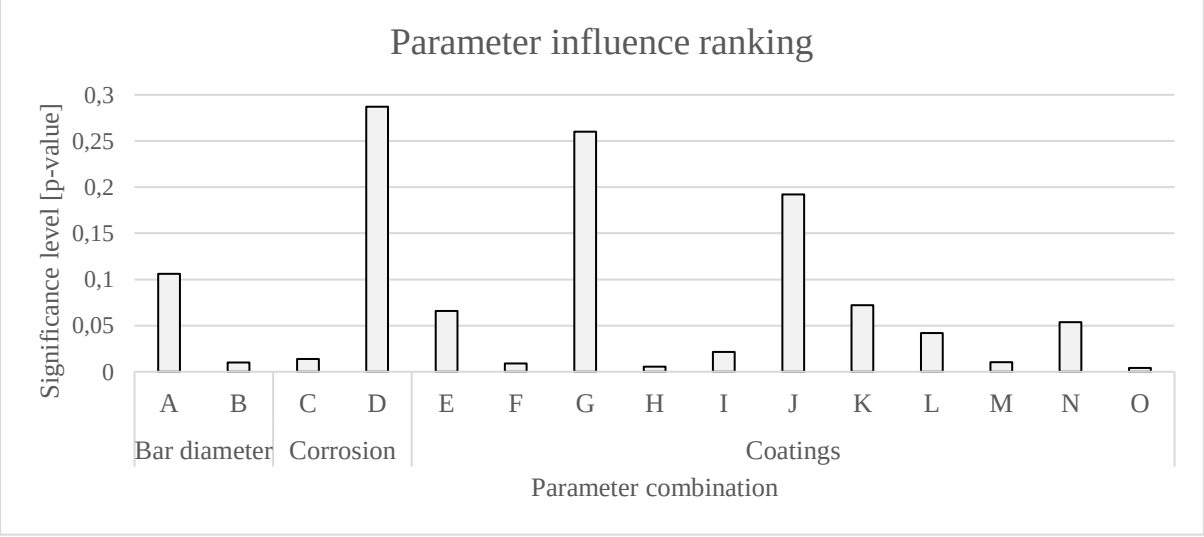

Figure 48: Parameter influence on pull-out force

Table 5: Categorization of influencing parameters

Designation	Comparison	Condition	p-value
A	12 vs 16 mm	0%	0.1
B		20%	0.01
C	0 vs 20%	12 mm	0.01
D		16 mm	0.3
E	0 vs 1 coat	0%	0.07
F		10%	0.009
G		20%	0.3
H	0 vs 2 coats	0%	0.006
I		10%	0.02
J		20%	0.2
K	0 vs 1 coat	0%	0.07
L		20%	0.04
M	0 vs 2 coats	0%	0.01
N		20%	0.06
O	M65 vs M45	Mortar w/b ratio	0.004

It must be noted that Figure 48 and Table 5 shows the influence of the different parameters in relation to M65 as all the variables could be compared in this regard, denoted A to N. Additionally, the influence of w/b ratio between M65 and M45 is shown. The parameters' influence is classified according to their significance indicators (p-values) which was obtained from statistical analysis of the pull-out test results. It was decided to rank the importance of the different parameters based on the p-values as they account for the difference in pull-out force and variation in results between the compared sets. A lower p-value indicates greater statistical difference in pull-out forces between the compared sets. The shaded areas in Table 5 indicate noteworthy influences from the parameters and the following can be noted:

1. Mortar w/b ratio of uncorroded specimens (O).
2. Applying two coats to uncorroded 12 mm and 16 mm rebar (H, M).
3. The influence of bar diameter at 20% steel mass loss (B).
4. Applying only one coat to 20% corroded 16 mm rebar (L).

The remainder of influences from the parameters shown in Figure 48 showed no significant influence on the pull-out force.

5. Conclusions

The main aim of this study was to investigate the influence of anti-corrosive coating thickness on the pull-out force of corrosion-damaged rebar. The motivation for this research involved demonstrating, through a review of the available literature, the importance of the bond in reinforced concrete, how corrosion affects the bond, and the importance of coatings used in the concrete repair industry. Pull-out testing was conducted to determine the effect of applying epoxy-modified cementitious coatings to uncorroded and corroded specimens, and the effect of their coating thickness on the bond in relation to different concrete repair materials and rebar sizes. From the results of this study, it was observed that:

- Most of the sound specimens failed by splitting as cracks developed in the repair material at the rebar interface with increasing load, while the corroded specimens failed by slip of the rebar when ribs were no longer present. The corrosion degree had a negative effect on the pull-out force for all mixes tested. Specimens with cleaned corroded rebar at 10% and 20% steel mass loss displayed pull-out forces 15% and 21% lower than the sound bars, showing that most of the bond was therefore lost during the early stages of corrosion. This highlights the importance of conducting patch repairs immediately as soon as corrosion is observed on in-situ structures. Despite the low p-values suggested by the statistical analysis, the pull-out force of all the specimens with cleaned corroded steel in this study only reduced by between 12 to 21 kN at most when the steel was at 20% steel mass loss, indicating no major influence of corrosion at this degree. The above results provide an estimate for engineers on the loss of pull-out capacity of corroded steel at 10% (Y12) and 20% mass loss (Y12 and Y16), if cleaned from corrosion and covered with the respective mortar/concretes used in this study. Applying no coating led to immediate corrosion therefore coatings are strongly advised for application to cleaned corroded steel during patch repairs.
- Cementitious coatings applied to uncorroded steel will accumulate between ribs and reduce the relative rib area that comprises majority of the bond. The presence of ribs on uncorroded coated steel caused slip with shear failure of the coating, and of a magnitude greater than what was seen for untreated specimens. Furthermore, specimens with Y16 showed more evidence of shear coating failure due to larger ribs, demonstrating the impracticality of applying coatings on sound ribbed bars. Concerning uncorroded steel during new construction, coatings should not be used as the bond was significantly reduced when two coats of 0.6 mm each were applied. As predicted, the uncorroded specimens with coatings

showed shear failure of the coating with its remnants between the steel ribs. The coating thickness showed minimal influence on the pull-out force of uncorroded (less than 10 kN on average) specimens and was therefore not significant.

At 10% and 20% steel mass loss, there was practically no difference between leaving the bars untreated or coating them, in terms of their pull-out strengths. Specimens at 10% steel mass loss with M65-12 and two coats of 0.6 mm each, showed pull-out forces measured as 75% compared to the control specimens. For specimens at 20% corrosion and two coats used, the pull-out force of the different mixes, and bar sizes, ranged from 74% to 80% compared to their respective control specimens. The pull-out force from corroded coated specimens with M65 at 10% and at 20% steel mass loss was the same, although this result should be strengthened by further research with additional repair materials used. Coatings are more suitable for repairing 20% corroded steel when all the ribs were gone, whereas for 10% corroded steel, shear failure of the coating can occur by the bearing forces of the ribs that are still present at 10% steel mass loss. It is not recommended to use a conventional repair mortar with w/b 0.47 (M45) due to differences in cement content between the 'high strength' mortar and cementitious coating, which led to poor bonding. Good contact between cementitious coatings, cleaned corroded 12 mm steel and M65 or C45 repair materials was seen. Epoxy-modified cementitious coatings such as the common construction repair coating used in South Africa is Sika Armatec® -110 EpoCem and is hence shown to be effective in repairing corrosion damaged steel up to 20% steel mass loss, as the pull-out force was hardly impacted by applying the first coat and second coat, compared to the untreated steel. The best performance of the coating with corroded (and uncorroded) steel was seen with C45-12. The coating thickness had no influence on the pull-out force of corroded specimens (less than 1 kN on average).

- The w/b ratio of mortars with CEM I 52.5N showed a significant effect on the pull-out force. Increasing the w/b ratio from 0.47 – 0.65 resulted in an 18% reduction in pull-out force between the uncorroded M45 and M65 specimens, respectively. There was no difference in pull-out force seen between the mortar and concrete of similar w/b ratios. C45 displayed the least effect of coatings on reducing the bond compared to untreated steel, which was the case for uncorroded and 20% corroded specimens. M65 and C45 showed good contact and bonding performance to corroded steel with coatings and hence could be considered as suitable OPC materials for repair scenarios.

- In general, as the rebar diameter was increased, the pull-out force increased which relates to a decrease in the bond strength. The effect of rebar diameter on uncorroded 12 mm and 16 mm steel was not significant, although for the corroded specimens, the difference was significant due to the absence of ribs. Here, the influence of nominal rebar diameter was clearly noticed. With M65 and uncorroded 16 mm steel, the initial high pull-out force displayed due to its larger ribs in comparison to 12 mm steel, was affected more by the coating and its thickness.

6. Recommendations

From the results of this study, it is recommended that:

- The loss in bond strength be tested by conducting experimental tests on actual corroded repaired RC members. For example, the flexural strength and other structural properties such as stiffness of repaired RC beams could be assessed to better understand the implications of coatings on bond strength, and the composite action between coated steel and repair material.
- Further testing on specimens that are either corroded naturally or by means of accelerated laboratory techniques, then cleaned and coated for pull-out testing, be carried out. This is mentioned on the basis that this study involved grinding the steel bars by using an angle grinder to simulate corrosion damage.
- Image analysis comparison of the microstructure between sound and cleaned corroded steel can be conducted to identify changes to the steels' adhesion and frictional bond components from corrosion damage and the steel cleaning process.
- The bond-slip relationships be obtained using linear variable differential transformers (LVDTs) to monitor slip behaviour, and that service life modelling on bond-degradation of corroded specimens be considered.
- A further detailed study is carried out to extend the current understanding of influence from the tested parameters on the pull-out force. For example, effects from the corrosion degrees at higher levels of steel mass loss of 30%, additional bar sizes such as Y10 and Y20, repair materials with different chemical compositions or extenders be assessed.
- Lastly, additional cementitious coating products, such as zinc-polyurethane primers, are tested to strengthen the conclusions made is this study, with respect to the effects from anti-corrosive coatings and their thickness on the bond.

References

Alexander et al., 2001. Research Monograph No 5 - *Repair principles for corrosion-damaged reinforced concrete structures* '. Concrete Materials and Structural Integrity Research Unit (CoMSIRU). pp. 1–36.

Al-Dulaijan, S. U. *et al.* (2002) *'Effect of rebar cleanliness and repair materials on reinforcement corrosion and flexural strength of repaired concrete beams'*, Cement and Concrete Composites, 24(1), pp. 139–149. doi: 10.1016/S0958-9465(01)00034-8.

Almusallam, A. A. *et al.* (1996) *'Effect of reinforcement corrosion on bond strength',* Construction and Building Materials, 10(2), pp. 123–129. doi: 10.1016/0950-0618(95)00077-1.

Angst, U. M. *et al.* (2017) *'The steel–concrete interface',* Materials and Structures/Materiaux et Constructions, 50(2). doi: 10.1617/s11527-017-1010-1.

Aryanto, A. and Shinohara, Y. (2012) *'Bond Behavior between Steel and Concrete in Low Level Corrosion of Reinforcing Steel'*, 15th World Conference on Earthquake Engineering, Lisbon Portugal, (1999).

Ballim, Y, Alexander, M & Beushausen, H. 2009. *'Durability of concrete', in G Owens (ed.), Ful- ton's Concrete Technology*, Cement and Concrete institute, Midrand.

Bashir, M. T., Ansar, M. and Muhammad, S. (2019) *'Investigation of Pullout Strength of Conventional Steel Reinforcement Bars in Normal and High Strength Concrete',* International Journal of Scientific Engineering and Science, 3(4), pp. 18–25.

Beushausen, H., Höhlig, B. and Talotti, M. (2017) *'The influence of substrate moisture preparation on bond strength of concrete overlays and the microstructure of the OTZ'*, Cement and Concrete Research, 92, pp. 84–91. doi: 10.1016/j.cemconres.2016.11.017.

Bouazaoui, L. and Li, A. (2008) *'Analysis of steel/concrete interfacial shear stress by means of pull out test',* International Journal of Adhesion and Adhesives, 28(3), pp. 101–108. doi: 10.1016/j.ijadhadh.2007.02.006.

de Brito, J. *et al.* (2020) *'Repair Techniques'*, Expert Knowledge-based Inspection Systems, pp. 301–355. doi: 10.1007/978-3-030-42446-6_5.

Choi, O. C. *et al.* (1991) *'Bond of epoxy-coated reinforcement: bar parameters',* ACI

Materials Journal, 88(2), pp. 207–217. doi: 10.14359/2023.

Diab, A. M. *et al.* (2014) *'Bond behavior and assessment of design ultimate bond stress of normal and high strength concrete',* Alexandria Engineering Journal. Faculty of Engineering, Alexandria University, 53(2), pp. 355–371. doi: 10.1016/j.aej.2014.03.012.

El Alami, E.; Fekak, F.-E.; Garibaldi, L.; Moustabchir, H.; Elkhalfi, A.; Scutaru, M.L.; Vlase, S. Numerical Study of the Bond Strength Evolution of Corroded Reinforcement in Concrete in Pull-Out Tests. *Appl. Sci.* **2022**, *12*, 654. https://doi.org/10.3390/app12020654

Fernandez, I., Lundgren, K. and Zandi, K. (2018) *'Evaluation of corrosion level of naturally corroded bars using different cleaning methods, computed tomography, and 3D optical scanning',* Materials and Structures/Materiaux et Constructions. Springer Netherlands, 51(3), pp. 1–13. doi: 10.1617/s11527-018-1206-z.

Gao, H., Zhang, X. and Zhang, Y. (2015) *'Effect of the entrained air void on strength and interfacial transition zone of air-entrained mortar',* Journal Wuhan University of Technology, Materials Science Edition, 30(5), pp. 1020–1028. doi: 10.1007/s11595-015-1267-6.

Guettala, A. and Abibsi, A. (2006) *'Corrosion degradation and repair of a concrete bridge',* Materials and Structures/Materiaux et Constructions, 39(288), pp. 471–478. doi: 10.1617/s11527-005-9046-z.

James, A. *et al.* (2019) *'Rebar corrosion detection, protection, and rehabilitation of reinforced concrete structures in coastal environments: A review'*, Construction and Building Materials. Elsevier Ltd, 224, pp. 1026–1039. doi: 10.1016/j.conbuildmat.2019.07.250.

Jorge, S., Dias-da-Costa, D. and Júlio, E. N. B. S. (2012) *'Influence of anti-corrosive coatings on the bond of steel rebars to repair mortars',* Engineering Structures. Elsevier Ltd, 36, pp. 372–378. doi: 10.1016/j.engstruct.2011.12.028.

Kamde, D. K. and Pillai, R. G. (2020) *'Effect of surface preparation on corrosion of steel rebars coated with cement-polymer-composites (CPC) and embedded in concrete',* Construction and Building Materials. Elsevier Ltd, 237, p. 117616. doi: 10.1016/j.conbuildmat.2019.117616.

Kearsley, E. P. and Joyce, A. (2014) *'Effect of corrosion products on bond strength and flexural behaviour of reinforced concrete slabs',* Journal of the South African Institution of

Civil Engineering, 56(2), pp. 21–29.

Khalaf, R. D. *et al.* (2020) *'Analytical Study on Effect of Bar Size on Pull-out force for Reinforcing Bar Embedded in Concrete Blocks',* IOP Conference Series: Materials Science and Engineering, 928(2). doi: 10.1088/1757-899X/928/2/022085.

Lin, H. *et al.* (2017) *'Bond strength evaluation of corroded steel bars via the surface crack width induced by reinforcement corrosion',* Engineering Structures, 152, pp. 506–522. doi: 10.1016/j.engstruct.2017.08.051.

Lin, H. *et al.* (2019) *'State-of-the-art review on the bond properties of corroded reinforcing steel bar',* Construction and Building Materials. Elsevier Ltd, 213, pp. 216–233. doi: 10.1016/j.conbuildmat.2019.04.077.

McClarty, Meghan (2021) ' Further investigation into the bond between repaired steel reinforcement and concrete repair materials' BSc thesis, University of Cape Town, Cape Town

Metelli, G. and Plizzari, G. A. (2014) *'Influence of the relative rib area on bond behaviour',* Magazine of Concrete Research, 66(6), pp. 277–294. doi: 10.1680/macr.13.00198.

Natino, M. R. L. *et al.* (2021) *'Experimental study on the effect of anti-corrosive coatings on bond behavior of corroded rebar'*, Construction and Building Materials. Elsevier Ltd, (xxxx), p. 121716. doi: 10.1016/j.conbuildmat.2020.121716.

Plesa, A. *et al.* (2016) *'Corrosion Effect on Bond Loss between Steel and Concrete'*, Intech, i(tourism), p. 13.

Pothisiri, T. *et al.* (2018) *'Effect of diameter on bond failure of steel rebar embedded into concrete using epoxies at high temperatures',* Engineering Journal, 22(3), pp. 93–107. doi: 10.4186/ej.2018.22.3.93.

Qasim, O. A. and Ahmed, A. S. (2018) *'Different variable effects on bond strength of normal, high and ultrahigh strength concrete'*, International Journal of Civil Engineering and Technology, 9(10), pp. 1923–1945.

Ramaswamy, S. N., Varalakshmi, R. (2016) *'Effect of Anti Corrosive Coatings To Steel - A State of Art Report',* International Journal of Scientific Research, 5(6), pp. 302–306.

Raupach, M. 2014. Concrete Repair to EN 1504: Diagnosis, Design, Principles and Practice.

CRC Press.

Seddelmeyer, J. D. *et al.* (2000) *'Feasibility of Various Coatings for the Protection of Reinforcing Steel--Corrosion and Bond Testing'*, 7(21), p. 72 p. http://www.utexas.edu/research/ctr/pdf_reports/4904_3.pdf.

Sonebi, M., Davidson, R. and Cleland, D. (2011) *'Bond between Reinforcement and Concrete – Influence of Steel Corrosion',* International Conference on Durability of Building Materials and Components, pp. 1–8.

South African Bureau of Standards (SABS). 2008. South African National Standard (SANS): *Sieve analysis, fines content and dust content of aggregates (SANS 201:2008)*. Pretoria. SABS Standards Division.

South African Bureau of Standards (SABS). 2006. South African National Standard (SANS): *Concrete tests – Consistence of freshly mixed concrete - Slump test (SANS 5862-1:2006)*. Pretoria. SABS Standards Division.

South African Bureau of Standards (SABS). 2006. South African National Standard (SANS): *Concrete tests – Consistence of freshly mixed concrete - Flow test (SANS 5862-2:2006)*. Pretoria. SABS Standards Division.

South African Bureau of Standards (SABS). 2006. South African National Standard (SANS): *Concrete tests — Compressive strength of hardened concrete (SANS 5863:2006)*. Pretoria. SABS Standards Division.

South African Bureau of Standards (SABS). 2006. South African National Standard (SANS): *Concrete tests — Compressive strength of mortar (SANS 6255:2006)*. Pretoria. SABS Standards Division.

Sørensen, P. A. *et al.* (2009) *'Anticorrosive coatings: A review',* Journal of Coatings Technology and Research, 6(2), pp. 135–176. doi: 10.1007/s11998-008-9144-2.

Taha, N. A. and Morsy, M. (2016) *'Study of the behavior of corroded steel bar and convenient method of repairing',* HBRC Journal. Housing and Building National Research Center, 12(2), pp. 107–113. doi: 10.1016/j.hbrcj.2014.11.004.

Teresa, M. *et al.* (2008) *'Analysis of the Relative Rib Area of Reinforcing Bars Pull Out Tests',* Material Research, 11(4), pp. 453–457.

Tondolo, F. (2015) *'Bond behaviour with reinforcement corrosion',* Construction and Building Materials. Elsevier Ltd, 93, pp. 926–932. doi: 10.1016/j.conbuildmat.2015.05.067.

Turk, K., Yildirim, M. S. and Caliskan, S. (2003) *'Effect of reinforcement size on the concrete / reinforcement bond strength'*, Role of Cement Science in Sustainable Development - Proceedings of the International Symposium - Celebrating Concrete: People and Practice, (September), pp. 47–57. doi: 10.1680/rocisd.32477.0005.

Vaysburd, A. M. and Emmons, P. H. (2000) *'How to make today's repairs durable for tomorrow-corrosion protection in concrete repair',* Construction and Building Materials, 14(4), pp. 189–197. doi: 10.1016/S0950-0618(00)00022-2.

Wang, C.-Y. (1963) 'A study of bond stress between concrete and steel', MSc thesis, Kansas State University, Manhattan

Xiao, J., Li, J. and Zha, Q. (2004) *'Experimental study on bond behavior between plain reinforcing bars and concrete',* Construction and Building Materials, 18(10), pp. 745–752. doi: 10.1016/j.conbuildmat.2004.04.026.

Zhang, W. *et al.* (2020) *'Influence of artificial cracks and interfacial defects on the corrosion behavior of steel in concrete during corrosion initiation under a chloride environment',* Construction and Building Materials. Elsevier Ltd, 253, p. 119165. doi: 10.1016/j.conbuildmat.2020.119165.

Appendix A – Laboratory schedule and repair material quantities

SUNDAY	MONDAY	TUESDAY	WEDNESDAY	THURSDAY	FRIDAY	SATURDAY
22-August	**23**	**24**	**25**	**26**	**27**	**28**
			Cast B1	Demould B1	Cast B2	Demould B2
29	**30**	**31**	**1 - September**	**2**	**3**	**4**
		Cast C1	Test B1 Demould C1	Cast C2	Test B2 Demould C2	
5	**6**	**7**	**8**	**9**	**10**	**11**
	Cast A1	Test C1 Demould A1	Cast A2	Test C2 Demould A2	Cast A3	Demould A3
12	**13**	**14**	**15**	**16**	**17**	**18**
	Test A1	Cast A4	Test A2 Demould A4	Cast A5	Test A3 Demould A5	
19	**20**	**21**	**22**	**23**	**24**	**25**
		Test A4		Test A5		

Specimens	Experiment 1	Experiment 2	Total
Total no. of specimens	84	24	108
Grinded specimens	48	12	60
Treated (coated)	56	16	72
Untreated	28	8	36

Repair material	Compressive strength	No. of specimens	Material required (liters)
Mortar – M65	30 MPa	60	203
Mortar – M45	45 MPa	24	81
Concrete – C45	45 MPa	24	81

Steel type	No. of specimens	Amount of steel required (m)	Total surface area to be coated (m^2)
Y12	100	100 x 0.275 = 28	0.37
Y16	16	16 x 0.275 = 5	0.061

Appendix B – Sieve analysis and grading

Dune sand						
sieve size	**sieve weight (g)**	**weight retained + sieve weight (g)**	**Weight retained (g)**	**Cumulative weight retained (g)**	**Cumulative percentage retained**	**Cumulative percentage passing**
4.75	446.4	455.9	9.5	9.50	1.90	98.1
2.36	408.2	413.9	5.7	15.20	3.04	97.0
1.18	541.3	573.1	31.8	47.00	9.40	90.6
0.6	340	433.2	93.2	140.20	28.05	72.0
0.3	280.6	417.4	136.8	277.00	55.41	44.6
0.15	488.9	668.8	179.9	456.90	91.40	8.6
0.075	251.8	293.2	41.4	498.30	99.68	0.3
pan	494.3	495.9	1.6	499.90	100.00	0.0
Total			499.9		189.20	

FM 1.89

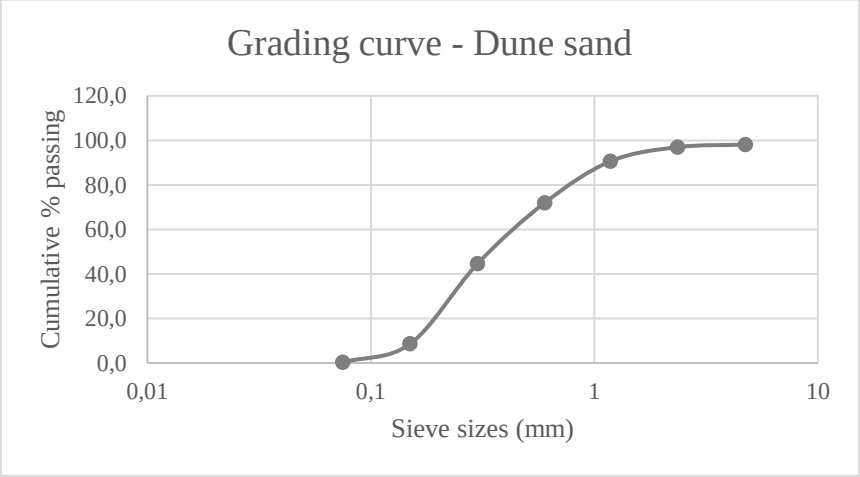

Crusher						
sieve size	**sieve weight (g)**	**weight retained + sieve weight (g)**	**Weight retained (g)**	**Cumulative weight retained (g)**	**Cumulative percentage retained**	**Cumulative percentage passing**
4.75	446.5	453.2	6.7	6.70	1.34	98.7
2.36	408.3	520	111.7	118.40	23.68	76.3
1.18	541.3	663.2	121.9	240.30	48.07	51.9
0.6	339.8	420.4	80.6	320.90	64.19	35.8
0.3	280.6	337.1	56.5	377.40	75.50	24.5
0.15	488.9	530.8	41.9	419.30	83.88	16.1
0.075	251.8	289.6	37.8	457.10	91.44	8.6
pan	494.3	536.9	42.6	499.70	99.96	0.0
Total			499.7		296.66	

FM 3.0

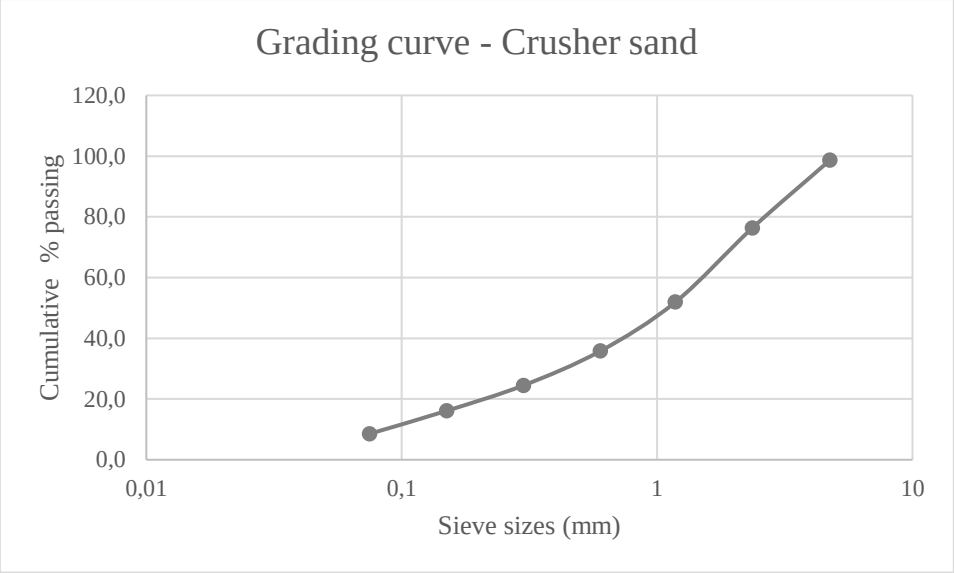

50/50 blend						
sieve size	**sieve weight (g)**	**weight retained + sieve weight (g)**	**Weight retained (g)**	**Cumulative weight retained (g)**	**Cumulative percentage retained**	**Cumulative percentage passing**
4.75	446.4	455.9	7.2	7.20	1.44	98.6
2.36	408.2	413.9	82.5	89.70	17.94	82.1
1.18	541.3	573.1	84.7	174.40	34.89	65.1
0.6	340	433.2	96.5	270.90	54.19	45.8
0.3	280.6	417.4	100.8	371.70	74.35	25.6
0.15	488.9	668.8	91.3	463.00	92.62	7.4
0.075	251.8	293.2	21.7	484.70	96.96	3.0
pan	494.3	495.9	15.3	500.00	100.02	0.0
Total			500		275.44	

FM 2.75

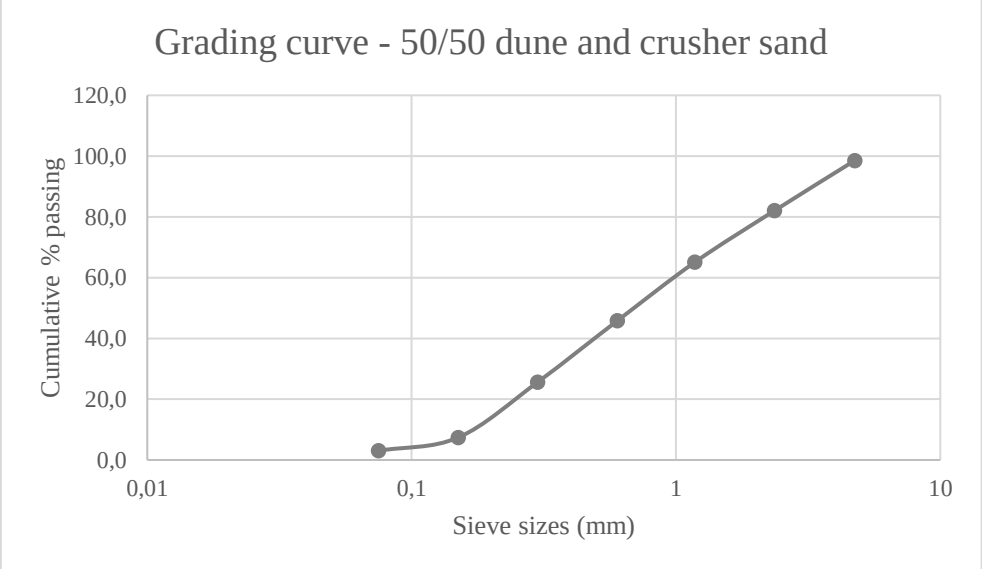

Appendix C – Detailed weights of grinded steel bars

B12 - 20 - untreated										
20% corrosion	**Mass before**	**Mass After**	**Mass loss (g)**	**Bar length**	**Corroded bar length**	**% Corroded length**	**Bar section (before)**	**Bar section (after)**	**Residual Mass (%)**	**Mass loss (%)**
1	400	374	26	456	158	0.35	138.60	112.60	81.24	18.8
2	398	368	30	457	170	0.37	148.05	118.05	79.74	20.3
3	394	366	28	455	156	0.34	135.09	107.09	79.27	20.7
4	390	362	28	455	168	0.37	144.00	116.00	80.56	19.4
									Average	19.8

B12 - 20 - 1 coat										
5	414	384	30	469	160	0.34	141.24	111.24	78.76	21.2
6	390	360	30	455	160	0.35	137.14	107.14	78.13	21.9
7	406	380	26	455	165	0.36	147.23	121.23	82.34	17.7
8	408	382	26	458	156	0.34	138.97	112.97	81.29	18.7
									Average	19.9

B12 - 20 - 2 coats										
9	386	358	28	457	160	0.35	135.14	107.14	79.28	20.7
10	402	370	32	456	160	0.35	141.05	109.05	77.31	22.7
11	408	378	30	455	157	0.35	140.78	110.78	78.69	21.3
12	386	360	26	441	165	0.37	144.42	118.42	82.00	18.0
									Average	20.7

A12 - 20 - untreated										
20% corrosion	**Mass before**	**Mass After**	**Mass loss (g)**	**Bar length**	**Corroded bar length**	**% Corroded length**	**Bar section (before)**	**Bar section (after)**	**Residual Mass (%)**	**Mass loss (%)**
13	384	358	26	448	160	0.36	137.14	111.14	81.04	19.0
14	406	376	30	455	165	0.36	147.23	117.23	79.62	20.4
15	398	368	30	458	160	0.35	139.04	109.04	78.42	21.6
16	410	382	28	460	165	0.36	147.07	119.07	80.96	19.0
									Average	20.0

A12 - 20 - 1 coat										
17	388	364	24	455	160	0.35	136.44	112.44	82.41	17.6
18	390	364	26	455	160	0.35	137.14	111.14	81.04	19.0
19	382	358	24	445	155	0.35	133.06	109.06	81.96	18.0
20	388	358	30	452	167	0.37	143.35	113.35	79.07	20.9
									Average	18.9

A12 - 20 - 2 coats										
21	400	368	32	447	165	0.37	147.65	115.65	78.33	21.7
22	386	362	24	451	165	0.37	141.22	117.22	83.01	17.0
23	388	362	26	454	165	0.36	141.01	115.01	81.56	18.4
24	388	364	24	455	155	0.34	132.18	108.18	81.84	18.2
									Average	18.8

C12 - 20 - untreated										
20% corrosion	**Mass before**	**Mass After**	**Mass loss (g)**	**Bar length**	**Corroded bar length**	**% Corroded length**	**Bar section (before)**	**Bar section (after)**	**Residual Mass (%)**	**Mass loss (%)**
25	380	354	26	452	160	0.35	134.51	108.51	80.67	19.3
26	380	354	26	446	165	0.37	140.58	114.58	81.51	18.5
27	388	362	26	453	157	0.35	134.47	108.47	80.67	19.3
28	382	354	28	448	164	0.37	139.84	111.84	79.98	20.0
									Average	19.3

C12 - 20 - 1 coat										
29	380	354	26	448	160	0.36	135.71	109.71	80.84	19.2
30	376	350	26	450	160	0.36	133.69	107.69	80.55	19.4
31	376	348	28	448	158	0.35	132.61	104.61	78.88	21.1
32	394	364	30	448	162	0.36	142.47	112.47	78.94	21.1
									Average	20.2

C12 - 20 - 2 coats										
33	388	360	28	454	160	0.35	136.74	108.74	79.52	20.5
34	390	364	26	446	160	0.36	139.91	113.91	81.42	18.6
35	382	356	26	450	161	0.36	136.67	110.67	80.98	19.0
36	412	382	30	462	158	0.34	140.90	110.90	78.71	21.3
									Average	19.8

A12 - 10 - untreated										
10% corrosion	**Mass before**	**Mass After**	**Mass loss**	**Bar length**	**Corroded bar length**	**% Corroded length**	**Bar section (before)**	**Bar section (after)**	**Residual Mass (%)**	**Mass loss (%)**
1	392	378	14	458	155	0.338	133	119	89.4	10.6
2	390	378	12	456	164	0.360	140	128	91.4	8.6
3	388	378	10	453	162	0.358	139	129	92.8	7.2
4	386	374	12	460	166	0.361	139	127	91.4	8.6
									Average	8.7

A12 - 10 - 1 coat										
5	396	382	14	448	164	0.366	145	131	90.3	9.7
6	382	368	14	445	160	0.360	137	123	89.8	10.2
7	386	370	16	445	159	0.357	138	122	88.4	11.6
8	400	388	12	456	166	0.364	146	134	91.8	8.2
									Average	9.9

A12 - 10 - 2 coats										
9	386	374	12	454	163	0.359	139	127	91.3	8.7
10	374	364	10	450	161	0.358	134	124	92.5	7.5
11	384	372	12	459	165	0.359	138	126	91.3	8.7
12	390	372	18	443	164	0.370	144	126	87.5	12.5
									Average	9.3

A16 - 20 - untreated										
20% corrosion	**Mass before**	**Mass After**	**Mass loss**	**Bar length**	**Corroded bar length**	**% Corroded length**	**Bar section (before)**	**Bar section (after)**	**Residual Mass (%)**	**Mass loss (%)**
1	683.3	631.1	52.2	454	161	0.35	242.32	190.12	78.46	21.54
2	689.8	634.6	55.2	451	158	0.35	241.66	186.46	77.16	22.84
3	686.3	643.5	42.8	446	160	0.36	246.21	203.41	82.62	17.38
4	677.6	631.7	45.9	453	159	0.35	237.83	191.93	80.70	19.30
									Average	20.3

A16 - 20 - 1 coat										
5	695	645	50	448	162	0.36	251.32	201.32	80.10	19.90
6	686.8	633.6	53.2	449	160	0.36	244.74	191.54	78.26	21.74
7	682.1	638.2	43.9	447	159	0.36	242.63	198.73	81.91	18.09
8	673.7	632.5	41.2	451	161	0.36	240.50	199.30	82.87	17.13
									Average	19.2

A16 - 20 - 2 coats										
9	684.3	635.5	48.8	452	161	0.36	243.74	194.94	79.98	20.02
10	690.7	644.2	46.5	455	158	0.35	239.85	193.35	80.61	19.39
11	677.4	634	43.4	455	160	0.35	238.21	194.81	81.78	18.22
12	688.7	640.1	48.6	451	159	0.35	242.80	194.20	79.98	20.02
									Average	19.4

Appendix D – Detailed bar diameter measurements

Batch 1 – C45

Bar #	External diameter (mm)					Average bar diameter (mm)
	d1	d2	d3	d4	d5	
1	13.16	13.35	13.28	13.07	13.14	13.2
2	12.3	13.14	13.16	13.14	13.12	12.972
3	13.13	13.23	13.08	13.06	13.15	13.13
4	13.4	13.1	13	13.1	13.1	13.14
5	13.16	13.32	13.43	13.18	13.17	13.252
6	13.15	13.04	13.13	13.06	13.25	13.126
7	13.35	13.4	13.5	12.7	13.4	13.27
8	13.6	13.6	13.7	13.7	13.7	13.66
9	13	13	12.8	13	13.5	13.06
10	13.1	13.3	13.5	13.35	13.4	13.33
11	13.1	13	13	13.1	13.05	13.05
12	13.1	13.13	13.2	13.1	13.4	13.186

Bar #	Internal diameter (mm)					Average bar diameter (mm)
	d1	d2	d3	d4	d5	
1	12.2	11.8	11.85	11.65	11.7	11.84
2	11.2	11.5	11.5	11.4	11.2	11.36
3	11.4	11.6	11.7	12.1	12.8	11.92
4	11.8	11.8	11.9	11.8	11.9	11.84
5	11.4	11.1	11	11	11	11.1
6	11	10.9	10.9	10.9	10.9	10.92
7	11	11.1	11	11	11.1	11.04
8	11.5	11.5	11.3	11.5	11.3	11.42
9	11.6	11.7	11.5	11.7	11.5	11.6
10	11.45	11.2	11.1	11	11	11.15
11	11.3	11.35	11.2	11.2	11.2	11.25
12	10.95	10.9	10.9	10.8	10.9	10.89

Bar #	External diameter (mm) after 1st coat					Average bar diameter (mm)
	d1	d2	d3	d4	d5	
5	13.87	13.8	13.95	14.1	14.12	13.968
6	13.84	13.7	13.94	14.04	14.17	13.938
7	14.16	14.02	14.13	13.34	13.81	13.892
8	14.51	14.38	14.8	14.28	14.07	14.408
9	14.44	14.56	14.41	13.64	14	14.21
10	14	14.41	13.96	13.86	13.86	14.018
11	13.98	13.85	13.84	13.71	13.67	13.81
12	13.93	13.88	13.95	13.79	13.87	13.884

Bar #	Internal diameter (mm) after 1st coat					Average bar diameter (mm)
	d1	d2	d3	d4	d5	
5	11.45	12.22	12.46	14.04	14.17	12.868
6	11.92	11.41	11.86	11.32	11.4	11.582
7	12.22	12.38	12.37	12.36	11.8	12.226
8	12.75	12.54	12.65	12.03	12.14	12.422
9	11.85	12	11.73	12.05	12.1	11.946
10	11.92	11.72	11.93	11.75	12.18	11.9
11	11.92	11.99	11.78	11.94	12.07	11.94
12	11.75	11.55	11.62	11.75	11.49	11.632

Bar #	External diameter (mm) after 2nd coat					Average bar diameter (mm)
	d1	d2	d3	d4	d5	
9	14.44	14.74	14.74	14.74	15.01	14.734
10	14.67	14.63	14.5	14.43	14.6	14.566
11	14.24	14.37	14.59	14.48	14.3	14.396
12	14.04	14.21	14.3	14.26	14.52	14.266

Bar #	Internal diameter (mm) after 2nd coat					Average bar diameter (mm)
	d1	d2	d3	d4	d5	
9	12.92	13.12	13.3	13.15	13.23	13.144
10	12.78	12.41	12.91	13.05	13.01	12.832
11	13.61	13.54	13.6	13.25	13.18	13.436
12	13	12.7	13.4	13.14	13.28	13.104

Batch 2 - C45

Bar diameter measured @ 15 mm intervals											
Bar #	**d1**	**d2**	**d3**	**d4**	**d5**	**d6**	**d7**	**d8**	**d9**	**d10**	**Average bar diameter (mm)**
1	10.05	9.6	8.9	10.2	9.05	10.1	9.8	9.65	9.8	10.95	9.81
2	10.6	9.2	10.7	9.3	9.7	9.6	9.3	10.5	10.5	10.8	10.02
3	10.4	8.2	10	10.1	10.15	10.5	10.3	8.1	10	10.5	9.825
4	10.9	10.9	8.7	8.3	10	10.6	9.7	9.9	10	10.8	9.98
5	9	8	8.6	9.8	10.4	9.8	10.3	10.5	10	9.9	9.63
6	10.8	10.1	8.5	10	9.7	8.5	9.5	10	10.5	10.8	9.84
7	10	10.1	10.9	10.3	8.4	10.7	10.7	9	10.6	10.9	10.16
8	10.3	9.1	11.2	8.8	10.8	10.8	11	9.7	9.6	10.4	10.17
9	10.55	10.7	10.25	9	10.75	10.6	10.75	9.95	10.7	10.6	10.385
10	10.85	9.7	10.5	11	10.7	9.8	10.9	9.6	10.6	11.2	10.485
11	10.5	10	10.6	10.6	7.1	10	9.6	10.1	9.7	10.8	9.9
12	10.4	10	9.85	10.6	9.5	11.1	10	9.3	10.7	10.9	10.235

Bar diameter measured @ 15 mm intervals after 1st coat											
Bar #	**d1**	**d2**	**d3**	**d4**	**d5**	**d6**	**d7**	**d8**	**d9**	**d10**	**Average bar diameter (mm)**
5	10.69	9.18	9	11.23	11.1	11.16	11.14	11.17	11.13	10.3	10.61
6	11.43	11.2	10.86	10.41	10.59	10	11.14	11.13	11.84	11.67	11.027
7	11.4	10.86	11.43	11.31	10.31	11.63	11.45	9.79	12.11	11.98	11.227
8	11.45	10.4	11.43	7.02	9.16	12.15	11.33	11.66	10.52	11.5	10.662
9	11.35	11.41	11.12	10.65	11.96	10.86	11.54	10.56	11.42	10.96	11.183
10	11.29	10.92	11.32	11.51	11.77	10.77	11.53	11.38	11.25	11.88	11.362
11	10.69	11.21	11.37	11.5	8.25	11.37	11.55	10.97	10.63	11.64	10.918
12	11.13	11.58	10.48	11.43	10.9	11.66	11.1	10.32	11.28	11.63	11.151

Bar diameter measured @ 15 mm intervals after 2nd coat											
Bar #	**d1**	**d2**	**d3**	**d4**	**d5**	**d6**	**d7**	**d8**	**d9**	**d10**	**Average bar diameter (mm)**
9	13.18	13.49	12.01	13.84	12.1	11.95	13	11.93	11.79	10.92	12.421
10	12.85	11.03	12.05	13.1	13.1	11.97	13.04	12.76	12.99	12.37	12.526
11	11.46	11.68	12.09	12.26	8.76	11.73	11.85	11.62	11.5	12.06	11.501
12	11.94	12.47	11.35	12.38	12.28	10.72	12.6	11.43	12.16	12.5	11.983

Batch 1 – M45

Bar #	External diameter (mm)					Average bar diameter (mm)
	d1	d2	d3	d4	d5	
1	13.0	13.0	13.1	13.2	13.1	13.1
2	12.9	13.0	12.9	12.9	12.8	12.9
3	12.9	12.9	13.0	13.0	12.9	12.9
4	13.0	13.1	13.1	13.2	13.2	13.1
5	13.5	13.3	13.2	13.2	13.2	13.3
6	13.0	13.1	13.2	13.2	13.1	13.1
7	12.9	12.9	12.9	12.9	12.8	12.9
8	12.8	12.9	13.0	12.7	12.9	12.9
9	13.2	13.4	13.3	13.2	13.2	13.2
10	13.0	13.9	12.9	13.0	13.0	13.2
11	13.0	13.1	13.0	13.1	13.1	13.1
12	12.9	13.1	13.1	13.0	13.0	13.0

Bar #	Internal diameter (mm)					Average bar diameter (mm)
	d1	d2	d3	d4	d5	
1	10.94	11.1	11.03	11.05	11.06	11.036
2	11.07	11.03	11.1	11.09	11.08	11.074
3	11.1	11.07	11.12	11.11	11.14	11.108
4	11.5	11.41	11.37	11.46	11.49	11.446
5	11.5	12	11.76	11.86	11.63	11.75
6	11.5	11.6	11.56	11.53	11.54	11.546
7	11.1	11.2	11.14	11.21	11.17	11.164
8	11.3	11.1	11.19	11.17	11.25	11.202
9	11.15	11	11.16	11.09	11.13	11.106
10	11.2	11.1	11.18	11.06	11.12	11.132
11	11.4	11.26	11.37	11.25	11.38	11.332
12	11.48	11.3	11.46	11.38	11.43	11.41

Bar #	External diameter (mm) after 1st coat					Average bar diameter (mm)
	d1	d2	d3	d4	d5	
5	13.61	14.29	14.06	13.98	14.12	14.012
6	13.39	13.38	13.43	13.65	13.38	13.446
7	13.3	13.5	13.67	13.54	13.78	13.558
8	13.45	13.56	13.54	13.56	13.49	13.52
9	14.57	14.01	14.29	14.15	14.27	14.258
10	14.04	14.45	14.35	14.02	14.17	14.206
11	14.1	14.16	14.28	14.09	14.15	14.156
12	13.76	14.08	13.96	13.78	13.99	13.914

Bar #	Internal diameter (mm) after 1st coat					Average bar diameter (mm)
	d1	d2	d3	d4	d5	
5	13.73	12.5	13.39	13.27	13.36	13.25
6	12.15	12.85	12.6	12.64	12.58	12.564
7	12.41	12.26	12.37	12.31	13.29	12.528
8	12.53	12.56	12.48	12.59	12.55	12.542
9	12.63	12.61	12.59	12.64	12.67	12.628
10	13.47	13.39	13.48	13.49	13.61	13.488
11	12.42	12.81	12.75	12.72	12.53	12.646
12	12.77	13.03	12.88	12.79	12.51	12.796

Bar #	External diameter (mm) after 2nd coat					Average bar diameter (mm)
	d1	d2	d3	d4	d5	
9	14.95	14.73	14.86	14.65	14.98	14.834
10	14.71	14.93	15.04	14.77	15.1	14.91
11	14.82	14.78	15.15	14.92	14.85	14.904
12	14.66	14.75	14.63	14.53	14.84	14.682

Bar #	Internal diameter (mm) after 2nd coat					Average bar diameter (mm)
	d1	d2	d3	d4	d5	
9	13.54	13.46	13.67	13.53	13.64	13.568
10	13.62	14.53	14.65	13.98	13.42	14.04
11	13.09	13.68	13.47	13.36	13.52	13.424
12	13.38	13.78	13.48	13.48	13.54	13.532

Batch 2 – M45

Bar diameter measured @ 15 mm intervals											
Bar #	**d1**	**d2**	**d3**	**d4**	**d5**	**d6**	**d7**	**d8**	**d9**	**d10**	**Average bar diameter (mm)**
1	11	9.7	11.4	10.3	10.25	10.7	10.8	10	11.2	11	10.635
2	9.6	10.7	9.4	9	10	9.5	8.5	10.15	10.4	8.9	9.615
3	11.8	9.7	10.1	10.9	9.6	10.7	10.4	10.2	10.5	11.5	10.54
4	10.8	10.3	10.7	10.5	10.6	10.6	9.1	10	10.8	10.6	10.4
5	10.25	10.7	9	10.8	10.3	8.95	11.1	10.4	10.6	11	10.31
6	10.1	10.15	9.25	10.5	10.5	10.8	8.7	10.5	10.8	10.9	10.22
7	10.75	11	10	11.1	11	10.4	9.7	11.2	10.7	11	10.685
8	10.6	10	10.3	10.8	9.75	9.9	9.3	10.8	10.9	10.8	10.315
9	10.2	10.3	10.25	10	10.3	9.4	10.3	10.9	9.7	10.6	10.195
10	10.1	10.6	9	9.7	10.25	10.5	10.1	9.5	10.2	10.7	10.065
11	10.8	9.7	10.7	9.8	9.9	10.7	10.9	10	10.7	11.1	10.43
12	10.3	10.6	9.5	10.5	10	9.3	9.4	11	9.65	10.1	10.035

Bar diameter measured @ 15 mm intervals after 1st coat											
Bar #	**d1**	**d2**	**d3**	**d4**	**d5**	**d6**	**d7**	**d8**	**d9**	**d10**	**Average bar diameter (mm)**
5	10.71	10.92	10.31	12.17	11.11	10.79	12.38	11.68	11.65	10.98	11.27
6	11.1	11.35	11.4	11.1	10.81	11.4	10.22	11.04	11.66	11.56	11.164
7	11.77	12.59	11.31	12.55	12.42	10.8	10.7	12.17	12.2	11.18	11.769
8	11.6	10.78	11.13	11.91	10.9	11.49	11.56	11.34	12.02	11.3	11.403
9	11.12	11.45	11.69	10.97	11.4	11.25	10.89	11.13	11.2	10.34	11.144
10	11.09	11.35	10.7	10.52	11.7	11.14	10.67	10	10.9	11.38	10.945
11	11.48	10.89	11.27	9.82	10.75	12.54	11.58	11.37	11.58	11.37	11.265
12	11.38	11.65	10.53	11.59	11.51	10.35	11.13	11.47	11	10.74	11.135

Bar diameter measured @ 15 mm intervals after 2nd coat											
Bar #	**d1**	**d2**	**d3**	**d4**	**d5**	**d6**	**d7**	**d8**	**d9**	**d10**	**Average bar diameter (mm)**
9	11.97	12.78	12.62	12.33	12.42	12.4	12.74	12.68	11.53	11.17	12.264
10	12.35	12.08	11.32	11.26	12.17	12.3	12.48	11.69	12.69	11.87	12.021
11	13.37	12.82	13.24	11.94	11.36	12.48	12.15	12.59	12.26	11.46	12.367
12	12.84	12.8	12.06	12.93	11.74	11.67	13.2	12.61	11.67	11.35	12.287

Batch 1 – M65

Bar #	External diameter (mm)					Average bar diameter (mm)
	d1	d2	d3	d4	d5	
1	13.12	13.03	13.03	13.06	12.91	13.03
2	13.01	13.12	13.14	13.12	13.08	13.094
3	12.98	13.03	13.17	13.18	13.18	13.108
4	13	12.92	13.03	13.16	12.96	13.014
5	12.86	13.07	12.97	13.09	13.15	13.028
6	12.95	12.87	12.84	13.12	13.04	12.964
7	13.14	13.02	13.16	13.04	13.12	13.096
8	13.09	13.01	13.02	12.92	12.79	12.966
9	13.17	13.17	13.04	13.13	13	13.102
10	13.11	13.13	12.95	12.88	12.82	12.978
11	13.16	12.98	13.08	13.01	12.94	13.034
12	12.99	13.05	13.16	12.94	13.07	13.042

Bar #	Internal diameter (mm)					Average bar diameter (mm)
	d1	d2	d3	d4	d5	
1	11.14	11.18	11.19	11.25	11.39	11.23
2	11.36	11.76	11.56	11.37	11.32	11.474
3	11.18	11.14	11.09	11.15	11.19	11.15
4	11.54	11.43	11.38	11.58	11.26	11.438
5	11.37	11.27	11.23	11.24	11.54	11.33
6	11.23	11.17	11.16	11.19	11.37	11.224
7	11.09	11.31	11.18	11.1	11.15	11.166
8	11.86	11.88	11.53	11.32	11.16	11.55
9	11.28	11.22	11.29	11.34	11.83	11.392
10	11.78	11.59	11.37	11.52	11.64	11.58
11	11.25	11.37	11.51	11.27	11.26	11.332
12	11.53	11.24	11.21	11.33	11.45	11.352

Bar #	External diameter (mm) after 1st coat					Average bar diameter (mm)
	d1	d2	d3	d4	d5	
5	13.96	13.72	13.55	13.85	13.91	13.798
6	13.46	13.51	13.5	13.67	13.74	13.576
7	13.61	13.78	13.9	13.84	13.79	13.784
8	14.28	14.07	14.16	14.13	14.09	14.146
9	13.87	13.93	14.1	14.08	14.16	14.028
10	13.98	14.04	14.02	14.02	13.88	13.988
11	13.93	13.97	13.85	14.02	14.04	13.962
12	13.87	14.16	14.07	13.98	13.92	14

Bar #	Internal diameter (mm) after 1st coat					Average bar diameter (mm)
	d1	d2	d3	d4	d5	
5	12.83	12.35	12.6	12.75	12.43	12.592
6	12.28	12.42	12.26	12.48	12.72	12.432
7	12.51	12.22	12.2	12.36	12.45	12.348
8	12.63	12.45	12.28	12.41	12.53	12.46
9	12.51	12.73	12.86	12.57	12.71	12.676
10	12.29	12.17	12.24	12.31	12.28	12.258
11	12.25	12.17	12.43	12.32	12.54	12.342
12	12.68	12.6	12.83	12.59	12.65	12.67

Bar #	External diameter (mm) after 2nd coat					Average bar diameter (mm)
	d1	d2	d3	d4	d5	
9	15.78	14.75	14.59	14.76	14.85	14.946
10	14.83	14.59	14.73	14.92	14.58	14.73
11	14.35	14.41	14.49	14.34	14.42	14.402
12	14.57	14.92	14.82	14.65	14.65	14.722

Bar #	Internal diameter (mm) after 2nd coat					Average bar diameter (mm)
	d1	d2	d3	d4	d5	
9	13.43	13.45	13.67	13.36	13.15	13.412
10	13.54	13.36	13.42	13.61	13.25	13.436
11	13.35	13.32	13.45	13.37	13.12	13.322
12	13.27	13.21	13.33	13.53	13.34	13.336

Batch 2 – M65

Bar diameter measured @ 15 mm intervals											
Bar #	**d1**	**d2**	**d3**	**d4**	**d5**	**d6**	**d7**	**d8**	**d9**	**d10**	**Average bar diameter (mm)**
1	10.8	10	10.4	10.8	10.7	11.2	11.7	10.3	10.7	12.6	10.92
2	12	11.4	10.5	11.7	10	9.4	11.1	10.5	11.2	10.5	10.83
3	11.1	11.15	10.3	11.25	10.8	11.15	11.1	11.2	11.1	11.4	11.055
4	12	11.9	11.2	11	10.1	11.5	11.8	11.2	11.3	11.1	11.31
5	11.2	10.9	11.3	10.5	11.4	12	11.2	10.4	11.4	12.5	11.28
6	11.3	10.9	10.7	11.2	10.8	11.1	10	10.1	11.1	11.2	10.84
7	11.3	9.1	10.4	12	11.5	12.7	11.8	11	11.2	11.8	11.28
8	11	11.5	12.2	11.8	10.8	11.8	11.5	12	11.9	11.7	11.62
9	11.2	10.4	10.5	11.8	11.3	9.8	10	10.9	11	11.5	10.84
10	11.1	10.9	10.9	10.1	10	11	11.1	10.5	11.8	11.5	10.89
11	10.7	10	10.8	11.8	9.9	10.6	11.5	12.2	12.1	11	11.06
12	13	12.3	11.1	10.6	11.3	11.1	10.5	11.8	11.1	10.9	11.37

1st coat - Bar diameter measured @ 15 mm intervals											
Bar #	**d1**	**d2**	**d3**	**d4**	**d5**	**d6**	**d7**	**d8**	**d9**	**d10**	**Average bar diameter (mm)**
5	12.72	11.38	12.07	11.39	13.32	12.78	12.17	11.55	13.8	12.77	12.395
6	13.1	13.25	12.69	12.66	13.06	13.34	12.6	12.92	13.19	13.36	13.017
7	13.08	10.47	12.17	12.77	13.16	13.53	13.4	13.16	12.7	13.38	12.782
8	12.92	12.51	13.08	12.5	12.7	12.74	12.05	11.76	12.77	13.04	12.607
9	13.17	12.15	12.98	13.41	12.76	12.55	13.01	12.78	12.89	12.11	12.781
10	12.34	12.78	12.53	12.96	12.68	12.68	12.83	12.75	12.55	12.69	12.679
11	12.88	12.64	12.73	12.03	12.97	12.54	12.86	12.91	12.89	12.43	12.688
12	12.95	12.75	12.58	12.49	12.53	12.27	12.24	12.38	12.17	12.05	12.441

Second coat - Bar diameter measured @ 15 mm intervals											
Bar #	**d1**	**d2**	**d3**	**d4**	**d5**	**d6**	**d7**	**d8**	**d9**	**d10**	**Average bar diameter (mm)**
9	14.15	12.76	13.7	14.07	13.37	13.04	14.26	14.33	14.47	12.71	13.686
10	13.48	13.94	13.5	13.6	13.65	13.54	13.51	14.11	13.52	13.73	13.658
11	13.97	13.67	13.82	13.92	12.6	13.34	13.85	13.75	14	13.01	13.593
12	14.68	13.36	13.41	13.37	14	14.05	13.58	13.51	13.66	12.86	13.648

Batch 3 – M65

Bar diameter measured @ 15 mm intervals											
Bar #	**d1**	**d2**	**d3**	**d4**	**d5**	**d6**	**d7**	**d8**	**d9**	**d10**	**Average bar diameter (mm)**
1	10.2	10	9.5	10.8	10.7	10.9	9.9	10.1	9.5	10.85	10.245
2	11	9.7	9.75	10.5	10.55	9.95	10.3	10	9.1	9.9	10.075
3	10.6	9.2	8.9	9.5	9.7	9.9	9.8	9.8	9.9	9.9	9.72
4	9.1	9.2	9.4	9.2	9.35	8	8.9	9.3	9.4	9	9.085
5	8.9	9.4	9.5	10	10.4	9	10.6	9.7	10.1	11.4	9.9
6	10.5	10.4	10.2	10.3	8.9	10.2	9.6	9.9	10.4	10.9	10.13
7	10.1	10.7	10.9	10	9.9	10.4	10	10	10.7	11	10.37
8	10.5	9	10.6	10.4	10.9	10.4	10.9	11	9.8	10.7	10.42
9	10.5	10.6	10	10.1	9.5	10.2	10.1	10.2	10.5	10.9	10.26
10	10	10.5	9.8	11	9.9	10.1	10.1	10.6	9.8	10.8	10.26
11	10.7	10.4	9.1	10.3	10.7	9.6	10.4	10.5	10.6	10.5	10.28
12	10.3	10.1	9.8	10.2	10	9.9	10.1	10.1	10.2	10.6	10.13

Bar diameter measured @ 15 mm intervals after 1st coat											
Bar #	**d1**	**d2**	**d3**	**d4**	**d5**	**d6**	**d7**	**d8**	**d9**	**d10**	**Average bar diameter (mm)**
5	10.95	11.24	11.69	11	11.87	9.97	11.59	10.54	10.84	12.69	11.238
6	11.15	11.79	11.29	11.2	10.07	11.24	10.78	11.43	11.41	11.58	11.194
7	11.44	11.29	11.69	11.3	11.1	11.41	10.93	11.25	12	11.98	11.439
8	11.1	10.56	11.69	11.24	11.65	11.39	11.63	11.65	11.34	11.55	11.38
9	11.28	11.97	11.42	11.36	11.01	11.31	11.45	11.16	11.25	11.65	11.386
10	11.38	11.76	11.45	12.38	11.37	11.94	11.68	11.97	12.03	11.33	11.729
11	11.48	11.38	11.29	12.47	11.39	11.98	11.56	11.84	11.97	11.38	11.674
12	11.45	11.33	11.04	11.16	11.18	11.46	11.27	11.19	11.32	11.21	11.261

Bar diameter measured @ 15 mm intervals after 2nd coat											
Bar #	**d1**	**d2**	**d3**	**d4**	**d5**	**d6**	**d7**	**d8**	**d9**	**d10**	**Average bar diameter (mm)**
9	12.66	13.24	11.98	12.21	11.8	12.55	13.32	12.09	13.14	12.87	12.586
10	12.11	12.95	12.53	13.73	12.17	13.08	12.74	13.07	13.08	12.4	12.786
11	12.31	12.82	12.1	12.58	13.37	12.31	12.75	13.4	13.57	12.18	12.739
12	12.63	12.46	11.83	12.35	12.26	12.59	11.89	12.22	12.52	11.9	12.265

Batch 4 – M65

Bar #	External diameter (mm)					Average bar diameter (mm)
	d1	d2	d3	d4	d5	
1	17.38	17.41	17.41	17.45	17.37	17.37
2	17.67	17.71	17.72	17.65	17.69	17.69
3	17.38	17.39	17.42	17.4	17.42	17.42
4	17.38	17.35	17.39	17.51	17.44	17.44
5	17.37	17.4	17.4	17.43	17.41	17.41
6	17.68	17.7	17.72	17.71	17.69	17.69
7	17.19	17.17	17.23	17.19	17.22	17.22
8	17.45	17.54	17.52	17.5	15.48	15.48
9	17.29	17.3	17.28	17.34	17.3	17.30
10	17.33	17.29	17.38	17.35	17.35	17.35
11	17.07	17.11	17.13	17.06	17.08	17.08
12	17.28	17.28	17.3	17.31	17.28	17.28

Bar #	Internal diameter (mm)					Average bar diameter (mm)
	d1	d2	d3	d4	d5	
1	15.11	15.05	15.06	15.12	15.09	15.09
2	15.38	15.4	15.39	15.44	15.52	15.43
3	15.14	15.11	15.17	15.03	15.09	15.11
4	15.2	15.22	15.27	15.21	15.09	15.20
5	15.02	14.97	14.99	15.01	15	15.00
6	15.05	15.15	15.08	15.16	15	15.09
7	15.12	15.12	15.04	15.06	15.1	15.09
8	15.39	15.33	15.38	15.37	15.42	15.38
9	15.19	15.18	15.23	15.22	15.21	15.21
10	15.56	15.55	15.59	15.6	15.61	15.58
11	15.33	15.41	15.37	15.35	15.37	15.37
12	15.09	15.08	15.1	15.13	15.09	15.10

Bar #	External diameter (mm) after 1st coat					Average bar diameter (mm)
	d1	d2	d3	d4	d5	
5	18.63	18.73	18.85	18.86	19.14	18.842
6	18.89	18.56	18.89	18.76	18.83	18.786
7	18.62	18.79	19.05	18.97	19.03	18.892
8	18.4	18.29	18.15	18.32	18.54	18.34
9	18.4	18.3	18.23	18.75	18.56	18.448
10	18.54	18.41	18.67	18.74	18.55	18.582
11	19.16	18.7	18.15	18.91	18.83	18.75
12	18.34	18.3	18.45	18.53	18.3	18.384

Bar #	Internal diameter (mm) after 1st coat					Average bar diameter (mm)
	d1	d2	d3	d4	d5	
5	16.76	16.56	17.47	17.07	17.2	17.012
6	16.95	16.21	16.48	16.52	16.39	16.51
7	16.92	16.59	16.54	16.72	16.35	16.624
8	16.52	16.5	16.3	16.27	16.65	16.448
9	16.53	16.45	16.62	16.31	16.74	16.53
10	16.7	17.02	17.05	17.1	16.89	16.952
11	16.82	16.5	16.49	16.38	16.41	16.52
12	15.27	15.99	15.44	15.63	16.03	15.672

Bar #	External diameter (mm) after 2nd coat					Average bar diameter (mm)
	d1	d2	d3	d4	d5	
9	18.8	19	18.98	19.14	19.23	19.03
10	18.74	18.96	19.2	19.15	19.07	19.024
11	19.4	18.87	18.78	19.33	19.48	19.172
12	18.98	19.01	18.94	19.54	18.93	19.08

Bar #	Internal diameter (mm) after 2nd coat					Average bar diameter (mm)
	d1	d2	d3	d4	d5	
9	16.9	17.01	17.55	17.41	17.86	17.346
10	17.09	17.61	17.41	17.43	17.29	17.366
11	17.32	16.75	16.97	16.72	16.97	16.946
12	16.93	16.95	17.01	16.72	17	16.922

Batch 5 – M65

Bar diameter measured @ 15 mm intervals											
Bar #	d1	d2	d3	d4	d5	d6	d7	d8	d9	d10	Average bar diameter (mm)
1	14.6	14	14.5	14.7	13.2	14.6	14	14.3	14.4	14.8	14.31
2	14.5	14.6	14.4	14.3	14.5	14.3	14.1	14.8	15	14.8	14.53
3	14	13.5	13.6	14.3	13.9	14	13.6	14.1	13.6	14.2	13.88
4	13.8	11.8	14.1	14.1	14	12.7	13	12.7	14	13.8	13.4
5	14.8	13.9	13.9	14.2	13	14.4	14.3	13.9	14.1	14.7	14.12
6	14.3	12.2	14.4	14.1	13.2	13.9	14.3	14.1	13.8	15	13.93
7	14.7	14.7	14.3	14.5	13.4	14.1	14.4	14.3	14	13.9	14.23
8	14.4	14.5	14.6	13.8	14	13.1	14.5	14.2	13.7	14.5	14.13
9	14.4	15	14	14.2	14.4	14.6	14.3	13.9	14.6	14.7	14.41
10	13.9	14.1	12.4	14.4	12.2	14.3	13.8	14.1	13.5	14.3	13.7
11	13	14.8	13.1	14.6	14	13.7	14.3	13.5	14.5	14.1	13.96
12	14	14.8	13.7	14.4	13.6	13.6	13.9	13.7	12.2	13.3	13.72

Bar diameter measured @ 15 mm intervals after 1st coat											
Bar #	**d1**	**d2**	**d3**	**d4**	**d5**	**d6**	**d7**	**d8**	**d9**	**d10**	**Average bar diameter (mm)**
5	15.98	15.14	14.46	15.4	12.41	14.5	14.54	14.32	15.65	16.15	14.855
6	15.38	13.55	15.35	14.68	15.1	15.07	15.32	15.09	15.13	15.62	15.029
7	15.47	15.24	15.45	15.05	14.14	14.7	15.96	14.07	15.78	14.8	15.066
8	15.35	15.72	15.51	15.1	15.98	15.49	15.76	15.18	15.5	15.36	15.495
9	15.13	15.29	14.85	15.03	15.12	15.14	15.04	15.13	15.02	15.28	15.103
10	15.18	15.04	15.01	14.89	14.93	15.34	15.28	14.79	15.15	15.26	15.087
11	15.28	15.37	15.19	15.28	15.32	15.17	15.49	15.13	15.29	15.16	15.268
12	15.06	15.43	15.18	15.02	14.68	14.72	15.16	15.01	14.93	15.07	15.026

Bar diameter measured @ 15 mm intervals after 2nd coat											
Bar #	**d1**	**d2**	**d3**	**d4**	**d5**	**d6**	**d7**	**d8**	**d9**	**d10**	**Average bar diameter (mm)**
9	15.97	17.25	15.2	16.5	15.94	16.36	15.97	16.19	15.8	16.47	16.165
10	15.99	15.79	15.52	15.5	15.27	16.33	16.4	15.09	16.42	16.32	15.863
11	16.68	17.73	16.22	17.04	16.52	15.57	17.63	15.55	16.94	15.91	16.579
12	16	17.14	15.79	15.37	15.12	15.56	15.83	15.77	15.81	16.16	15.855

Appendix E – Coating thickness for each bar

Treatment	Bar diameter (mm)	12							16	
	Coating thickness (mm)	C45 - 0	C45 - 20	B45 - 0	B45 - 20	M65 - 0	M65 - 10	M65 - 20	M65 - 0	M65 - 20
1 coat	5	0.6	0.5	0.6	0.5	0.5	0.6	1.3	0.9	0.4
	6	0.4	0.6	0.3	0.5	0.5	1.1	1.1	0.6	0.5
	7	0.5	0.5	0.5	0.5	0.5	0.8	1.1	0.8	0.4
	8	0.4	0.2	0.5	0.5	0.5	0.5	1.0	0.6	0.7
2 coats	9	0.8	1.0	1.0	1.0	1.0	1.4	2.3	1.3	0.9
	10	0.7	1.0	1.2	1.0	0.9	1.4	2.5	1.2	1.1
	11	0.9	0.8	1.0	1.0	0.8	1.3	2.5	1.2	1.3
	12	0.8	0.9	0.9	1.1	0.9	1.1	2.1	1.0	1.1
Average		0.6	0.7	0.8	0.8	0.7	1.0	1.7	1.0	0.8

Appendix F – Trial Mix and Detailed Compressive strength results

Compressive strength – Trial mix results

Trial No. 1	**M65 (w/b – 0.65)**	**M45 (w/b – 0.47)**	**C45 (w/b – 0.45)**
TAS (MPa)	32	53	53
3 days age	22.2	33.6	52.9
	22.4	34.0	51.8
	21.8	33.3	49.9
7 days age	28.4	38.4	53.4
	28.4	42.0	52.8
	28.3	40.2	54.4
28 days age	34.6	50	62
	33.8	49.7	61.8
	34	51.5	63.2
Trial No. 2	**M65 (w/b – 0.65)**	**M45 (w/b – 0.47)**	**C45 (w/b – 0.45)**
TAS (MPa)	32	53	53
3 days age	23.0	35	42.2
	20.2	35.8	40.4
	22.2	35.8	42.5
7 days age	28.5	43.4	46.3
	28.6	43.6	48.4
	28.2	44.4	49.0
28 days age	35.2	55.4	60.3
	33.7	53.7	62.1
	34.5	54	61.4

Compressive strength results for each batch

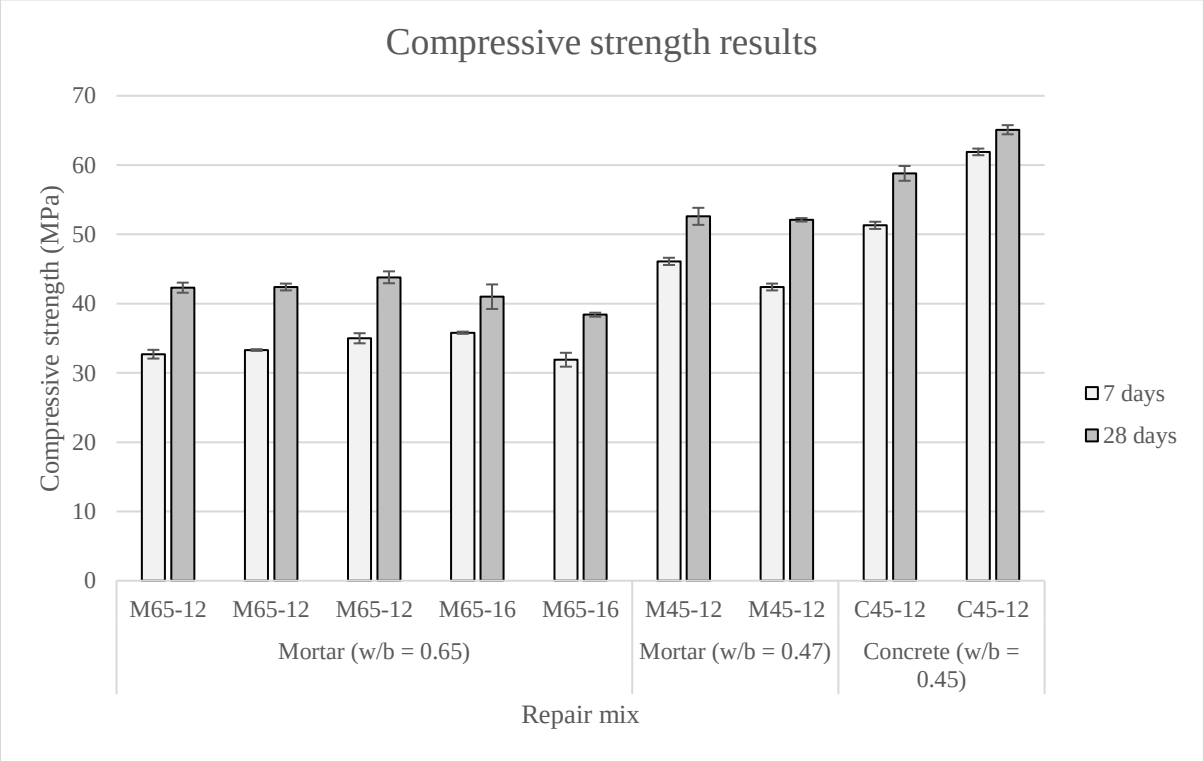

Detailed Compressive strength results

Ref. Mix	Mix C1
Composition	CEM I 52.5N
w/b	0.45
Cast date	25/08/2021

Date - 25/08	**Cube**	**Length (mm)**	**Breadth (mm)**	**Height (mm)**	**Mass (kg)**	**Failure load (kN)**	**Compressive strength (Mpa)**
	1	100.00	100.00	101.47	2.342	510	51.0
	2	100.00	100.00	101.20	2.258	508	50.8
Age: 7 days	3	100.00	100.00	100.97	2.341	520	52.0
					Average	513	51.3

Date - 01/09	**Cube**	**Length (mm)**	**Breadth (mm)**	**Height (mm)**	**Mass (kg)**	**Failure load (kN)**	**Compressive strength (Mpa)**
	1	100.00	100.00	100.45	2.467	570	57.4
	2	100.00	100.00	100.23	2.455	590	59
Age: 28 days	3	100.00	100.00	100.63	2.445	600	60
					Average	587	58.80

Ref. Mix	Mix C2
Composition	CEM I 52.5N
w/b	0.45
Cast date	27/08/2021

Date - 27/08	**Cube**	**Length (mm)**	**Breadth (mm)**	**Height (mm)**	**Mass (kg)**	**Failure load (kN)**	**Compressive strength (Mpa)**
	1	100.00	100.00	100.89	2.387	621	62.1
	2	100.00	100.00	100.92	2.346	623	62.3
Age: 7 days	3	100.00	100.00	100.96	2.431	612	61.2
					Average	618.67	61.87

Date - 03/09	**Cube**	**Length (mm)**	**Breadth (mm)**	**Height (mm)**	**Mass (kg)**	**Failure load (kN)**	**Compressive strength (Mpa)**
	1	100.00	100.00	100.48	2.432	650	65
	2	100.00	100.00	100.37	2.434	644	64.4
Age: 28 days	3	100.00	100.00	100.43	2.378	660	66
					Average	651.33	65.13

Ref. Mix	Mix B1
Composition	CEM I 52.5N
w/b	0.47
Cast date	31/08/2021

Date - 31/08	**Cube**	**Length (mm)**	**Breadth (mm)**	**Height (mm)**	**Mass (kg)**	**Failure load (kN)**	**Compressive strength (Mpa)**
	1	100.00	100.00	100.29	2.355	458	45.8
	2	100.00	100.00	100.35	2.376	456	45.6
Age: 7 days	3	100.00	100.00	100.48	2.387	468	46.8
					Average	460.67	46.07

Date - 07/09	**Cube**	**Length (mm)**	**Breadth (mm)**	**Height (mm)**	**Mass (kg)**	**Failure load (kN)**	**Compressive strength (Mpa)**
	1	100.00	100.00	101.38	2.421	516	51.6
	2	100.00	100.00	101.28	2.388	518	51.8
Age: 28 days	3	100.00	100.00	101.4	2.412	543	54.3
					Average	525.67	52.57

Ref. Mix	Mix B2
Composition	CEM I 52.5N
w/b	0.47
Cast date	02/09/2021

Date - 02/09	**Cube**	**Length (mm)**	**Breadth (mm)**	**Height (mm)**	**Mass (kg)**	**Failure load (kN)**	**Compressive strength (Mpa)**
	1	100.00	100.00	100.57	2.298	430	43
	2	100.00	100.00	100.39	2.306	418	41.8
Age: 3 days	3	100.00	100.00	100.48	2.301	425	42.5
					Average	424.33	42.43

Date - 09/09	**Cube**	**Length (mm)**	**Breadth (mm)**	**Height (mm)**	**Mass (kg)**	**Failure load (kN)**	**Compressive strength (Mpa)**
	1	100.00	100.00	102.18	2.432	524	52.4
	2	100.00	100.00	101.96	2.215	518	51.8
Age: 28 days	3	100.00	100.00	101.92	2.318	522	52.2
					Average	521.33	52.13

Ref. Mix	Mix A1
Composition	CEM I 52.5N
w/b	0.65
Cast date	06/09/2021

Date - 06/09	**Cube**	**Length (mm)**	**Breadth (mm)**	**Height (mm)**	**Mass (kg)**	**Failure load (kN)**	**Compressive strength (Mpa)**
	1	100.00	100.00	101.1	2.293	336	33.6
	2	100.00	100.00	100.97	2.304	325	32.5
Age: 7 days	3	100.00	100.00	101.22	2.303	321	32.1
					Average	327.33	32.73

Date - 13/09	**Cube**	**Length (mm)**	**Breadth (mm)**	**Height (mm)**	**Mass (kg)**	**Failure load (kN)**	**Compressive strength (Mpa)**
	1	100.00	100.00		2.358	420	42
	2	100.00	100.00		2.301	416	41.6
Age: 28 days	3	100.00	100.00		2.311	433	43.3
					Average	423	42.3

Ref. Mix	Mix A2
Composition	CEM I 52.5N
w/b	0.65
Cast date	08/09/2021

Date - 08/09	**Cube**	**Length (mm)**	**Breadth (mm)**	**Height (mm)**	**Mass (kg)**	**Failure load (kN)**	**Compressive strength (Mpa)**
	1	100.00	100.00		2.267	333	33.3
	2	100.00	100.00		2.256	335	33.5
Age: 7 days	3	100.00	100.00		2.305	332	33.2
					Average	333	33.33

Date - 15/09	**Cube**	**Length (mm)**	**Breadth (mm)**	**Height (mm)**	**Mass (kg)**	**Failure load (kN)**	**Compressive strength (Mpa)**
	1	100.00	100.00		2.234	423	42.3
	2	100.00	100.00		2.294	418	41.8
Age: 28 days	3	100.00	100.00		2.271	430	43
					Average	424	42.4

Ref. Mix	Mix A3
Composition	CEM I 52.5N
w/b	0.65
Cast date	10/09/2021

Date - 10/09	**Cube**	**Length (mm)**	**Breadth (mm)**	**Height (mm)**	**Mass (kg)**	**Failure load (kN)**	**Compressive strength (Mpa)**
	1	100.00	100.00		2.293	347	34.7
	2	100.00	100.00		2.312	343	34.3
Age: 7 days	3	100.00	100.00		2.311	360	36
					Average	350	35

Date - 17/09	**Cube**	**Length (mm)**	**Breadth (mm)**	**Height (mm)**	**Mass (kg)**	**Failure load (kN)**	**Compressive strength (Mpa)**
	1	100.00	100.00		2.271	426	42.6
	2	100.00	100.00		2.288	442	44.2
Age: 28 days	3	100.00	100.00		2.34	446	44.6
					Average	438	43.8

Ref. Mix	Mix A4
Composition	CEM I 52.5N
w/b	0.65
Cast date	14/09/2021

Date - 14/09	**Cube**	**Length (mm)**	**Breadth (mm)**	**Height (mm)**	**Mass (kg)**	**Failure load (kN)**	**Compressive strength (Mpa)**
	1	100.00	100.00		2.253	356	35.6
	2	100.00	100.00		2.273	360	36
Age: 7 days	3	100.00	100.00		2.248	358	35.8
					Average	358	35.8

Date - 21/09	**Cube**	**Length (mm)**	**Breadth (mm)**	**Height (mm)**	**Mass (kg)**	**Failure load (kN)**	**Compressive strength (Mpa)**
	1	100.00	100.00		2.249	385	38.5
	2	100.00	100.00		2.255	422	42.2
Age: 28 days	3	100.00	100.00		2.251	423	42.3
					Average	410	41.0

Ref. Mix	Mix A5
Composition	CEM I 52.5N
w/b	0.65
Cast date	16/09/2021

Date - 16/09	**Cube**	**Length (mm)**	**Breadth (mm)**	**Height (mm)**	**Mass (kg)**	**Failure load (kN)**	**Compressive strength (Mpa)**
	1	100.00	100.00		2.247	324	32.4
	2	100.00	100.00		2.24	328	32.8
Age: 7 days	3	100.00	100.00		2.237	305	30.5
					Average	319	31.9

Date - 23/09	**Cube**	**Length (mm)**	**Breadth (mm)**	**Height (mm)**	**Mass (kg)**	**Failure load (kN)**	**Compressive strength (Mpa)**
	1	100.00	100.00		2.218	387	38.7
	2	100.00	100.00		2.239	384	38.4
Age: 28 days	3	100.00	100.00		2.24	380	38
					Average	384	38.4

Appendix G – Pull-out test results & statistical significance values

Pull-out force (kN)	C45-12-0	C45-12-20	M45-12-0	M45-12-20	M65-12-0	M65-12-10	M65-12-20	M65-16-0	M65-16-20	Coating treatment
1	78.60	60.60	68.60	58.00	58.80	54.00	44.70	86.00	52.70	Untreated
2	66.10	56.30	68.00	56.30	54.00	46.80	50.00	58.00	66.50	
3	64.40	60.40	70.80	62.80	60.30	48.40	50.30	74.30	62.00	
4	74.20	57.20	72.50	60.10	64.20	52.00	42.30	66.80	70.80	
5	64.40	61.80	52.30	54.50	52.80	44.20	43.20	56.80	54.50	1 coat
6	62.10	55.00	70.20	48.80	58.30	44.20	43.00	54.00	52.00	
7	72.30	58.00	64.20	54.00	50.30	44.50	44.10	60.00	50.60	
8	62.00	56.80	58.40	52.10	50.80	42.00	46.40	60.80	54.00	
9	58.30	60.00	58.40	50.80	47.40	46.00	44.80	52.30	50.00	2 coats
10	61.00	56.00	62.60	50.80	52.80	46.00	44.20	42.20	52.50	
11	64.00	59.00	52.80	54.00	47.40	42.50	42.20	46.50	50.50	
12	71.00	53.00	60.20	50.30	48.00	43.80	44.00	50.80	58.00	

p-values	20% steel mass loss				10%
Specimen set	C45-12	M45-12	M65-12	M65-16	M65-12
Untreated, corroded	0.013609	0.000863946	0.004986	0.287144	0.014942343
One coat	0.012271	4.03737E-05	0.00052	0.021574	0.000381912
Two coats	0.009814	8.94662E-06	0.000387	0.024509	0.000645573

p-values	Repair materials			
	0%		20%	
	M65/M45	M45/C45	M65/M45	M45/C45
Untreated	0.0040	0.8170	0.0021	0.7178

p-vales	Coating - 12mm					
	M65		M45		C45	
	0-1 coat	0-2 coats	0-1 coat	0-2 coats	0-1 coat	0-2 coats
0%	0.066	0.00567	0.071	0.00263	0.224	0.145
10%	0.009	0.0216	-	-	-	-
20%	0.260	0.192	0.011	0.00308	0.703	0.431

p-values	Corrosion			
	M65 – 16 – 0/20	M65 - 12-0/20	M45 - 12-0/20	C45 - 12-0/20
Untreated	0.287	0.014	0.001	0.005

p-vales	Coating - 16mm	
	0-1 coat	0-2 coats
0%	0.072	0.0104
20%	0.042	0.0539

p-values	Bar diameter	
	M65 - 0-12/16	M65 - 20-12/16
Untreated	0.106	0.010
1 coat	0.090	0.00036
2 coats	0.730	0.003

Appendix H – Failure Mode status

Treatment type	Bar #	C45-12-0	C45-12-20	M45-12-0	M45-12-20	M65-12-0	M65-12-10	M65-12-20	M65-16-0	M65-16-20
Untreated	**1**	Slip	Slip	Slip	Slip	Splitting	Splitting	Splitting	Splitting	Splitting
	2	Splitting	Rupture	Slip	Rupture	Splitting	Splitting	Slip	Splitting	Slip
	3	Splitting	Slip	Splitting	Slip	Splitting	Slip	Slip	Splitting	Slip
	4	Rupture	Slip	Splitting	Slip	Slip	Splitting	Slip	Splitting	Splitting
One coat (0.6 mm)	**5**	Slip (c)	Slip	Splitting	Slip	Splitting (c)	Splitting (c)	Slip	Splitting (c)	Slip
	6	Slip	Slip	Slip (c)	Slip	Slip	Splitting (c)	Slip	Slip	Slip (c)
	7	Splitting	Slip	Slip (c)	Slip (c)	Splitting	Slip (c)	Slip	Splitting (c)	Slip
	8	Slip (c)	Slip	Slip	Slip	Slip (c)	Slip	Slip	Splitting	Slip
Two coats (0.6 mm each)	**9**	Splitting	Splitting	Slip	Slip (c)	Slip (c)	Slip	Splitting	Splitting (c)	Slip (c)
	10	Slip (c)	Slip (c)	Slip (c)	Slip	Splitting (c)	Slip	Slip	Splitting	Splitting
	11	Slip (c)	Slip	Slip	Slip	Slip	Slip (c)	Slip (c)	Splitting (c)	Slip
	12	Slip	Slip	Slip (c)	Slip	Slip	Splitting (c)	Slip	Splitting (c)	Slip

Appendix I – Ethics form